HELSINGIN YLIOPISTO
HELSINGFORS UNIVERSITET
UNIVERSITY OF HELSINKI

APPLICATION OF A NOVEL MOLECULAR METHOD FOR CANCER DIAGNOSTICS:

The detection of AR-V7 mRNA

Sonja Elf

Master's thesis
University of Helsinki
Faculty of Biological and Environmental Sciences
Master's Degree Programme in Biotechnology (MBIOT)
October 2018

HELSINGIN YLIOPISTO
HELSINGFORS UNIVERSITET
UNIVERSITY OF HELSINKI

Tiedekunta – Fakultet – Faculty Faculty of Biological and Environmental Sciences	**Laitos – Institution– Department** Department of Biosciences	
Tekijä – Författare – Author Sonja Elf		
Työn nimi – Arbetets titel – Title Application of a novel molecular method for cancer diagnostics: detection of AR-V7 mRNA		
Oppiaine – Läroämne – Subject Master's Degree Programme in Biotechnology (MBIOT)		
Työn laji – Arbetets art – Level Master's thesis	**Aika – Datum – Month and year** 31.10.2018	**Sivumäärä – Sidoantal – Number of pages** 66 + 17

Tiivistelmä – Referat – Abstract

Despite recent advances in understanding, diagnosis and treatment of cancer, this complex and versatile disease remains one of the leading causes of death worldwide. New and rapid diagnostic methods are needed to detect cancers at their early stages of development, thus enabling earlier prognosis, better risk assessment and more efficient treatment of the disease. There has been an increasing interest in specific molecular biomarkers as the hallmark for cancer research, and the detection of these markers from liquid biopsies using advanced molecular diagnostics methods provides major advantages over the conventional imaging methods currently used in oncology.

The aims of this thesis were to examine the applicability of a novel molecular method, SIBA® (Strand Invasion Based Amplification), for the detection of cancer biomarkers, and to develop an assay targeting androgen receptor splice variant 7 (AR-V7) mRNA. The AR-V7 is proposed as a treatment-response biomarker in patients with castration-resistant metastatic prostate cancer (mCRPC). The expression of this variant can indicate resistance to hormonal therapies used for the treatment of advanced prostate cancer. Prostate cancer is the most common cancer after lung cancer in men worldwide and can gradually develop into a highly advanced lethal form, mCRPC, that is not responsive to androgen deprivation therapies. Positive AR-V7 status is suggested to represent the phenotype of this advanced stage of prostate cancer, and its detection can assist in treatment selection for the mCRPC patients.

SIBA is a novel isothermal method for the amplification and detection of nucleic acids. The technology offers significant advantages over the more conventional molecular detection method, polymerase chain reaction (PCR), since the amplification reaction occurs at constant temperature and does not require sophisticated laboratory equipment for the thermal cycling. Reverse transcription SIBA (RT-SIBA) enables reverse transcription of RNA to cDNA as well as the simultaneous amplification and detection of the cDNA in one-step reaction under isothermal conditions. The method displays both high analytical sensitivity and specificity to the target nucleic acids. The RT-SIBA technology has not formerly been applied for the detection of human DNA or RNA.

The main finding of this thesis was, that the RT-SIBA technology can be applied for rapid detection of specific molecular cancer biomarkers such as the AR-V7 mRNA. In this study, two RT-SIBA assays targeting the full-length androgen receptor (AR-FL) mRNA and the AR splice variant 7 mRNA were developed and optimized. Performance of the assays were evaluated by testing RNA isolates from AR-V7 positive and negative prostate cancer cell lines in the presence of human whole blood and plasma in the reaction. The developed RT-SIBA assays provided high analytical sensitivity and specificity: low copies of the target mRNA were amplified within 20 minutes without the production of non-intended amplicons. The results suggest that the RT-SIBA technology can be utilized for easy and rapid detection of AR-V7 and AR-FL mRNA directly from liquid sample material without a need for time-consuming sample treatment. Further performance evaluation using real AR-V7 positive clinical samples from mCRPC patients is necessary for the reliable validation of the developed assays.

Avainsanat – Nyckelord – Keywords
Cancer diagnostics, biomarker, molecular method, SIBA, mCRPC, AR-V7

Ohjaaja tai ohjaajat – Handledare – Supervisor or supervisors
Kevin Eboigbodin, PhD

Säilytyspaikka – Förvaringställe – Where deposited
Viikki campus library, University of Helsinki

Muita tietoja – Övriga uppgifter – Additional information

HELSINGIN YLIOPISTO
HELSINGFORS UNIVERSITET
UNIVERSITY OF HELSINKI

Tiedekunta – Fakultet – Faculty	Laitos – Institution– Department
Bio- ja ympäristötieteellinen tiedekunta	Biotieteiden laitos

Tekijä – Författare – Author
Sonja Elf

Työn nimi – Arbetets titel – Title
Uuden molekulaarisen menetelmän soveltaminen syöpädiagnostiikkaan: AR-V7 mRNA:n detektio

Oppiaine – Läroämne – Subject
Master's Degree Programme in Biotechnology (MBIOT)

Työn laji – Arbetets art – Level	Aika – Datum – Month and year	Sivumäärä – Sidoantal – Number of pages
Pro-gradu tutkielma	31.10.2018	66 + 17

Tiivistelmä – Referat – Abstract

Huolimatta viimeaikaisista edistysaskelista syöpädiagnostiikan ja syöpähoitojen saralla, on tämä kompleksi ja monitahoinen tauti yhä yksi maailman yleisimmistä kuolinsyistä. Uusia ja nopeita diagnostisia menetelmiä tarvitaan syöpätautien tunnistamiseen niiden aikaisessa kehitysvaiheessa, jotta tautien aiempi prognoosi, parempi riskienhallinta ja tehokkaampi hoito olisivat mahdollisia. Kiinnostus spesifisiin molekulaarisiin biomerkkiaineisiin, jotka toimivat syövän tunnusmerkkeinä, on vähitellen kasvamassa. Näiden merkkiaineiden tunnistaminen nestemäisistä näytemateriaaleista kehittyneiden molekulaaristen diagnostiikkamenetelmien avulla tarjoaa huomattavia etuja perinteisiin onkologiassa käytettäviin kuvantamismenetelmiin verrattuna.

Tämän tutkielman tavoite oli tutkia uuden molekulaarisen menetelmän, SIBA®:n (Strand Invasion Based Amplification), soveltuvuutta syöpämerkkiaineiden tunnistamiseen, sekä kehittää testi androgeenireseptorin silmukointivariantti 7 (AR-V7) mRNA:n tunnistamiseen. AR-V7:ä on esitetty hoitovaste-biomerkkiaineeksi potilaissa, joilla on metastaattinen kastraatioresistentti eturauhassyöpä (mCRPC). Tämän variantin ekspressio voi ilmaista kehittynyttä resistenssiä edistyneen eturauhassyövän hoitoon käytetyille hormonaalisille hoidoille. Eturauhassyöpä on maailmanlaajuisesti toiseksi yleisin miehillä esiintyvä syöpä keuhkosyövän jälkeen, ja se voi vähitellen kehittyä pitkälle edenneeksi kuolettavaksi metastaattiseksi kastraatioresistentiksi eturauhassyöväksi, johon androgeeni-deprivaatiohoito ei enää toimi. Positiivisen AR-V7-statuksen on esitetty edustavan tämän pitkälle edenneen eturauhassyövän fenotyyppiä, ja sen tunnistaminen voi auttaa sopivan hoitomuodon valinnassa mCRPC-potilaille.

SIBA on uusi isotermaalinen menetelmä nukleiinihappojen monistamiseen ja tunnistamiseen. Teknologia tarjoaa merkittäviä etuja perinteiseen molekulaariseen tunnistusmenetelmään, polymeraasiketjureaktioon (PCR) verrattuna, sillä SIBA-monistus tapahtuu vakiolämpötilassa eikä vaadi lämpösykliseen monistamiseen tarvittavaa hienostunutta laboratoriovälineistöä. Käänteistranskriptio-SIBA (RT-SIBA) mahdollistaa RNA:n käänteistranskription cDNA:ksi samanaikaisesti cDNA:n monistuksen ja tunnistuksen kanssa yksivaiheisessa reaktiossa ja isotermaalisissa olosuhteissa. Menetelmä on osoittanut korkeaa analyyttistä herkkyyttä sekä spesifisyyttä kohdenukleiinihapoille. RT-SIBA-teknologiaa ei ole aiemmin sovellettu ihmisperäisen DNA:n tai RNA:n tunnistamiseen.

Tämän tutkielman tärkein havainto oli, että RT-SIBA-teknologiaa voidaan soveltaa molekulaaristen syöpämerkkiaineiden, kuten AR-V7 mRNA:n, nopeaan ja spesifiseen tunnistamiseen. Tässä tutkimuksessa kehitettiin ja optimoitiin kaksi RT-SIBA-testiä, jotka kohdistuivat täyspitkän androgeenireseptori (AR-FL) mRNA:n sekä androgeenireseptorin silmukointivariantti 7 (AR-V7) mRNA:n tunnistamiseen. Näiden testien suorituskykyä arvioitiin testaamalla RNA:ta, joka oli eristetty AR-V7 positiivisista sekä negatiivisista eturauhassyöpäsoluista. Reaktiossa oli samanaikaisesti läsnä myös nestemäistä näytemateriaalia; kokoverta tai plasmaa. Kehitetyt RT-SIBA-testit olivat analyyttisesti erittäin spesifisiä ja herkkiä: ne monistivat alhaisia kopiomääriä kohde-mRNA:ta alle 20 minuutissa ilman epäspesifisten amplikonien muodostumista. Tulokset osoittavat, että RT-SIBA-teknologiaa voidaan hyödyntää AR-V7 ja AR-FL mRNA:n helppoon ja nopeaan tunnistukseen suoraan nestemäisestä näytemateriaalista ilman aikaa vievää näytteenkäsittelyä. Jatkokokeet todellisilla AR-V7-positiivisilla mCRPC-potilaiden kliinisillä näytteillä ovat tarpeellisia, jotta kehitetyt testit voidaan validoida luotettavasti.

Avainsanat – Nyckelord – Keywords
Syöpädiagnostiikka, biomerkkiaine, molekulaarinen menetelmä, SIBA, mCRPC, AR-V7

Ohjaaja tai ohjaajat – Handledare – Supervisor or supervisors
Kevin Eboigbodin, PhD

Säilytyspaikka – Förvaringställe – Where deposited
Viikin kampuskirjasto, Helsingin yliopisto

Muita tietoja – Övriga uppgifter – Additional information

Table of contents

List of abbreviations

2-DE	2-dimensional gel electrophoresis
ADT	androgen deprivation therapy
AR	androgen receptor
AR-FL	full-length androgen receptor
ARSI	androgen receptor signaling inhibitor
AR-V7	androgen receptor splice variant 7
bp	base pair
CI	confidence interval
C_q	quantification cycle
CTC	circulating tumor cell
ctDNA	circulating tumor-derived DNA
DBD	DNA-binding domain
ddPCR	droplet digital polymerase chain reaction
DNA	deoxyribonucleic acid
DRE	digital rectal examination
EDTA	ethylenediaminetetraacetic acid
FISH	fluorescence in situ hybridization
HRPC	hormone-refractory prostate cancer
IO	invasion oligonucleotide
LBD	ligand-binding domain
LoD	limit of detection
mCRPC	metastatic castration-resistant prostate cancer
MgAc	magnesium acetate
mRNA	messenger RNA
MS	mass spectrometry
NCI	National Cancer Institute
NGS	next-generation sequencing
NTD	N-terminal binding domain
OD	optical density
PBS	phosphate-buffered saline
PCa	prostate cancer
PCR	polymerase chain reaction

PSA	prostate-specific antigen
RFU	relative fluorescence unit
RNA	ribonucleic acid
RT	reverse transcription
RT-qPCR	quantitative reverse transcription polymerase chain reaction
RT-SIBA	reverse transcription strand invasion based amplification
SIBA	strand invasion based amplification
SQ	Starting quantity
T_m	melt temperature

1 Introduction

1.1 Cancer diagnostics

1.1.1 Cancer in general

According to World Health Organization (WHO) estimates, “cancer is the first or second leading cause of death before the age of 70 years in 91 of 172 countries” (Bray et al. 2018). Cancer is a highly complex and versatile disease that involves genomic changes causing normal cells to turn into cancer cells. The range of genomic changes behind the cancer development can vary from subtle point mutations on a nucleotide level to changes in a whole chromosome complement. (Hanahan & Weinberg 2000.) In addition to these genetic alterations, the human cancer genome also includes the potentially reversible epigenetic modifications to DNA and the histone proteins (Chin & Gray 2008).

Whereas the molecular background of cancer is versatile, so is the range of the subsequent disease types and symptoms. More than 100 different types of cancer have been identified, and a diverse scale of tumor subtypes specific to certain tissues can be found. However, these heterogenous complex diseases all share a few similar physiological characteristics of the cancer cells: (1) self-sufficiency in growth signals, (2) ability to evade antiproliferative signals, (3) ability to evade apoptosis, (4) limitless replicative potential, (5) ability to induce and sustain angiogenesis, and (6) tissue invasion and metastasis. The development of cancer is a multistep process during which the cells acquire these novel capabilities and progressively evolve from normal to pre-malignant states, and finally into invasive metastatic cancers. (Hanahan & Weinberg 2000.)

1.1.2 Molecular biomarkers

One of the aims of Cancer research is to map out the changes in the cancer genome and epigenome responsible for the disease mechanisms (Chin & Gray 2008). The genetic and epigenetic changes result in altered protein expression levels or functions in the affected cells, further causing changes in cell physiology, proliferation and signaling. Molecules that indicate the presence of affected cancer cells in the body are referred to as the molecular cancer biomarkers. These biomarkers can be found in blood, urine,

cerebrospinal fluid and other tissues. They include genomic variations, differences in messenger RNA (mRNA) expression, protein expression and metabolite levels, and posttranslational protein variants. Identification of these molecular disease indicators is applied for risk assessment, early detection, diagnosis, prognosis, treatment planning, progression monitoring and anti-cancer drug development. (Maruvada et al. 2005; Sawyers 2008; Schiffman et al 2015).

Molecular biomarkers may have a critical role in the success of therapies that target specific genomic alterations, and they can provide information on individualized treatment responses paving the way for personalized medicine. (Maruvada et al. 2005; Chin and Gray 2008). These predictive biomarkers can be used to assess the probability of patients benefiting from a particular treatment, indicating sensitivity or resistance to a specific drug (Sawyers 2008). For instance, lung cancer patients with mutations in the *EGFR* gene can be treated with gefitinib or erlotinib medication (Paez et al. 2004), patients with chronic myeloid leukemia caused by the *BCR-ABL* translocation can be treated with imatinib mesylate (Druker et al. 2001), and breast cancer patients with the amplification of the oncogene *HER2* can be treated with trastuzumab or lapatinib (Pegram & Slamon 2000).

Detection of the alterations acting as biomarkers can also be used for risk assessment for the development of a certain type of cancer (Chin and Gray 2008; Maruvada et al. 2005). For example, mutations in the *BRCA1* or *BRCA2* genes are associated with an increased risk for development of hereditary breast or ovarian cancer (King et al. 2003). Testing for prognostic biomarkers in turn allows the prediction of the disease progression and outcome and guides the decision-making on whom to treat with adjuvant therapy in order to prevent the cancer recurrence (Sawyers 2008).

Pharmacodynamic biomarkers are used in the clinical development of anti-cancer drugs to measure the treatment effects on the tumor and to guide dosage planning. In addition to the use in clinical trials, the pharmacodynamic biomarkers can potentially be applied for personalized medicine in selection of effective drug doses for patients with differing clinical responses. (Sawyers 2008).

1.1.3 Cancer diagnosis methods

1.1.3.1 Traditional methods

In cancer diagnostics, screening is the testing for disease indicators, and it is used for early disease detection and surveillance (Schiffman et al. 2015). Radiographic imaging is the most common screening method used for the detection of non-active, asymptomatic latent cancers: mammography for breast cancer, colonoscopy for colon cancer and X-ray for lung cancer screening. Nevertheless, these methods can be insensitive and lead to unnecessary radiation exposure or biopsies. (Maruvada et al. 2005; Schiffman et al. 2015).

When the indication of a solid tumor is found, a surgical biopsy sample is traditionally obtained from the cancer tissue and analyzed under a microscope using histopathological staining and imaging. Then, the potential changes in cell structures and tissue patterns are identified and used for both confirmation of the presence or absence of cancer and grading of the disease stage. Diagnosis is always subjective, since it is based on the personal assessment of the pathologist and can easily lead to considerable diagnostic variability. Automated systems and computational algorithms have been developed to ease the work load relating to the histopathological imaging, as the handling of the pathological sections can be laborious and time-consuming. (Demir & Yener 2005.)

1.1.3.2 Molecular methods

Molecular cancer diagnosis methods comprise of techniques used to detect and monitor changes on genomic, proteomic and metabolomic levels. The method used for the detection and diagnosis depends on the type of the target alteration. Common genetic technologies used for monitoring genetic alterations include DNA microarrays, PCR-based assays and fluorescence *in situ* hybridization (FISH). DNA microarrays allow wide-range expression profiling of thousands of genes, thereby enabling the identification of differentially expressed genetic factors in cancer tissue and classification of the tumor types. Modern quantitative microarray platforms utilizing comparative genomic hybridization can be used to detect changes in cancer cell chromosomes. Structural rearrangements, including deletions, insertions and translocations, can be detected

using cytogenetic techniques, such as FISH, or sequencing-based methods such as end-sequence profiling. (Maruvada et al. 2005; Chin and Gray 2008.)

Quantitative PCR (qPCR) is a common molecular method that provides rapid and versatile information on gene expression levels, gene amplification or loss and small-scale alterations such as point mutations. The method includes both amplification and analysis of the target nucleic acid without a need for gel electrophoresis, radioactivity or sample manipulation. The use of DNA dyes and fluoroprobes enables real-time monitoring and quantification of the targets, and the multiplex detection provides the possibilities to use internal controls, lower reagent costs and to simultaneously analyze multiple genetic targets from a single sample within a single reaction tube. The qPCR technology can be applied for gene copy number determination in cancer cells and for the detection of various genetic mutations. (Bernard & Wittwer 2002; Maruvada et al. 2005.)

In addition to the genetic technologies, molecular techniques for the identification of epigenetic changes in DNA methylation and chromatin structure have been established. These methods include restriction-landmark genomic scanning, microarray analysis, bisulphate sequencing, methylation-specific digital karyotyping and chromatin immunoprecipitation. (Chin and Gray 2008.)

Proteomic molecular technologies in cancer diagnostics cover the functional and structural analysis of proteins responsible for carcinogenesis. High-throughput quantitative proteomic approaches for identification of key proteins in cancer development include two-dimensional gel electrophoresis (2-DE), isotope-coded affinity tag (ICAT), stable isotope labeling with amino acids in cell culture (SILAC), isobaric tags for relative and absolute quantification (iTRAQ) and several other techniques utilizing mass spectrometry (MS). Robust microarray platforms composed of recombinant proteins or antibodies can be applied for multiplexed detection of several tumor-specific antigens and utilized as a screening tool for specific cancers. (Maruvada et al. 2005; Liang et al. 2012.)

The metabolomic diagnostic technologies target molecules that are the final products of cell metabolism and gene expression. The metabolites exposed to carcinogenic changes can often be detected from body fluids. The metabolomic analytical approaches

comprise several spectroscopic and chromatographic methods, and their use as a tool for cancer diagnostics is becoming more general. (Maruvada et al. 2005.)

1.1.3.3 Future methods

New methods for enhanced cancer detection are constantly being developed. Novel PCR-based technologies, such as the droplet digital PCR (ddPCR), have already been applied for cancer diagnostics, thereby providing improved sensitivity, specificity and precision for the detection and quantitation of genetic alterations. Another newly developed approach for cancer detection and classification is the utilization of optimized next-generation sequencing (NGS) technologies. These advanced methods are utilized for the detection of cancer biomarkers from liquid biopsies and can furthermore be used for screening as well as for real-time monitoring and regular follow-up of the disease on whole-genome level. (Postel et al. 2018.) The future cancer diagnosis methods also likely include applications of innovative nanotechnology. Various nanodevices comprising *i.a.* nanometer-sized shells, wires, diamonds, carbon tubes, quantum dots and supermagnetic nanoparticles can be utilized for the identification of various molecules, including tumor-specific biomarkers. (Jaishree & Gupta 2012.)

1.1.4 Liquid biopsies in molecular cancer diagnostics

The use of tissue biopsies for tumor profiling limits the sampling frequencies and exposes patients to a risk, since surgical complications may occur while clinically obtaining the tissue samples. Furthermore, not all tumors are accessible for a biopsy. Analysis of a single biopsy from heterogenic tumor can cause diagnostic biases and the histological analysis of biopsy samples obtained from several sites may delay the treatment initiation. Therefore, the non-invasive methods lacking these limitations are an attractive alternative, enabling the use of more accessible liquid biopsies and profiling of the disease on molecular level. (Crowley et al 2013; Postel et al. 2017.)

The non-invasive strategies include the analysis of circulating tumor cells (CTCs) and cell-free circulating tumor-derived DNA (ctDNA) isolated from blood, proteomic studies on serum or plasma, *in situ* tumor imaging on molecular level and assessment of tumor cell-specific autoantibodies. (Sawyers 2008; Schiffman et al. 2015.) The use of CTC isolation in cancer management especially provides advantages in morphologic identification and molecular characterization of the tumors, and they can be applied for

disease screening at early stage as well as for prognosis and treatment response assessment of more advanced cancers. The ctDNA detection is currently used for targeting mutations from the circulation and for the identification of tumor cells responsive or resistant to therapies. (Crowley et al 2015; Schiffman et al. 2015.)

The use of liquid biopsies, such as blood, as the sample material for cancer diagnostics can ensure rapid and safe systematic sampling in contrast to tissue biopsies. The use of liquid biopsies shortens the sample analysis time thereby enabling faster diagnosis and treatment initiation as well as regular disease monitoring. The non-invasive liquid biopsies and molecular biomarkers can be used in combination with traditional diagnostic imaging for efficient first-hand screening: if indications for the disease are found by biomarker screening, the more expensive and accurate imaging tests can be performed to confirm the diagnosis and individualize the treatment. (Crowley et al 2015; Maruvada et al. 2005).

1.2 Prostate cancer and metastatic castrate-resistant prostate cancer (mCRPC)

Prostate cancer is a disease, where cancer is developed in the prostate gland tissues in the male reproductive system (NCI, Dictionary of Cancer Terms: Prostate cancer 2018). Prostate cancer is the second most commonly diagnosed cancer worldwide after lung cancer, and in 105 countries, including Finland, the most frequently diagnosed cancer in men. It is the leading cause of cancer-related deaths among men in 46 countries. It is estimated that almost 1,3 million new prostate cancer cases are diagnosed, and that the disease causes nearly 360 000 deaths worldwide in 2018 (Bray et al. 2018). The increase in prostate cancer incidence in recent decades is due to improved awareness of prostate-related symptoms, better health care access and the diagnosis of latent cancers during prostate surgeries or screening of asymptomatic individuals. (Kvåle et al. 2007). Whereas the disease incidence rates have been increasing, the death rates for prostate cancer are decreasing in several developed countries. This results from both earlier diagnosis due to screening of latent cancers, and improved treatment. (Bray et al. 2018.)

Metastatic castrate-resistant prostate cancer (mCRPC) is an advanced stage of prostate cancer that has progressed despite established androgen-targeting therapies (Tan et al.

2017).10–20% of prostate cancer patients undergo the disease translation to this lethal phenotype within five years from the initial diagnosis (Kirby et al. 2011).

1.2.1 Clinical characteristics

Prostate cancer is more common in older men, and it is typically diagnosed in men around the age of 70 years. Urinary tract symptoms, such as urgency, frequency and weak flow, can be signs of prostate cancer. The disease is slow-growing when compared to most of the cancers. All men with circulating androgens will eventually develop microscopic prostate cancer if they just live long enough, and most people die with the disease rather than from it. Typical prostate cancer characteristics include multifocality and heterogeneity: the presence of several prostate tumors instead of only one, and variability in the cancer morphology and genotype, suggesting that the disease is a result of multiple carcinogenic mechanisms. (Bostwick et al. 2004; Moyer 2012.)

Age, African American origin and family background are known risk factors for developing prostate cancer. 5–10% of all prostate cancer cases are hereditary, and the clinical and pathological characteristics of both familial and nonfamilial prostate cancer are similar (Bostwick et al. 2004; Bratt et al. 2002). Altered androgen metabolism due to elevated testosterone levels may increase the risk for prostate cancer. In addition, a set of exogenous risk factors including diet and environmental agents have been linked to the development of prostate cancer. (Bostwick et al. 2004.)

Most diagnosed prostate cancer cases have a good prognosis, and the survival rate is 98,2% (NCI, Cancer Stat Facts: Prostate Cancer 2018). However, the stage of the cancer at the initial point of diagnosis has a strong effect on the survival rate: the earlier the disease is detected, the better the prognosis. The disease stages include the localized stage, where the primary tumor is only found at one site, and the more advanced metastatic regional and distant stages, where tumors have spread to several sites in the body, most commonly to the bone tissue. (Moyer 2012; Shen & Abate-Shen 2010). Patients diagnosed with advanced prostate cancer have a median survival of two years, and the survival of patients with tumor metastases is remarkably reduced (Kirby et al. 2011).

The early stages are often asymptomatic and treatable. Nevertheless, the majority of prostate cancer patients ultimately develop advanced metastatic tumors that are

resistant to the most common hormonal androgen deprivation treatments. This lethal disease stage is termed metastatic castrate-resistant prostate cancer (mCRPC), or formerly referred to as hormone-refractory prostate cancer (HRPC). (Haile & Sadar 2011; Antonarakis et al. 2014.) This lethal phenotype is associated with bone metastases, reduced survival and poor life quality (Kirby et al. 2011). Several different molecular factors can induce the conversion of previously androgen-dependent cells into androgen-independent cells resistant to androgen deprivation therapy. These may include mutations in the AR gene, altered cell proliferation and genetic and epigenetic changes that induce the conversion of the previously androgen-dependent cells into androgen-independent cells under the androgen deprivation therapy. (Shen & Abate-Shen 2010.)

1.2.2 Diagnosis

Conventional prostate cancer detection methods include ultrasonography and digital rectal examination (DRE). These methods may display varying sensitivity and specificity (Maruvada et al. 2005; Moyer 2012). A more sensitive screening method is the testing for a proteomic molecular marker, prostate-specific antigen (PSA). PSA is a glycoprotein secreted by the epithelial cells of the prostate tissue. The PSA level is elevated in patients with prostate cancer and it increases as the clinical stage of the disease progresses. (Stamey et al. 1987.) Determination of PSA is used for both screening and monitoring of the disease. PSA is detected from serum, and PSA values above 4 ng/ml indicate the potential presence of prostate cancer. PSA is not only specific to prostate cancer. Consequently, the false positive results are common during PSA screening. (Maruvada et al. 2005).

The most remarkable benefit of the PSA screening is the initiation of early treatment and reduction in the development of symptomatic metastatic disease. (Fleshner et al. 2017.) After PSA testing became available in the Nordic countries around 1990, a considerable increase in the prostate cancer incidence was detectable (Kvåle et al. 2007). A similar impact was reported in the United States during the 1980s and 1990s, where the incidence rates of prostate cancer were doubled due to the initiation of PSA screening (Hankey et al. 1999).

Nevertheless, PSA screening for early detection of prostate cancer is controversial, since the benefits versus the pitfalls of PSA testing remain questionable. Harms of the PSA

screening include a high rate of false-positive results, leading to negative mental effects, unnecessary biopsies, overdiagnosis and overtreatment. PSA screening often reveals a latent benign disease that would have remained asymptomatic throughout one's life. (Moyer 2012; Mottet et al. 2017.)

Based on the indications of DRE and elevated PSA levels, the presence of prostate cancer is confirmed by a biopsy, and the tumor is classified based on the histopathological findings. The most used prostate cancer classification methods are the Gleason scoring determining the differentiation level of localized tumors, and the TNM classification, which covers the status of primary tumor (T), lymph node involvement (N) and the metastatic degree of the disease (M). (Shen & Abate-Shen 2010; Mottet et al. 2017.)

1.2.3 Treatment

PSA detected prostate cancer is initially managed by observation, physical examination and palliative treatment. The potential disease development is monitored by active surveillance strategies such as PSA tests and repeated biopsies. Conventional early treatment of localized progressive prostate cancer includes prostate surgery and radiation therapy. The more advanced prostate cancer is commonly treated with androgen deprivation therapy (ADT), that includes both surgical and medical castration to reduce the tumor burden and PSA levels by inhibiting the activity of androgens. (Moyer 2012; Shen & Abate-Shen 2010: Hu et al. 2009.) The surgical castration, radical prostatectomy, is the only effective treatment for localized prostate cancer (Mottet et al. 2017). The hormonal ADT comprises the use of luteinizing hormone-releasing hormone (LHRH) analogues and AR antagonists (Tan et al. 2017).

Eventually, most of the patients treated with ADT develop metastatic castration-resistant prostate cancer (mCRPC) that is no longer responsive to the AR-targeting therapies. To improve the survival of patients with mCRPC, they can be treated with chemotherapies that decrease the proliferation of cancer cells, such as taxanes docetaxel or cabazitaxel, immunotherapies such as Sipuleucel-T and radium-223 dichloride. However, these therapies are only remotely effective, and most patients pass away within 2 years of the disease onset. (Haile & Sadar 2011; Antonarakis et al. 2014; Tan et al. 2017.)

The most common hormonal treatment for advanced prostate cancer is the use of androgen receptor signaling inhibitors (ARSIs), that either suppress the androgen synthesis or directly target the AR by binding to its LBD. Currently, the progressive metastatic prostate cancer is treated with continuous ARSI therapies, such as androgen-synthesis inhibitor abiraterone and androgen receptor antagonist enzalutamide. Abiraterone and enzalutamide are the most recently licensed FDA-approved hormonal agents that can improve the overall survival of men with mCRPC progression after taxane therapies. (Antonarakis et al. 2014; Tan et al. 2017.)

1.2.4 AR and AR-Vs in mCRPC

Androgen receptor (AR) gene is considered the most significant gene in prostate cancer, since the development of prostate cancer is always dependent on the interactions between androgens and the androgen receptor. The human AR is single-copy gene located on Xq11-12 in the male genome. It is over 90 kb long and is composed of eight exons. The gene encodes a multidomain protein with four functional regions: an N-terminal domain (NTD), a DNA-binding domain (DBD), a hinge region and a COOH-terminal ligand-binding domain (LBD). Androgens are nuclear hormones acting as ligand for the AR protein, and the most abundant androgen in men is testosterone synthetized by the testis. The androgen receptor protein acts as a hormone activated transcription factor and is expressed in several tissues. (Lu & Luo 2013; Shen & Abate-Shen 2010; Hu et al. 2009; Guo et al. 2009.)

The AR plays several cell-type specific roles in the development of prostate cancer together with other key regulators of epithelial differentiation in the prostate. Several different molecular mechanisms including the AR overexpression and gain-of-function mutations in the LBD of AR have been suggested to lead to the resistance to hormonal androgen deprivation therapy and the development of mCRPC. (Shen & Abate-Shen 2010; Hu et al. 2009.)

More than 20 alternative splicing isoforms encoding constitutively active transcript variants of AR have been identified. The AR splice variants (AR-Vs) encode alternative AR proteins that lack the hinge region and the LBD due to splicing of cryptic exons containing the stop codons (Dehm et al. 2008; Hu et al 2009; Guo et al. 2009). Androgen receptor splice variant 7 (AR-V7), formerly referred to as AR3, is the most frequently expressed AR variant encoding a functional protein that is detectable in prostate cancer

cell lines as well as in clinical specimens. The AR-V7 protein acts as an androgen-independent transcription factor and its activity is not affected by AR signaling inhibitors. Consequently, the alternative AR gene splicing can have a central role in the activation of AR signaling in prostate cells. The AR-V7 is expressed in both the normal prostate tissues and malignant glands, but the level of cytoplasmic expression is considerably increased in the cancerous tissues, whereas in normal tissues the expression is mainly restricted to basal and stromal cells. (Guo et al. 2009; Hörnberg et al. 2011). The elevated AR-V7 expression level has been associated with worse prognosis and clinical outcome in patients with prostate cancer (Hu et al. 2009; Hörnberg et al. 2011; Antonarakis et al. 2017).

1.2.4.1 The importance of AR-V7 detection in mCRPC

Antonarakis et al. first demonstrated in 2014, that the detection of AR-V7 mRNA transcript in CTCs of men with advanced mCRPC was associated with resistance to the androgen receptor signaling inhibitors abiraterone and enzalutamide (Antonarakis et al. 2014) and later showed that the positive AR-V7 status was not an indication of primary resistance to taxane chemotherapy, such as docetaxel or cabazitaxel (Antonarakis et al. 2015). These findings and several supporting studies suggest that the AR-V7 can act as a predictive treatment-response biomarker in patients with progressive mCRPC and guide the selection of an appropriate treatment method: taxane chemotherapy is more effective in AR-V7-positive men, whereas the AR-V7 negative men can be treated with ARSI therapies. Novel alternative therapies for efficient treatment of advanced mCRPC can be applied for patients identified as AR-V7 positive, thus preventing them for undergoing unnecessary, inefficient and costly treatments. (Onstenk et al. 2015; Scher et al. 2016; Antonarakis et al. 2017; Del Re et al. 2017).

Most methods for the analysis of AR-V7 status in mCRPC patients target the of AR-V7 mRNA or protein present in the CTCs in blood (Antonarakis et al. 2014; Onstenk et al. 2015; Scher et al. 2016), but alternative molecular methods have also been presented: Hu et al. (2009) extracted RNA from prostate tissue specimens, Hörnberg et al. (2011) from bone metastases and Del Re et al (2017) from exosomes present in plasma. Among these studies, the multiplex reverse transcription quantitative PCR is the most common method used for the simultaneous detection of AR-V7 mRNA and full-length androgen receptor (AR-FL) mRNA in the clinical specimens.

1.3 Reverse Transcription Strand Invasion Based Amplification® (RT-SIBA®)

Strand Invasion Based Amplification (SIBA®) is an isothermal nucleic acid amplification method patented in 2011 and first described by Hoser et al. in 2014. The technique utilizes recombinase-dependent insertion of a single-stranded invasion oligonucleotide (IO) into the double-stranded target nucleic acid. Amplification of the target sequence occurs at constant temperature of approximately 41°C, and thus no sophisticated laboratory equipment is necessarily required for the repeated thermal cycling, in contrast to polymerase chain reaction (PCR) -based methods. The SIBA technology is sensitive to detect a single molecule of a target nucleotide, resistant to non-specific amplification and does not require complex target-specific probes for distinction of intended and un-intended amplification products, unlike several other isothermal amplification methods or real-time PCR (Hoser et al- 2014; Kumar et al. 2018).

In SIBA reaction, a recombinase protein called UvsX (from bacteriophage T4) first assist the invasion of the IO into the complementary region of target duplex by polymerizing to the IO DNA sequence, and the double-stranded target partially separates. After depolymerization of the UvsX protein, the IO can fully invade the target duplex, and the double-stranded sequence becomes completely dissociated. The target-specific single-stranded forward and reverse primers hybridize to the single-stranded complementary regions of the target area which then act as templates for the amplification reaction. The template is then extended by a polymerase enzyme from the 3'-end of the bound primers, and two copies of the target duplex are produced. During the extension, the IO is displaced by the forward primer and released to bind to another target duplex, and therefore is not consumed. The invasion and the primer extension cycles are repeated, leading to exponential amplification of the initial target duplex. (Hoser et al. 2014.) The mechanistic description of the RT-SIBA reaction steps is presented in Figure 1.

The single-stranded forward and reverse primers are designed to be below the minimum length required for the formation of a complex between an oligonucleotide and the UvsX recombinase enzyme; 25–30 nucleotides (Formosa & Alberts 1986), whereas the IO is above this length. Therefore, the primers do not act as substrates for the recombinase enzyme due to their shortness and are unable to hybridize to the target sequence without the presence of the IO. All single-stranded elements in the SIBA reaction, including forward and reverse primers, IO and the partially separated target duplex sequence, are coated with a stabilizing recombinase cofactor called Gp32 (a single-stranded DNA-

binding enzyme from bacteriophage T4), except for the complementary 3'-end of the IO sequence. The 3'-terminus of the IO is modified with additional 2'-O-methyl RNA nucleotides, that are hydrolysis-resistant analogue of RNA bases (Hoser et al. 2014; Stump et al. 1999). Since 2'-O-methyl RNA does not act as a template for a DNA polymerase, the IO cannot be extended or produce artifacts during the amplification reaction. These characteristics assure that the target nucleotides are specifically amplified without exponential production of primer dimers or other un-intended amplicons during the SIBA reaction. (Hoser et al. 2014.)

The components needed for the strand-invasion reaction and exponential template amplification include the recombinase system (such as the UvsX and Gp32 enzymes), the single-stranded forward and reverse primers (at least partly complementary to the target region), the IO (at least partly complementary to the target region, intervening the primer sequences and comprising a modified non-extendable 3'-end and a non-homologous seeding region at the 5'-end), a polymerase enzyme (preferably with strand-displacement activity and without 3'→5' exonuclease activity), deoxyribonucleotide triphosphates (dNTPs), an energy generation system (comprising such as ATP, sucrose and sucrose phosphorylase, phosphocreatine and creatine kinase, and magnesium ions) and other various factors affecting the reaction efficiency, such as pH adjusters, reducing agents or crowding agents. For real-time monitoring of the amplification reaction, intercalating dyes such as SYBR Green I, or target-specific probes can be utilized. The nucleic acid sequence used as a template in SIBA can be DNA, reverse transcribed complementary DNA (cDNA) or genomic DNA. (Hoser 2011; Hoser et al. 2014.)

The addition of reverse transcriptase enzyme into the SIBA reaction enables the detection and amplification of RNA targets, and the technology is termed reverse transcription SIBA (RT-SIBA). The presence of the reverse transcriptase enzyme allows simultaneous one-step reverse transcription of RNA into cDNA and amplification of the cDNA under isothermal SIBA reaction conditions. Contrary to several reverse transcription PCR methods, an additional step for reverse transcription prior to nucleic acid amplification is thus not needed. (Eboigbodin et al. 2016.)

Until now, the utility of SIBA and RT-SIBA has only been reported for the detection of infectious bacterial pathogens including *Salmonella* (Hoser et al. 2014), *Chlamydia trachomatis*, *Neisseria gonorrhoeae* (Eboigbodin & Hoser 2016) and *Streptococcus pyogenes* (Elf et al. 2018), and viral pathogens such as influenza virus (Eboigbodin et

al. 2016), respiratory syncytial virus (Eboigbodin et al. 2017) and rhinovirus (Kainulainen et al. 2018). Application of SIBA technology for the detection of human DNA or RNA has not been previously reported, and the use of molecular cancer markers as targets for strand invasion based amplification is a novel approach that could be possibly utilized in the field of oncology.

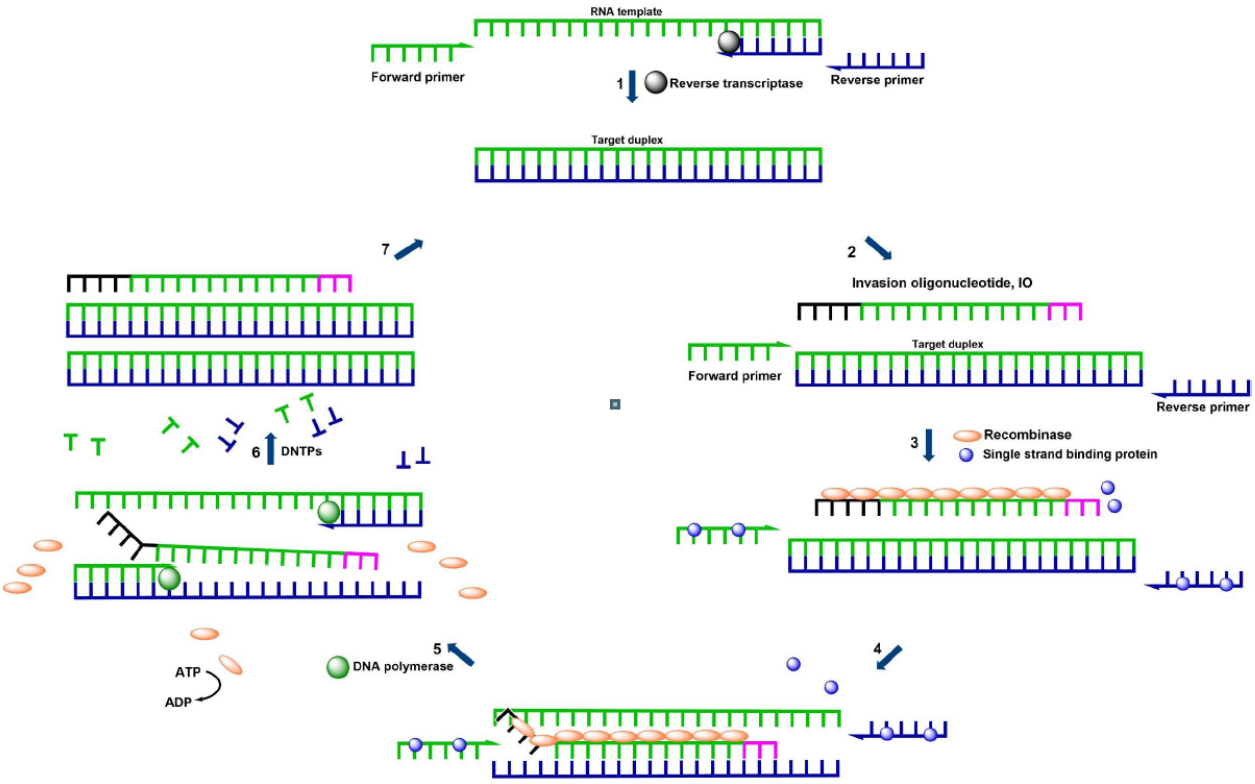

Figure 1. Mechanistic description of reverse-transcription strand invasion–based amplification (RT-SIBA) reaction. **1)** Reverse transcription of RNA target to cDNA by the reverse transcriptase enzyme. **2)** An invasion oligonucleotide (IO) and two target-specific primers are required for the amplification. **3)** A recombinase cofactor protein, Gp32, binds to single-stranded oligonucleotides to reduce the formation of secondary structures. The recombinase protein, UvsX, coats the IO displacing the bound Gp32. **4)** The IO invades the complementary region of the target duplex with the assistance of UvsX. **5)** After complete separation of the target duplex, the target-specific primers bind and extend the target via the action of a DNA polymerase. **6)** Two copies of the target duplex are synthesized. **7)** The continuous recombinase-mediated target duplex separation and template extension via DNA polymerase action leads to an exponential amplification under isothermal conditions. (Adapted from Kainulainen et al. 2018.)

2 Aims of the study

The aims of this study were to examine the applicability of a novel molecular method, the Reverse Transcription Strand Invasion Based Amplification (RT-SIBA), for the diagnosis of cancer. Specifically, the method was used to develop a new nucleic acid amplification assay for the detection of androgen receptor splice variant 7 (AR-V7) messenger RNA. The AR-V7 mRNA can be used as the predictive biomarker for resistance to hormonal androgen receptor-targeting therapy in patients with metastatic castrate resistant prostate cancer (mCRPC) (Antonarakis et al. 2014). A supportive assay targeting the wild type full-length androgen receptor (AR-FL) was also to be developed. The SIBA technology has been previously utilized in the detection of microbial and viral nucleic acids (Hoser et al. 2014; Eboigbodin & Hoser 2016; Eboigbodin et al. 2016; Eboigbodin et al. 2017; Elf et al. 2018; Kainulainen et al. 2018), but not applied for the detection of human DNA or RNA. The specific target region for the developed assay was selected based on the genetic properties as well as known characteristics of SIBA technology. The RT-SIBA assays to be developed should be specific to the detection of the target region mRNA sequences, as well as providing rapid amplification and sensitivity to low levels of the target nucleic acids.

The thesis research included development of the two assays targeting AR-V7 and AR-FL mRNA. The development comprised of analysis of the AR-V7 and AR-FL target sequence, RT-SIBA assay design and screening of potential oligonucleotides for the RT-SIBA assays. Assay optimization and performance evaluation of the developed assays were also conducted. Furthermore, these assays were further evaluated using limited number of clinical prostate cancer positive specimens. The study was conducted at the R&D department of Orion Diagnostica Oy, Espoo, Finland.

3 Materials and methods

3.1 Materials

3.1.1 PCa Cell lines

A total of four different human prostate cancer (PCa) cell lines were used in this study. 22Rv1, VCaP, and DU-145 cells were generously provided by Orion Pharma (Turku, Finland) and LNCaP cells by the University of Tampere (Finland). Cells were delivered in ready pelleted form from Orion Pharma ($8 \times 10^6 – 10^7$ cells per pellet), and in PBS suspension from the University of Tampere (10^7 cells/ml). 22Rv1, VCaP and LNCaP cells are known to express both AR-V7 and full-length AR, and DU-145 cell line is negative for both AR-V7 and AR-FL at the transcript level (Wadowsky & Koochekpour 2017). Cell pellets as well as cell suspension were stored at -70°C prior to RNA isolation.

3.1.2 Sample matrixes

Commercial human plasma was obtained from Sigma-Aldrich (St. Louis, MO, USA). Plasma was delivered as powder and reconstituted with nuclease-free water (Sigma-Aldrich) prior to use. Human whole blood sample was obtained from the European Reference Laboratory for Glycohemoglobin (Netherlands) and stored at +8°C. The AR and AR-V status of the blood was unknown, but unlikely to be positive for AR-V7.

3.1.3 Clinical PCa samples

Four prostate cancer positive K2 EDTA plasma samples were obtained from the Magellan Research Sample Biobank (Discovery Life Sciences Inc, CA). Sample information is listed in the Appendix 1. The samples had been collected from patients under pre-treatment for prostate cancer. No samples from patients with more advanced PCa were available. Ages of the patients ranged between 64–69 years, Gleason scores between 6–9 and PSA levels between 12,3–18,3 ng/ml. The AR-V7 status of the samples was unknown. Samples were stored at -70 °C prior to RNA isolation.

3.1.4 GeneArt™ Strings™ DNA Fragments control templates

Synthetic androgen receptor splice variant 7 (AR-V7) and full-length androgen receptor (AR-FL) control templates were designed according to AR-V7 mRNA (GenBank NM_001348064.1) and full-length AR mRNA (GenBank L29496.1) sequences, and commercially synthetized by Invitrogen, Thermo Fisher Scientific Inc. (USA) as GeneArt™ Strings™ DNA Fragments in lengths of 980 base pairs (bp). Sequences of the templates are presented in Appendix 2.

Copy numbers of the DNA templates were calculated utilizing the Avogadro's number and an assumed 660 Dalton average weight of one base pair of double-stranded DNA (dsDNA) (Kravetz & Womble 2003). Both templates were first reconstituted with nuclease-free water (Sigma-Aldrich) to 20 ng/µl concentration. Equation 1 was used for the conversion of nanogram concentrations to dsDNA copy numbers:

Equation 1. Copy number conversion for AR-V7 and AR-FL DNA control templates.

$$dsDNA\ copy\ number = \frac{\boldsymbol{X}\ ng \times 6{,}0221 \times 10^{23}\ molecules/mole}{(\boldsymbol{N} \times 660\ g/mole) \times 1 \times\ 10^{9}\ ng/g}$$

$$= \frac{20\ ng \times 6{,}0221 \times 10^{23}\ molecules/mole}{(980 \times 660\ g/mole) \times 1 \times\ 10^{9}\ ng/g} = \mathbf{1{,}9 \times 10^{10}\ copies\ /\ \mu l}$$

Where:
X = amount of dsDNA (ng)
N = length of dsDNA template

According to the conversion calculation, 20 ng of the control template DNA corresponded $1{,}9 \times 10^{10}$ DNA copies. The templates were then further diluted with nuclease-free water (Sigma-Aldrich) to 10^6 copies per microliter, aliquoted and stored at -70 °C.

3.2 RNA extraction and quantification

3.2.1 RNA extraction from PCa cell lines

First, 0,5 ml of LNCaP cell suspension was pelleted by centrifuging for 5 minutes at 3000 x g. mRNA from all four PCa cell pellets (22Rv1, VCaP, LNCaP and DU-145) was extracted using the RNeasy Mini Kit (Qiagen, Hilden, Germany) according to manufacturer's instruction. On average, 8×10^6 cells of each cell line were used for the extraction. RNA was finally eluted twice in 30 µl of RNase-free water. Quality and quantity of the extracted RNA were determined using the NanoDrop 2000 spectrophotometer (Thermo Scientific, Waltham, MA, USA).

3.2.2 RNA extraction from PCa clinical samples

Two RNA extraction protocols were used for the clinical human prostate cancer positive samples: exoRNeasy Serum/Plasma Midi Kit (Qiagen) for the isolation of exosomal RNA, and miRNeasy Serum/Plasma Advanced Kit (Qiagen) for the purification of cell-free circulating total RNA. Before using the plasma samples for the exoRNeasy kit protocol, 250 µl of each thawed sample was first centrifuged at 3000 x *g* for 15 minutes at 4 °C to remove residual cellular material. 200 µl of clear supernatant was then used for the vesicle isolation and exosomal RNA extraction according to the manufacturer's instructions. 200 µl of each thawed plasma sample was used for the miRNeasy kit protocol, and the cell-free small RNA was extracted according to the manufacturer's instructions. At the end of both protocols, RNA was eluted in 20 µl of RNase-free water (Qiagen), and the quality and quantity of the extracted RNA were determined using the NanoDrop 2000 spectrophotometer.

3.2.3 RT-qPCR quantification of mRNA extracted from PCa cell lines

The quantities of AR-V7 and AR-FL mRNA in prostate cancer positive cell line isolates were determined utilizing the absolute quantification method by measuring the RNA copy numbers relative to the concentrations of the control DNA templates, that were used as quantification calibrators (Bustin 2000). A tenfold dilution series from 10^6 copies/µl to 1 copy/µl of both synthetic AR-V7 and AR-FL control DNA templates (Thermo Fisher Scientific) were prepared for construction of standard curves and calculation of copy

numbers for AR-V7 and AR-FL mRNA transcripts. 1:10, 1:100 and 1:1000 dilutions of mRNA isolates from 22Rv1, VCaP, LNCaP and DU-145 cells were prepared.

Real-time quantitative reverse-transcriptase polymerase chain reaction (RT-qPCR) assay was used for AR-V7 and AR-FL mRNA detection and quantification. Oligonucleotides used for the duplex one-step RT-qPCR as well as the cycling protocol were taken after the publication by Ma et al. 2016 and are presented in Appendix 3. The assay included primers and probes for simultaneous detection of both AR-V7 (FAM labelled probe) and AR-FL (HEX labelled probe). Primers and probes were synthesized by Eurofins MWG Synthesis GmbH (Ebersberg, Germany). 20 µl one-step RT-qPCR reaction mixtures were set up containing 10 µl iTaq Universal Probes One-Step Reaction Mix (Bio-Rad Laboratories Inc, Hercules, CA), 0,5 µl iScript™ reverse-transcriptase enzyme (Bio-Rad Laboratories Inc.), 500 nM of each forward and reverse primer, 250 nM of each probe and 2 µl of extracted mRNA sample, control DNA in known concentration or nuclease-free water for negative controls. Real-time detection of RT-qPCR reactions was performed in a 96-well plate using a CFX96 Real-Time System C1000 Thermal Cycler (Bio-Rad Laboratories Inc.). First, reverse transcription was performed at 50°C for 10 minutes. Then, amplification was performed at 95°C for 10 min, followed by 40 cycles at 95°C for 30 s and at 55°C for 60 s. Fluorescence detection was measured after every cycle.

Standard curves were generated according to the control DNA template dilution series (two replicates for each diluted concentration), and average concentrations of four replicates for each mRNA extract dilution were calculated using the Bio-Rad CFX Manager software and baseline threshold level of 50 RFU (relative fluorescence units). Then, concentration of each mRNA stock was calculated based on the average concentrations and dilution coefficients of 1:10, 1:100 and 1:1000 diluted samples (10, 100 and 1000, respectively). All of the RNA extracts were quantified against both the AR-V7 DNA (FAM detection) and the full-length AR DNA standard dilution series (HEX detection) to determine the expression ratios of AR-V7 and AR-FL mRNA. The RNA stocks were then further diluted to 10^4 copies/µl of AR-V7 and 10^4 copies/µl of AR-FL mRNA according to the quantification results, aliquoted and stored at -70 °C.

3.3 RT-SIBA assay development and optimization

Two functional Reverse Transcription Strand Invasion Based Amplification (RT-SIBA) assays were developed in this study. One was designed to detect the androgen receptor splice variant 7 (AR-V7) mRNA and the other the full-length androgen receptor (AR-FL) mRNA. The AR-V7 assay was the main assay to be used for the detection of AR-V7 in the mCRPC patients (Antonarakis et al. 2014), and the AR-FL assay was developed as a supporting assay to detect the presence of the transcript of wild type AR.

3.3.1 Assay design

Design of the SIBA assays included target sequence alignment analysis and design of the SIBA oligonucleotides. The target sequences for AR-V7 and AR-FL mRNA were retrieved from GenBank database (https://www.ncbi.nlm.nih.gov/genbank/, March 2018). The used target sequence for the AR-V7 located within the GenBank mRNA sequence NM_001348064.1, and the target for the full-length AR located within the GenBank mRNA sequence L29496.1. The RT-SIBA assays targeting the AR-V7 mRNA were designed to span the unique AR-V7 splice junction area located in between exon 3 (E3) and the splice variant specific cryptic exon 3 (CE3) within the AR intron 3 sequence (Luo 2016). The RT-SIBA assays targeting the full-length AR mRNA were designed to amplify the wild-type sequences within the AR exons 4 to 8. Locations of the AR exon sequences were retrieved from the Ensembl database (http://www.ensembl.org/index.html, May 2018, gene accession ID ENSG00000169083). The detection areas of the AR-V7 and AR-FL mRNA within the AR gene transcripts are visually represented in Figure 2.

SIBA oligonucleotide sequences, including one forward and one reverse primer and one invasion oligo (IO) per assay, were designed according to the protocol previously found to be optimal for specific SIBA-based target amplification presented by Hoser et al. (2014) and Eboigbodin et al. (2016). Oligonucleotides for a total of five AR-V7 assays and three AR-FL assays were designed and synthesized. Forward and reverse primers were synthesized and HPLC-purified by Eurofins MWG Synthesis GmbH (Ebersberg, Germany), and HPLC-purified invasion oligos were purchased from Integrated DNA Technologies GmbH (München-Flughafen, Germany).

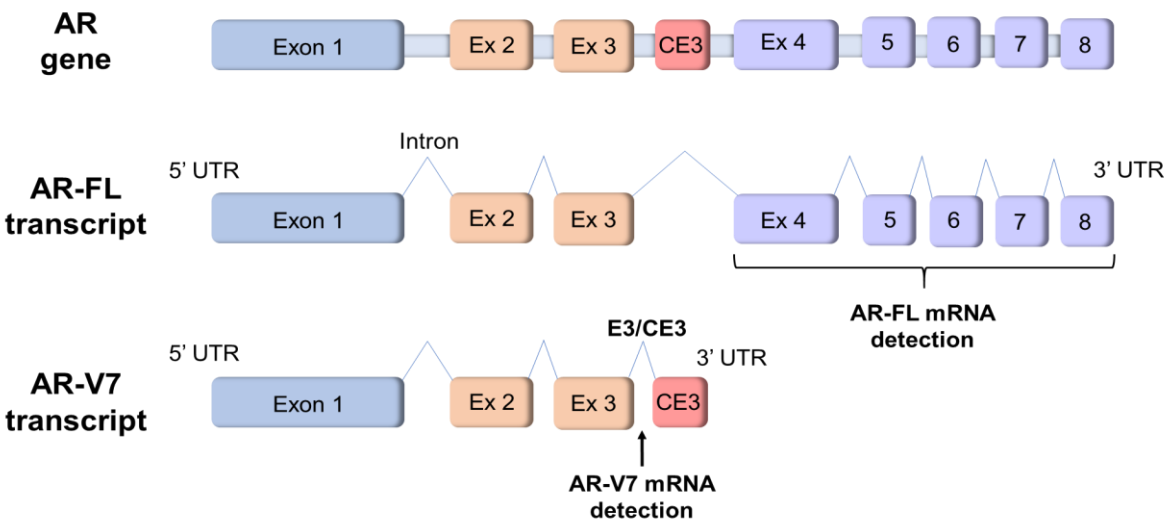

Figure 2. Visual representation of AR gene, AR-FL mRNA transcript and AR-V7 mRNA transcript structures. The designed AR-FL RT-SIBA assays targeted the mRNA sequences between exons 4 and 8 within the full-length AR transcript, and the AR-V7 RT-SIBA assays targeted the splice variant specific junction area between exon 3 and cryptic exon 3 mRNA sequence within the AR-V7 transcript. AR, androgen receptor; AR-FL, full-length androgen receptor; AR-V7, androgen receptor splice variant 7; UTR, untranslated region; E, exon; CE, cryptic exon. (Adapted from Figure 1, Nakazava et al. 2014 and Figure 1 A, Zhu et al. 2017.)

The designed AR-V7 RT-SIBA assays differed in the target sequence location around the E3/CE3 junction mRNA area, and the AR-FL assays differed in the target sequence location within the full-length AR exons; AR-FL assay 1 targeted the mRNA sequence flanking AR exons 4 and 5, assay 2 targeted the AR exon 4 sequence and assay 3 targeted the sequence flanking AR exons 7 and 8. Two of the AR-V7 assays (assay 4 and 5) were designed to amplify the reverse complement strand of the target area mRNA due to the lower content of guanines. This is because UvsX protein bind more efficiently to pyrimidines (Formosa & Alberts 1986). The 70–75 bp target sequences of each AR-V7 and AR-FL RT-SIBA assay are presented in Appendix 4.

Sets of 15 to 20 forward and reverse primer pairs in lengths between 16–21 bp were designed for each assay framing the assay target area. The primers differed in their lengths of homologous and non-homologous regions in relation to the IO sequence. IOs in lengths between 48–52 bp were designed to overlap both primers on the target sequence area. The non-homologous seeding region comprising of 10–12 nucleotides was added in the 5' end and 10–14 nucleotides of 2′-O-methyl RNA were added in the

3’ end of each designed IO. Secondary structures and oligo interactions were evaluated using the Oligo Analyzer 1.0.2 software (https://oligo-analyzer.software.informer.com/1.0).

3.3.2 Oligonucleotide screening

The SIBA assay development was initiated by screening through all the designed oligonucleotides and selecting the best primer pairs for specific and efficient amplification of the assay target sequences. RT-SIBA reactions were performed in 20 µl reaction volume, using the commercial SIBA reagent kit (Orion Diagnostica Oy, Espoo, Finland). The unoptimized RT-SIBA reaction conditions were used for the screening as follows: UvsX and Gp32 enzymes at 0,25 mg/ml concentrations, 0,1 x SYBR® Green I (Thermo Fisher Scientific, USA) and 8 units of GoScript™ Reverse Transcriptase (Promega Corporation, Madison, USA). Forward and reverse primers as well as IOs were each used at a final concentration of 200 nM, and the reactions were started using 10 mM magnesium acetate (Sigma-Aldrich, St. Louis, MO, USA). Real-time detection of RT-SIBA reactions was performed in a 96-well plate using a CFX96 Real-Time System C1000 Thermal Cycler (Bio-Rad Laboratories Inc, Hercules, CA). 60 cycles were run at a constant 41°C temperature for 60 seconds, and fluorescence readings were taken after each cycle. A melt curve analysis from 40°C to 95°C was run after the incubation for further evaluation of the reaction specificity.

First, all of the possible forward and reverse primer pairs of each assay were tested in the presence of the IO and without any template in the SIBA reaction. A minimum of two duplicate reactions were run per each primer pair combination. To develop a target-specific SIBA assay, primer pairs producing non-specific amplification due to oligonucleotide interactions during the 60 min run time were excluded from further experiments. Then, 2 µl of the synthetic AR-V7 and AR-FL DNA templates and extracted mRNA template from the 22Rv1 cell line in known copy number concentrations were used to assess the amplification efficacy of different primer pairs; primer pairs that amplified the correct target DNA or mRNA in the fastest reaction time, when comparing the cycle thresholds and melt temperatures, were selected for further assay optimization.

3.3.3 Selection of best assays

After the screening of the most optimal oligo combinations for each SIBA assay, one primer pair was selected for each assay, and performances of the five unoptimized assays targeting the AR-V7 mRNA were compared by adding 2 µl of the synthetic AR-V7 or AR-FL DNA template at 10^3 copies per reaction, or extracted AR-V7 mRNA template from the 22Rv1 cell line at 100 copies per reaction concentrations. The RT-SIBA reactions were set up as previously described (section 3.3.2.). The performance of the three assays targeting the AR-FL mRNA were also similarly compared and quantified 100 cp AR-FL mRNA isolate from 22Rv1 cells was used in addition to the DNA control templates. One out of five AR-V7 RT-SIBA assays and one out of three AR-FL RT-SIBA assays were selected for further optimization based on the template amplification specificity and efficacy. Oligonucleotide sequences as well as the amplicon lengths for each AR-V7 and AR-FL assay that were compared are listed in the Appendix 5.

3.3.4 Assay optimization

Since the optimal conditions and concentrations of recombinase and its cofactors used in SIBA differ depending on a target analyte seqience (Hoser et al. 2014), the reaction conditions of the SIBA assays developed for the detection of AR-V7 mRNA and AR-FL mRNA were briefly optimized. Optimization included titration of oligonucleotide concentrations, UvsX and Gp32 protein concentrations, reverse transcriptase concentration and magnesium acetate concentration in the reaction, and the determination of optimal reaction temperature.

To find optimal oligonucleotide concentrations for the AR-V7 and AR-FL RT-SIBA assays, 200 nM, 300 nM and 400 nM final concentrations of forward and reverse primers as well as the IO were tested in different combinations. Other RT-SIBA reaction conditions were the same as described in section 3.3.2. When the optimal oligonucleotide concentrations were found, concentrations of the UvsX and Gp32 enzymes were shortly titrated: 0,25 mg/ml, 0,35 mg/ml and 0,4 mg/ml final concentrations of both enzymes were compared for optimal assay performance. Since the titration of the oligonucleotide concentrations and UvsX and Gp32 enzyme concentrations were performed in several different experiments and separately for both AR-V7 and AR-FL RT-SIBA assays, experiment setups for these optimization experiments are not described here in more detail.

The optimized oligonucleotide concentrations as well as concentrations of Gp32 and UvsX proteins (see Table 9) were then compared to the original, unoptimized conditions (200 nM oligonucleotides and 0,25 mg/ml enzymes) by amplifying 100 copies of quantified AR-V7 mRNA isolated from 22Rv1 cells in the AR-V7 RT-SIBA assay and 100 copies of quantified AR-FL mRNA from 22Rv1 cells in the AR-FL assay. Four RNA replicates were tested at each condition, and four negative control reactions containing nuclease-free water were included per each reaction condition in order to evaluate the reaction specificity. 20 µl reaction volume and the commercial SIBA reagent kit (Orion Diagnostica Oy) were used as previously described, amplification was detected using 0,1 x SYBR® Green (Thermo Fisher Scientific), and the reactions were incubated for 60 minutes using a CFX96 Real-Time System C1000 Thermal Cycler (Bio-Rad Laboratories Inc). Fluorescence readings were taken at 60 second intervals and a melt curve analysis from 40°C to 95°C was run after the incubation for further evaluation of the reaction specificity.

The selected most optimal oligonucleotide concentrations and UvsX and Gp32 enzyme concentrations were used in the following RT-SIBA optimization. First, the concentrations of magnesium acetate (MgAc) and reverse transcriptase (RT) enzyme were titrated simultaneously for both developed AR-V7 and AR-FL assays. The RT-SIBA reactions were otherwise set up as previously described, and 41 °C incubation temperature and 60 min run time were used. MgAc (Sigma-Aldrich) was tested at final concentrations of 7,5 mM, 10 mM, 12,5 mM, 15 mM, 17,5 mM and 20 mM. The GoScript™ Reverse Transcriptase (Promega Corporation) was tested at 3 units, 8 units, 12 units and 16 units per reaction. 100 copies of AR-V7 and AR-FL mRNA from the 22Rv1 cells were used to assess the amplification efficacy of alternative reaction conditions in four replicate reactions, and four negative control reactions containing nuclease-free water were included. MgAc and RT enzyme concentrations that allowed rapid amplification of the target AR-V7 or AR-FL mRNA and did not produce any non-specific amplification, were selected for further RT-SIBA optimization experiments (see Table 9).

Optimal RT-SIBA reaction temperature was determined for efficient and specific oligonucleotide annealing and target sequence amplification using the thermal gradient feature of the CFX96 Real-Time System C1000 Thermal Cycler (Bio-Rad). Previously described RT-SIBA reaction conditions and a thermal gradient ranging from 41°C to 45°C were used. 100 copies of quantified AR-V7 and AR-FL mRNA extracted from the 22Rv1

cell line were amplified in the AR-V7 and AR-FL assays, respectively. Three replicate reactions containing template mRNA, and three negative control reactions were included at each temperature to evaluate the reaction efficiency and specificity. Finally, the optimized reaction conditions (magnesium acetate and reverse transcriptase concentrations as well as optimal incubation temperature, see Table 9) were compared with the original, unoptimized conditions (10 mM MgAc, 8 units of RT enzyme and 41°C incubation temperature).

3.4 Evaluation of the SIBA assay performance

To evaluate the performance of the two developed RT-SIBA assays for the detection of AR-V7 mRNA and AR-FL mRNA, three approaches were used: (1) analytical specificity determination using cell lines with known AR-V7 and full-length AR statuses, (2) analytical sensitivity and limit of detection determination using quantified target mRNA, and (3) exposal of the assays for liquid biopsy matrixes and determination of the matrix tolerance levels.

RT-SIBA reactions in total volume of 20 µl were set up as previously described and optimized reaction conditions (listed in Table 9) were used for the performance evaluation of both AR-V7 and AR-FL assays.

3.4.1 Analytical specificity

To determine the analytical specificity of the two developed RT-SIBA assays, *i.e.* the specific detection of the target mRNA sequence present in the sample (Bustin et al. 2009), 1 ng of each mRNA extract from four prostate cancer cell lines (22Rv1, LNCaP, VCaP and DU-145) with known AR-V7 and AR-FL status was added into RT-SIBA reaction and amplified with both AR-V7 and AR-FL assays. Four replicate reactions of each mRNA extract were tested with both assays. In addition, reactions containing either synthetic AR-V7 or AR-FL DNA at 10^3 copies per reaction were used as positive controls, and nuclease-free water as negative control.

3.4.2 Analytical sensitivity

Serial dilutions (1000, 500, 100, 50, 10, 5, 2.5 and 1 copy) of mRNA extracted from three known AR-V7 and AR-FL expressing prostate cancer cell lines (22Rv1, LNCaP and VCaP) were used for empirical determination of analytical sensitivity, *i.e.* the minimum copy number in a sample that can be accurately measured by the developed AR-V7 and AR-FL RT-SIBA assays (Bustin et al. 2009). Ten replicate reactions were run per each RNA concentration. Synthetic AR-V7 and AR-FL DNA templates were included as positive controls, and reactions containing nuclease-free water as negative controls.

Limits of detection, *i.e*. the lowest quantities of AR-V7 and AR-FL mRNA that can be consistently detected with 95% certainty by the developed RT-SIBA assays (Bustin et al. 2009), were calculated using the Probit regression analysis and the statistical MiniTab® 18 software (version 18.1.0, MiniTab Inc, State College, PA). The Probit analysis is commonly used for the determination of the lowest, reliably detectable analyte concentrations by molecular assays (Burd 2010). Normal distribution, confidence level of 95% and maximum likelihood as an estimation method were used. Since eight descending concentrations of AR-V7 and AR-FL mRNA and ten replicates of each concentration were used, there was a total of 80 data points. Detected and non-detected reactions acted as binomial response variables for the analysis: the number of positive reactions out of ten replicates was analyzed. Reaction was called as positive, if mRNA amplification was detected during the 60-minute run time, and negative, if no amplification occurred.

3.4.3 Assay tolerance of sample matrix

To evaluate the possible use of liquid biopsies in RT-SIBA reaction for the detection of molecular biomarkers, two liquid sample matrixes were tested: human whole blood and plasma. Low quantities (10 and 100 copies) of AR-V7 and AR-FL mRNA extracted from 22Rv1, VCaP and LNCaP cells were amplified with the AR-V7 and AR-FL RT-SIBA assays in the presence of various concentrations (0%, 1%, 2.5%, 5%, 7.5%, 10%, 12.5%, 15%, 17.5%, 20%, 22.5% and 25%) of plasma or whole blood per 20 µl reaction volume. The inhibitive effects of these liquid sample matrixes were observed by comparing mRNA amplification efficiency in relation to the sample matrix concentrations. Liquid biopsy concentration that did not remarkably weaken the amplification efficacy of AR-V7 and AR-FL mRNA in the RT-SIBA assays were considered to display tolerated

levels, while concentrations that considerably weakened the amplification efficiency, were considered as inhibitive.

After preliminary determination of possible inhibitive levels of the matrixes, 100 copies of AR-V7 mRNA from LNCaP cells were amplified in the AR-V7 assay in three replicate reactions, and 100 copies of AR-FL mRNA from LNCaP cells in the AR-FL assay in three replicate reactions, in the presence of lower concentrations (0%, 0.25%, 0.5%, 1%, 1.5%, 2%, 2.5%, 3%, 3.5%, 4%, 4.5% and 5%) of human plasma or whole blood per reaction volume, and the final tolerated levels of the matrixes were determined. Two replicates of negative controls containing nuclease-free water were included per each condition. Hence, the blood and plasma dilutions were also tested as such in the RT-SIBA assays, without added AR-V7 or AR-FL mRNA. Determined assay tolerance level of plasma was used for following testing of clinical prostate cancer plasma samples.

3.5 Testing of clinical samples

To shortly validate the practical performances of the developed mRNA-based AR-V7 and AR-FL RT-SIBA assays, four prostate cancer positive K2 EDTA plasma samples were tested with both assays. Each sample was tested in three forms: (1) exosomal RNA extract, (2) cell-free total mRNA extract and (3) diluted plasma sample without RNA extraction.

Exosomal RNA and total mRNA were previously extracted from the samples using two RNA isolation kits by Qiagen (Hilden, Germany): exoRNeasy and miRNeasy serum/plasma kits. 2 µl of each RNA extract was added into total volume of 20 µl RT-SIBA reaction, and previously described optimized reaction conditions (Table 9) were used. In addition, the four plasma samples were diluted 1:10 in nuclease-free water and 2 µl of each diluted sample was added into AR-V7 and AR-FL RT-SIBA reactions to acquire 1% plasma concentration per reaction. Two replicate reactions were run per each sample with both assays. Reactions containing either synthetic AR-V7 or AR-FL DNA at 10^3 copies per reaction were used as positive controls, and nuclease-free water as negative control.

To reliably examine the presence of AR-V7 or AR-FL mRNA in the clinical samples, identical 2 µl volume of each sample (exosomal RNA extract, mRNA extract and 1:10

plasma dilution) was also analyzed using the published RT-qPCR (described in section 3.2.3) in two replicate reactions. The same positive and negative controls were used as in the RT-SIBA runs.

4 Results

4.1 RNA extraction from PCa cell lines

The determined RNA concentrations as well as optical density ratios A_{260}/A_{280} ($OD_{A260/A280}$) of mRNA extracted from the prostate cancer positive cell lines are presented in Table 1. Mean values of the RNA yields ranged from 513,6 to 1719,1 ng/µl, indicating that the isolation was successful. Mean values of the optical density ratios A_{260}/A_{280} ranged from 2,03 to 2,07. The 260 nm / 280 nm ratio for pure RNA is around 2,0 (Gallagher 2017). Hence, the purity of each PCa cell mRNA isolate was satisfactory, and presumably no remarkable protein contamination remained.

Table 1. Determined RNA concentrations and optical density ratios for PCa cell line isolates. OD, optical density.

Cell line	Express	RNA concentration (ng/µl)	$OD_{A260/A280}$
22Rv1	AR-FL+ AR-V7+	911,6	2,03
DU-145	AR-FL- AR-V7-	1719,1	2,07
VCaP	AR-FL+ AR-V7+	513,6	2,05
LNCaP	AR-FL+ AR-V7+	581,2	2,04

4.2 RNA extraction from clinical samples

Determined RNA concentrations as well as optical density ratios A_{260}/A_{280} ($OD_{A260/A280}$) of exosomal RNA isolated with the exoRNeasy plasma kit (Qiagen) and cell-free total RNA isolated with the miRNeasy plasma kit (Qiagen) from the prostate cancer positive clinical plasma samples, are presented in Table 2. Mean values of the RNA yields ranged

from 5,1 to 34,8 ng/µl, which were quite low quantities. Mean values of the optical density ratios A_{260}/A_{280} ranged from 1,3 to 1,7.

Table 2. Determined RNA concentrations and optical density ratios for the clinical PCa plasma sample isolates. OD, optical density.

No.	Sample ID	Isolation kit	RNA concentration (ng/µl)	$OD_{A260/A280}$
1a	DLS17-049910-K2	exoRNeasy	16,1	1,5
1b	DLS17-049910-K2	miRNeasy	5,1	1,5
2a	DLS17-049930-K2	exoRNeasy	13,2	1,5
2b	DLS17-049930-K2	miRNeasy	13,6	1,3
3a	DLS17- 050017-K2	exoRNeasy	18,3	1,5
3b	DLS17- 050017-K2	miRNeasy	34,8	1,3
4a	DLS17- 050029-K2	exoRNeasy	20,0	1,6
4b	DLS17- 050029-K2	miRNeasy	38,7	1,7

The miRNeasy kit yielded in higher RNA concentrations than the exoRNeasy kit for three out of four samples. According to the kit manufacturer, the miRNAeasy plasma kit purifies all small cell-free total RNA from serum and plasma samples, and the exoRNeasy is designed for specific isolation of total vesicular RNA from serum or plasma. Thus, the amount of total RNA is likely higher in RNA samples extracted using the miRNeasy kit than in samples extracted using the exoRNeasy kit.

The purity levels between the two isolation methods were not considerably different. Although according to the A_{260}/A_{280} ratios, the purity of two RNA samples isolated using the exoRNeasy kit were slightly higher than those extracted with the miRNeasy kit. Furthermore, one plasma sample extracted using the miRNeasy kit resulted in higher A_{260}/A_{280} ratio.

The low $OD_{A260/280}$ ratios indicate poor nucleic acid purity levels, as proteins have a peak absorbance at 280 nm, which reduces the A_{260}/A_{280} ratio (Gallagher 2017). The A_{260}/A_{280} ratios below 2.0 suggest that the samples likely had residual protein contamination after the exosomal RNA and total cell-free RNA isolations. Alternatively, the use of the optical density ratios for the RNA quality assessment could be omitted from the result analysis, as the quantities of the plasma RNA isolates were that low, and the RNA quality estimate is not very reliable here (Bustin et al. 2009).

4.3 PCR quantification of mRNA extracted from PCa cell lines

AR-V7 RT-qPCR primers and the FAM-labelled probe produced some late unintended amplification products after 37 PCR amplification cycles, when 50 RFU (relative fluorescence units) was used as a threshold. This was presumably due to primer dimers. The produced primer dimers were identified when the negative control reactions as well as other reactions negative for AR-V7 had similar C_q (quantification cycle) values. When calculating the quantities of AR-V7 mRNA, reactions having C_q values above 37 were considered as AR-V7 negative to exclude the false-positive amplification. The AR-FL primers and probe labelled with HEX did not produce any non-specific amplification, and there was no need for data rejection when examining the AR-FL amplification.

The qRT-PCR assay was specific to the detection of AR-V7 and AR-FL, since the AR-V7 probe did not detect the AR-FL DNA template, and vice versa the AR-FL probe did not detect the AR-V7 DNA. The RT-qPCR assay was able to detect 1 copy of both AR-V7 and AR DNA template. Amplification curves of serially diluted synthetic AR-V7 DNA template are presented in Figure 3A, and the standard curve constructed from these dilutions by plotting the log of the template starting quantity against the C_q value, is presented in Figure 3B. Amplification efficiency (E) of the AR-V7 control DNA was 116,8%, which is above the optimum range. This is most likely to be due to the produced primer-dimers or pipetting errors (Taylor et al. 2010). To increase the efficiency, the lowest DNA concentration (10^0 copies/µl) could have been left out of the standard curve data. However, the correlation coefficient (R^2) value of 0,986 was acceptable and indicated, that the standard curve data was linear, and the efficiency was similar for each control template dilution replicate.

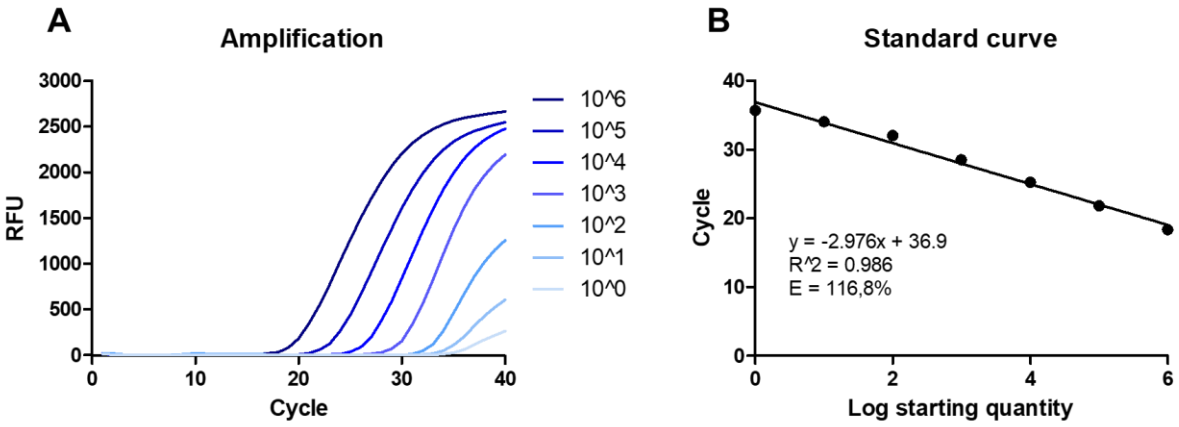

Figure 3A. RT-qPCR amplification curves of serial diluted synthetic AR-V7 DNA control template in concentrations 10^6, 10^5, 10^4, 10^3, 10^2, 10^1 and 10^0 copies per µl. RFU, relative fluorescent units. **Figure 3B.** Standard curve constructed from the serial dilutions of AR-V7 control DNA. E, amplification efficiency; R^2, correlation coefficient.

Amplification curves of serially diluted synthetic AR-FL DNA template are presented in Figure 4A, and the standard curve for AR-FL template dilutions is presented in Figure 4B. Amplification efficiency of the AR-FL control DNA was very optimal, 98,4%, and was an indicator of a robust assay (Taylor et al. 2010). The correlation coefficient value for AR-FL standard curve was also slightly better than that for the AR-V7 standard curve (0,995 vs. 0,986) and indicated high data linearity.

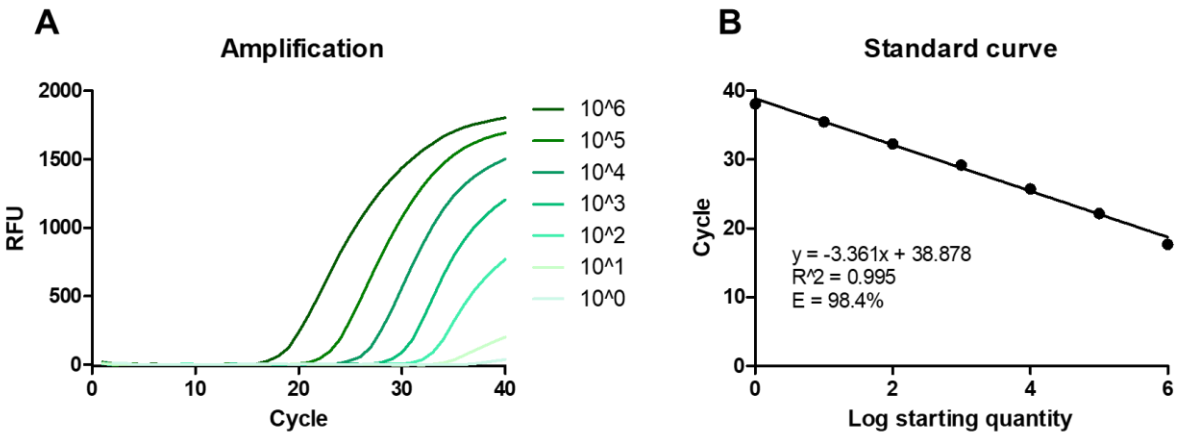

Figure 4A. RT-qPCR amplification curves of serial diluted synthetic AR-FL DNA control template in concentrations 10^6, 10^5, 10^4, 10^3, 10^2, 10^1 and 10^0 copies per µl. RFU, relative fluorescent units. **Figure 4B.** Standard curve constructed from the serial dilutions of AR-FL control DNA. E, amplification efficiency; R^2, correlation coefficient.

The average starting quantitity (SQ) of each RNA isolate dilution was calculated according to the constructed standard curves. Both AR-V7 and AR-FL mRNA quantities of the original mRNA isolate stocks were then calculated. The quantification data of the mRNA isolate stocks is presented in Table 3. 22Rv1, VCaP and LNCaP cell isolates were all positive for both AR-V7 and AR-FL mRNA, and DU-145 was negative for both AR-V7 and AR-FL mRNA, as expected (Wadowsky & Koochekpour 2017). Each AR-V7 and AR-FL positive PCa cell isolate had higher copy number of AR-FL mRNA than AR-V7 mRNA, which is also in line with earlier studies (Hu et al. 2009).

Table 3. Quantification results of mRNA isolates from PCa positive cells. SQ, starting quantity; N/D, no data.

	RNA isolate dilution	SQ mean (copies/µl)	Dilution coefficient	Stock conc.	Mean stock conc. (copies/µl)
22Rv1: AR-V7 mRNA	1:10	$9{,}3 \times 10^4$	10	$9{,}3 \times 10^5$	**$6{,}3 \times 10^5$**
	1:100	$5{,}7 \times 10^3$	100	$5{,}7 \times 10^5$	
	1:1000	$3{,}7 \times 10^2$	1000	$3{,}7 \times 10^5$	
22Rv1: AR-FL mRNA	1:10	$1{,}8 \times 10^5$	10	$1{,}8 \times 10^6$	**$1{,}5 \times 10^6$**
	1:100	$1{,}4 \times 10^4$	100	$1{,}5 \times 10^6$	
	1:1000	$1{,}3 \times 10^3$	1000	$1{,}3 \times 10^6$	
DU-145: AR-V7 mRNA	1:10	N/D	10	N/D	**0,0**
	1:100	N/D	100	N/D	
	1:1000	N/D	1000	N/D	
DU-145: AR-FL mRNA	1:10	N/D	10	N/D	**0,0**
	1:100	N/D	100	N/D	
	1:1000	N/D	1000	N/D	
VCaP: AR-V7 mRNA	1:10	$1{,}3 \times 10^5$	10	$1{,}4 \times 10^6$	**$8{,}9 \times 10^5$**
	1:100	$8{,}3 \times 10^3$	100	$8{,}4 \times 10^5$	
	1:1000	$4{,}7 \times 10^2$	1000	$4{,}8 \times 10^5$	
VCaP: AR-FL mRNA	1:10	$1{,}4 \times 10^6$	10	$1{,}4 \times 10^7$	**$1{,}1 \times 10^7$**
	1:100	$1{,}1 \times 10^5$	100	$1{,}1 \times 10^7$	
	1:1000	$8{,}6 \times 10^3$	1000	$8{,}6 \times 10^6$	
LNCaP: AR-V7 mRNA	1:10	$1{,}1 \times 10^3$	10	$1{,}1 \times 10^4$	**$7{,}7 \times 10^3$**
	1:100	$7{,}5 \times 10^1$	100	$7{,}5 \times 10^3$	
	1:1000	$4{,}3 \times 10^0$	1000	$4{,}3 \times 10^3$	
LNCaP: AR-FL mRNA	1:10	$2{,}1 \times 10^5$	10	$2{,}1 \times 10^6$	**$1{,}9 \times 10^6$**
	1:100	$2{,}1 \times 10^4$	100	$2{,}1 \times 10^6$	
	1:1000	$1{,}6 \times 10^3$	1000	$1{,}6 \times 10^6$	

The copy numbers per microliter of mRNA isolate were then converted into RNA copies per nanogram using the previously determined RNA concentration data (Table 1) to compare the expression levels in PCa cell lines. The AR-V7 and AR-FL copy numbers per one nanogram of mRNA isolate as well as the relation of AR-V7 and AR-FL mRNA are presented in Table 4. Consistent to previous studies (Hu et al. 2009; Ma et al. 2016), the VCaP cells expressed the highest levels of both AR-FL and AR-V7, 22Rv1 cells the

second highest level of AR-V7 and the LNCaP cells expressed the lowest level of AR-V7. The VCaP cells expressed higher level of AR-FL than the LNCaP cells as previously demonstrated by Makkonen et al. (2010). The ratios of expressed AR-V7 and AR-FL RNA in the three AR-V7 positive PCa cell lines were considerably in line with the study by Ma et al. (2016): when measured in percentages, the AR-V7/AR-FL ratio for 22Rv1 was now 40,8%, whereas previously measured it was 26%, the ratio for VCaP was now 8% and previously 1,3%, and the ratio for LNCaP was now 0,4% whereas previously measured 0,9 %. The differences in the ratios between the two studies can be explained by different analysis methods, since the previous study utilized droplet digital PCR (ddPCR) for determination of the exact AR-V7 and AR-FL mRNA copy numbers in exosomes of PCa cells. Furthermore, the cultivation method could also account for these differences.

Table 4. AR-V7 and AR-FL RNA quantities of PCa positive cell isolates. Copies/ng were calculated from copies/µl and ng/µl RNA concentration data. N/D, no data.

Cell line	AR-V7 copies/ng	AR-FL copies/ng	AR-V7 / AR-FL (%)
22Rv1	$6{,}9 \times 10^2$	$1{,}7 \times 10^3$	40,8
DU-145	0,0	0,0	N/D
VCaP	$1{,}7 \times 10^3$	$2{,}2 \times 10^4$	8,0
LNCaP	$1{,}3 \times 10^1$	$3{,}3 \times 10^3$	0,4

Expression levels of AR-V7 and AR-FL mRNA within the PCa cell lines according to the RT-qPCR quantification are presented simplified in Table 5.

Table 5. Simplified representation of AR-V7 and AR-FL mRNA expression levels in PCa cell lines according to the RT-qPCR quantification. +, positive expression; -, no expression.

	AR-V7 expression	AR-FL expression
22Rv1	**++**	**++**
DU-145	**-**	**-**
VCaP	**++**	**+++**
LNCaP	**+**	**++**

4.4 SIBA assay development and optimization

4.4.1 Oligonucleotide screening and selection of best assays

After several oligonucleotide screening experiments (results not presented), a single primer and IO triplet was selected for each of the five AR-V7 and three AR-FL assays based on their performance: the selected oligonucleotides produced the most specific amplicons in the shortest reaction time (Appendix 5).

When selecting the most optimal SIBA assays for the detection of AR-V7 and AR-FL RNA, the assay specificity was considered as the most important feature; assays producing non-specific amplicons with differing melt temperatures were excluded. Detection time and melt temperature (T_m) data of AR-V7 mRNA isolate from 22Rv1 cells, positive DNA controls and negative water controls amplified with the five AR-V7 RT-SIBA assays are presented in Table 6. The amplification is expressed as the average detection time of four replicate reactions, using a threshold level of 20 RFU. Since the protocol cycling, 60 × 60 s cycles, equates a 60-minute run, the detection times are presented as minutes.

Table 6. Average detection time and melt temperature (T_m) comparison of 100 AR-V7 mRNA copies from 22Rv1 cells, AR-V7 and AR-FL DNA controls and negative controls for five different AR-V7 RT-SIBA assays. AR-V7 assay 5 was the only assay, that amplified specifically the correct target mRNA. N/D, no data (negative reaction); cp, copies. Number of positive replicate reactions accounting for the average detection times is marked in brackets, if differing from 4/4 positive replicate reactions.

	100 cp AR-V7 mRNA		10^3 cp AR-V7 DNA		10^3 cp AR-FL DNA		Negative control	
	Detection (min)	T_m (°C)	Detection (min)	T_m (°C)	Detection (min)	T_m (°C)	Detection (min)	T_m (°C)
AR-V7 assay 1	28,2	73	29,2	73	38,4 (1/4)	72,5	44,3 (1/4)	72,5
AR-V7 assay 2	20,4	72,5	18,9	72,5	45,9 (3/4)	73,5	49,8 (3/4)	73
AR-V7 assay 3	20,5	73	19,9	73	33	73	24,8	73
AR-V7 assay 4	14,1	73	14,3	73	18,6	75	17,5	75
AR-V7 assay 5	28,9	72	28,4	72	N/D	N/D	N/D	N/D

When the five AR-V7 targeting RT-SIBA assays were compared, the AR-V7 assay 5 was the most specific to the target region. The assay 5 amplified the target AR-V7 mRNA and

DNA relatively late (within 29 minutes), but assays that amplified the target AR-V7 RNA and DNA most efficiently, also tended to produce non-specific amplification. Four out of five assays produced non-specific amplicons during the 60-minute incubation; assays 1–4 not only amplified the AR-V7 mRNA and control DNA templates, but also showed positive reactions for the AR-FL DNA and water controls. The non-specific amplicons were detected later, within 38–50 minutes by the AR-V7 assays 1 and 2, but quite rapidly by the AR-V7 assays 3 and 4 (within 24–33 and 18 minutes, respectively).

When the melt temperatures of AR-V7 amplicons were compared, the AR-V7 assay 5 had the lowest T_m: 72 °C. This is most likely due to the amplicon size, since the amplicon of assay 5 is only 66 bp in length, whereas other assays have amplicons in length of 68–69 bp, and longer templates require higher temperature to melt (Ririe et al. 1997). The only assay, that distinguished the specific and non-specific amplicons by T_m, was AR-V7 assay 4: T_m of AR-V7 amplicons was 73°C whereas T_m of negative control and AR-FL DNA template was 75°C. This was unexpected, since non-specific products are usually short and have lower T_m than the target products, at least when PCR amplification products are in question (Ririe et al. 1997).

The AR-V7 assay 5 showed high preliminary specificity for the AR-V7, since the negative control reactions as well as reactions containing the AR-FL control DNA template remained negative during the 60-minute RT-SIBA run, and no melting peak was observed for other than the desired amplification products. The AR-V7 assay 5 was selected out of the five AR-V7 targeting RT-SIBA assays for further optimization.

Detection time and melt temperature (T_m) data of AR-FL mRNA isolate from 22Rv1 cells, positive DNA controls and negative water controls amplified with the three AR-FL RT-SIBA assays are presented in Table 7. When the three AR-FL targeting RT-SIBA assays were compared, the AR-FL assay 2 performed the best: 100 copies of quantified AR-FL mRNA isolate from 22Rv1 cells amplified within 18,5 minutes, whereas with other assays the mRNA amplified right before 33 minutes. The AR-FL assays 2 and 3 were highly specific to the detection of AR-FL, since the negative control reactions and reactions containing the AR-V7 control DNA template remained negative during the 60-minute RT-SIBA run.

Table 7. Average detection time and melt temperature (T_m) comparison of 100 AR-FL mRNA copies from 22Rv1 cells, AR-V7 and AR-FL DNA controls and negative controls for three different AR-FL RT-SIBA assays. AR-FL assays 2 and 3 did not produce unintended amplicons. N/D, no data (negative reaction); cp, copies. Number of positive replicate reactions accounting for the average detection times is marked in brackets, if differing from 4/4 positive replicate reactions.

	100 cp AR-FL mRNA		10^3 cp AR-V7 DNA		10^3 cp AR-FL DNA		Negative control	
	Detection (min)	T_m (°C)	Detection (min)	T_m (°C)	Detection (min)	T_m (°C)	Detection (min)	T_m (°C)
AR-FL assay 1	32,9	77	29,6 (1/4)	76,5	28,4	77	41,3 (1/4)	77
AR-FL assay 2	18,5	73,5	N/D	N/D	14,6	73,5	N/D	N/D
AR-FL assay 3	32,5	73	N/D	N/D	22	74	N/D	N/D

The differences between the melt temperatures for the AR-FL amplicons between the different assays could again be explained by the amplicon length: AR-FL assay 1 amplified AR-FL sequence in length of 69 base pairs and had the highest T_m, 77°C, whereas the assays 2 and 3 had shorter amplicons (64 bp and 63 bp) as well as lower melt temperatures (73-74 °C).

According to the results of this experiment, the AR-FL assay 2 was the most optimal for amplification of AR-FL target mRNA. However, later optimization experiments (data not presented) showed evidence, that the AR-FL assay 3 was more robust than the assay 2, when comparing assay specificities. The AR-FL RT-SIBA assay 2 targeted only one exon, the full-length androgen receptor exon 4, whereas all other assays targeted two exons. When designing RT-PCR assays, it is recommended for PCR primers to bind to separate exons to avoid false positive results and contamination caused by the amplification of genomic DNA (Bustin 2000). Even though the design of isothermal nucleic acid amplification assays differs from RT-qPCR assays, this might have been one reason, why the AR-FL assay 2 might not have been optimal for the detection of full-length AR. Out of the three AR-FL targeting RT-SIBA assays, AR-FL assay 3 was selected for further optimization.

The selected oligonucleotides for both RT-SIBA assays are listed in Table 8, and the hybridization of the oligonucleotides is illustrated in Figure 5. Henceforth, the AR-V7 assay 5 is called AR-V7 RT-SIBA assay, and the AR-FL assay 3 is called AR-FL RT-SIBA assay.

Table 8. Selected oligonucleotides for the RT-SIBA assays targeting AR-V7 and AR-FL mRNA.

RT-SIBA assay	Oligocucleotide name	Sequence (5'→3')
AR-V7 assay 5	AR-V7 forward	CAATTGCCAACCCGGAA
	AR-V7 reverse	TTGTCGTCTTCGGAAAT
	AR-V7 IO	CCCCCCCCCCCCAATTTTTCTCCCAGAGTCATCCCTGCTT mCmAmUmAmAmCmAmUmUmUmC
AR-FL assay 3	AR-FL forward	GTGCAGCCTATTGCG
	AR-FL reverse	CATGTGTGACTTGATTA
	AR-FL IO	CCCCCCCCCCCGAGAGAGCTGCATCAGTTCACTTTTG mACmCmUmGmCmUmAmAmUmC

A

```
5'-CAATTGCCAACCCGGAATTTTTCTCCCAGAGTCATCCCTGCTTCATAACATTTCCGAAGACGACAA-3'
   ||||||||||||||||||||||||||||||||||||||||||||||||||||||||||||||||||||
3'-GTTAACGGTTGGGCCTTAAAAAGAGGGTCTCAGTAGGGACGAAGTATTGTAAAGGCTTCTGCTGTT-5'
```

B

```
5'-GTGCAGCCTATTGCGAGAGAGCTGCATCAGTTCACTTTTGACCTGCTAATCAAGTCACACATG-3'
    ||||||||||||||||||||||||||||||||||||||||||||||||||||||||||||||||||||
3'-CACGTCGGATAACGCTCTCTCGACGTAGTCAAGTGAAAACTGGACGATTAGTTCAGTGTGTAC-5'
```

Figure 5A. Hybridization of AR-V7 RT-SIBA oligonucleotides to the target AR-V7 mRNA sequence. **Figure 5B.** Hybridization of AR-FL RT-SIBA oligonucleotides to the target AR-FL mRNA sequence. Forward primers are marked with red, reverse primers with light blue and IO sequences are underlined**.**

4.4.2 Assay optimization

The performance of optimized oligonucleotide concentrations as well as UvsX and Gp32 enzyme concentrations compared to the unoptimized conditions (200 nM oligonucleotide concentration and 0,25 mg/ml enzyme concentration) are presented in Figure 6, where the average detection times of 100 copies of AR-V7 mRNA isolate from 22Rv1 cells in the optimized versus unoptimized AR-V7 RT-SIBA assay, and 100 copies of AR-FL mRNA from 22Rv1 cells in AR-FL assay are described. All the negative control reactions remained negative and thus are not presented in the figure. For the optimized AR-V7 assay, forward primer was used at final concentration of 300 nM, reverse primer at 200 nM and IO at 300 nM. For the AR-FL assay, forward primer was used at final concentration of 400 nM, and both the reverse primer and IO at 300 nM. Optimized 0,4

mg/ml final concentration of both UvsX and Gp32 was used for the AR-V7 assay, and 0,35 mg/ml for the AR-FL assay.

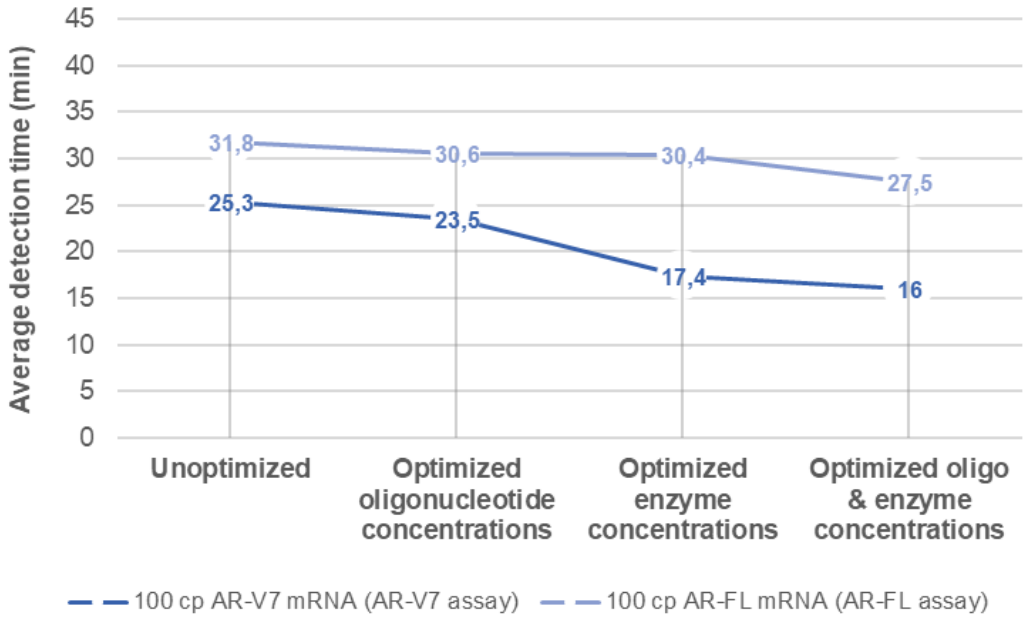

Figure 6. Average detection time comparison of 100 AR-V7 mRNA copies from 22Rv1 cells for the AR-V7 RT-SIBA assay, and 100 AR-FL mRNA copies for the AR-FL assay using unoptimized reaction conditions (200 nM oligonucleotide concentration and 0,25 mg/ml UvsX and Gp32 enzyme concentration) versus altered, optimized reaction conditions (oligonucleotide and enzyme concentrations). Optimized oligonucleotide concentrations for the AR-V7 assay: 300 nM forward primer, 200 nM reverse primer and 300 nM IO. Optimized enzyme concentration for the AR-V7 assay: 0,4 mg/ml. Optimized oligonucleotide concentrations for the AR-FL assay: 400 nM forward primer, 300 nM reverse primer and 300 nM IO. Difference between the optimized and unoptimized conditions was 9,3 minutes for the AR-V7 assay, and 4,3 minutes for the AR-FL assay. Optimized enzyme concentration for the AR-V7 assay: 0,35 mg/ml. Cp, copies.

Optimization of the oligonucleotide concentrations of AR-V7 assay improved the amplification efficacy of 100 copies of AR-V7 mRNA by 1,8 minutes, and optimization of UvsX and Gp32 enzyme concentrations improved the amplification efficacy by 7,9 minutes. Since UvsX and Gp32 act as recombinant proteins responsible for the target duplex invasion in the SIBA reaction (Hoser et al. 2014), the optimal concentration of these proteins can have a considerable effect on the amplification efficiency. When both optimized conditions, oligonucleotide and enzyme concentrations, were compared to the original conditions, 100 AR-V7 copies were detected on average 9,3 minutes faster, which accounts for 36,6% improvement in the detection time.

Optimization of the oligonucleotide concentrations of AR-FL assay improved the amplification efficacy of 100 copies of AR-FL mRNA extract from 22Rv1 cells by 1,2 minutes, and optimization of UvsX and Gp32 enzyme concentrations by 1,4 minutes. When both optimized conditions were compared to the original conditions, 100 AR-FL copies were detected on average 4,3 minutes faster, accounting for 13,5% improvement. The results suggest, that the RT-SIBA reaction efficacy can be notably improved by discovering the optimal oligonucleotide and enzyme concentrations. However, the improvement in the detection time was more remarkable for the optimized AR-V7 assay than for the AR-FL assay. Amplification curves of 100 copies AR-V7 mRNA isolate in optimized versus unoptimized AR-V7 RT-SIBA conditions are presented in Figure 7A, and 100 copies AR-FL mRNA isolate in optimized versus unoptimized AR-FL reaction conditions are presented in Figure 7B. In addition to the improved detection time, also the signal levels of the amplification curves were higher at the optimized conditions.

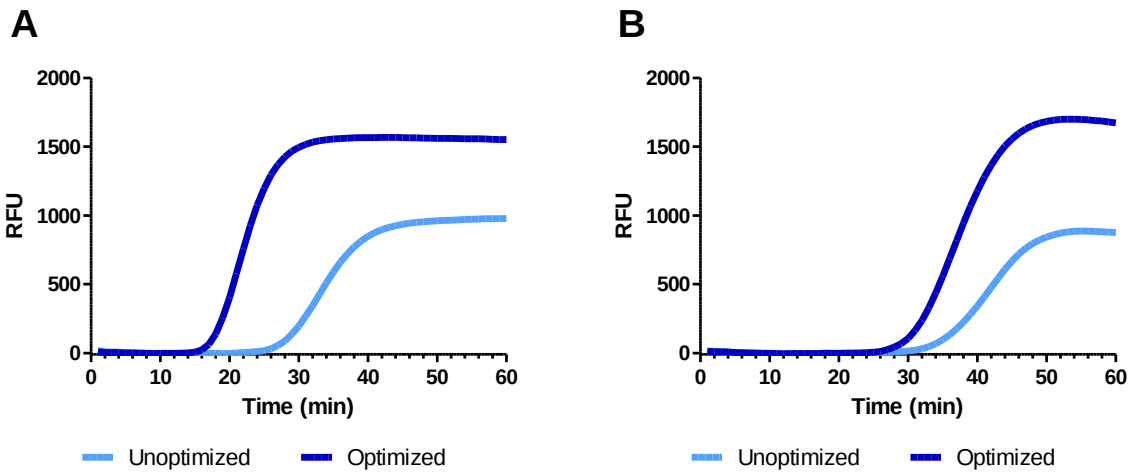

Figure 7A. Amplification curves for 100 copies of AR-V7 mRNA in unoptimized (200 nM oligonucleotide concentration and 0,25 mg/ml UvsX and Gp32 enzyme concentration) versus optimized AR-V7 RT-SIBA reaction conditions (300 nM forward primer, 200 nM reverse primer and 300 nM IO, 0,4 mg/ml UvsX and Gp32 enzyme concentration). **Figure 7B**. Amplification curves for 100 copies of AR-FL mRNA in unoptimized (200 nM oligonucleotide concentration and 0,25 mg/ml UvsX and Gp32 enzyme concentration) versus optimized AR-FL RT-SIBA reaction conditions (400 nM forward primer, 300 nM reverse primer and 300 nM IO, 0,35 mg/ml UvsX and Gp32 enzyme concentration). RFU, relative fluorescence units.

Optimization of the magnesium acetate (MgAc) concentration was performed simultaneously with optimization of the reverse-transcriptase (RT) enzyme concentration. Magnesium acetate plays a role in the SIBA reaction energy generating system (Hoser et al. 2014). Some alternative conditions of MgAc and RT concentrations produced some random, non-specific amplification during the 60-minute RT-SIBA

reactions in both AR-V7 and AR-FL assays. This demonstrated the importance of optimal conditions for the SIBA reaction components to function correctly.

Detection times of 100 copies of AR-V7 mRNA isolate from the 22Rv1 cells using alternative MgAc and RT enzyme conditions for the AR-V7 assay are presented in Figure 8. 10 mM MgAc concentration and 16 units of RT enzyme per reaction were selected to be used for the AR-V7 assay, because no false-positive amplification of the negative controls occurred, and the detection time of 100 AR-V7 mRNA copies was the shortest (20 minutes) when using these conditions. Altered, higher and lower concentrations of MgAc inhibited the amplification of AR-V7 mRNA. The differences between the different RT enzyme conditions were not remarkable, and the highest 16 U concentration was selected due to the lack of false-positive amplification of negative controls.

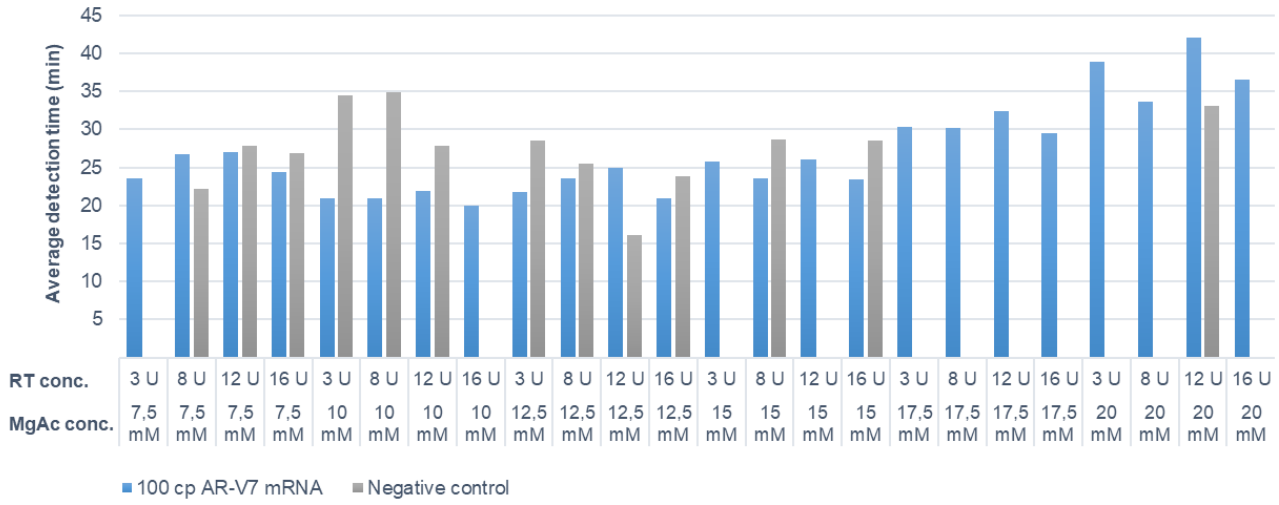

Figure 8. Average detection time comparison of 100 AR-V7 mRNA copies from 22Rv1 cells and negative controls using alternative magnesium acetate (MgAc) and reverse-transcriptase (RT) enzyme concentrations for the AR-V7 RT-SIBA assay. 10 mM MgAc and 16 U RT enzyme concentration were selected to be used as the optimized assay conditions. Cp, copies.

Detection times of 100 copies of AR-FL mRNA isolate from the 22Rv1 cells using alternative MgAc and RT enzyme conditions for the AR-FL assay are presented in Figure 9. The most optimal conditions for the AR-FL RT-SIBA assay were 15 mM MgAc and 16 U RT enzyme, since the detection time of 100 cp AR-FL mRNA was the shortest (21 min) and no unintended amplicons were produced. However, though higher

concentrations of MgAc (12,5 mM and 15 mM) would have improved the amplification efficacy of AR-FL mRNA, the same 10 mM MgAc concentration was selected to be used for both assays due to practical, experimental reasons: all the reactions could be started using the same MgAc aliquot. The highest 16 U RT concentration was clearly the most optimal, since detection times of the AR-FL mRNA template were the shortest when compared to lower RT concentrations. The lowest 7,5 mM and the highest 20 mM concentrations of MgAc inhibited the RT-SIBA reaction efficacy nearly by 9 minutes, when compared to the most optimal 15 mM concentration.

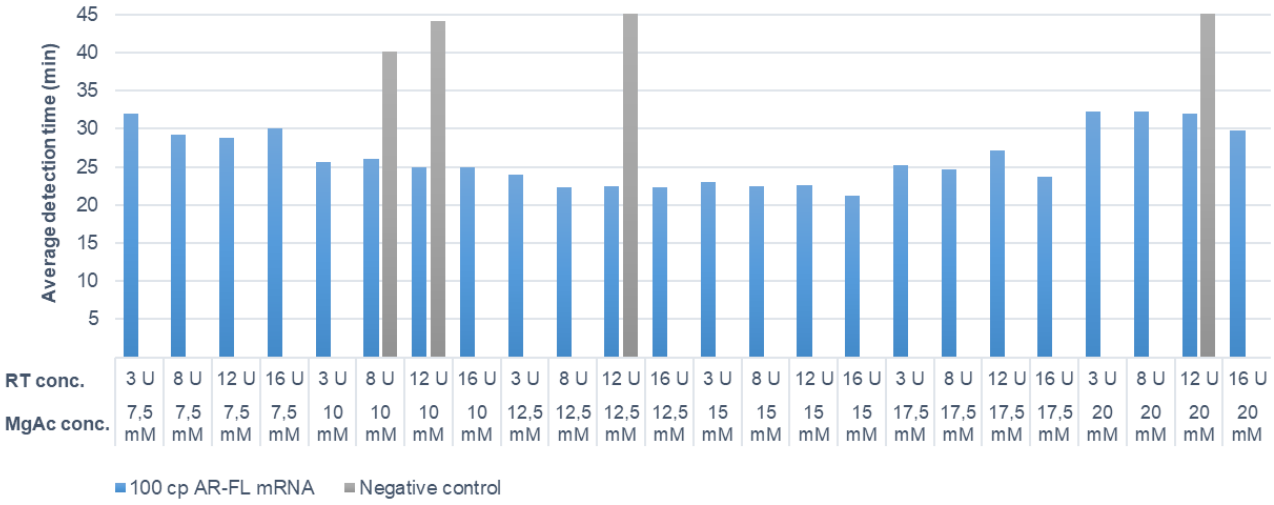

Figure 9. Average detection time comparison of 100 AR-FL mRNA copies from 22Rv1 cells and negative controls using alternative magnesium acetate (MgAc) and reverse-transcriptase (RT) enzyme concentrations for the AR-FL RT-SIBA assay. 10 mM MgAc and 16 U RT enzyme concentration were selected to be used as the optimized assay conditions. Cp, copies.

Temperature gradient ranging from 41–45°C was used for the determination of optimal RT-SIBA incubation temperature for both AR-V7 and AR-FL RT-SIBA assays. The results of reaction temperature optimization are presented in Figure 10. The optimal temperatures for the two assays did slightly differ, since increased temperatures between 42,6–45°C were more optimal for the AR-V7 assay, and increased temperatures between 41,8–44,3°C for the AR-FL assay, when compared to the original 41°C incubation temperature. 100 copies of AR-V7 mRNA amplified the fastest at 44,8°C (12,2 min) with the AR-V7 assay, and 100 copies of AR-FL mRNA amplified the fastest at 43,5°C (17,5 min) with the AR-FL assay. Even though the average detection times were shorter at higher temperatures for the AR-V7 assay, the signal (RFU) levels slightly

decreased, when the temperature got above 44,3°C. All the negative control reactions remained negative at all temperatures during the 60-minute SIBA run, and thus are not presented in the result chart.

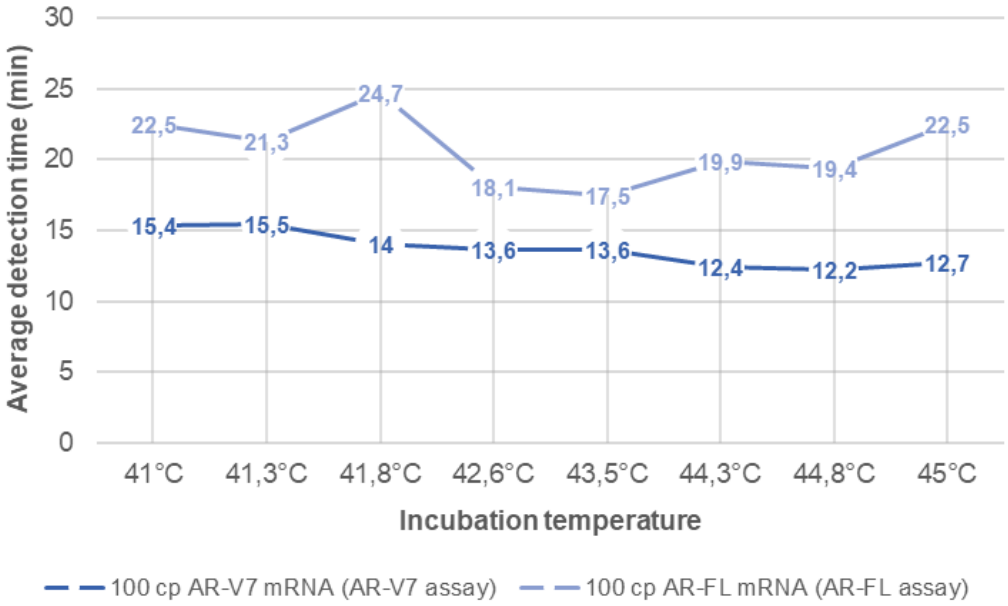

Figure 10. Average detection time comparison of 100 AR-V7 mRNA copies from 22Rv1 cells for the AR-V7 RT-SIBA assay, and 100 AR-FL mRNA copies for the AR-FL assay using alternative incubation temperatures. 43,5°C was selected to be used as optimized incubation temperature for both assays. Cp, copies.

For practical and experimental reasons, same incubation temperature was selected to be used for both AR-V7 and AR-FL RT-SIBA assays: 43,5°C. The chosen temperature was within the optimal temperature range for both assays. The optimized conditions of both AR-V7 and AR-FL assays are compared to unoptimized conditions in Figure 10, where RT-SIBA amplification curves of quantified 100 AR-V7 mRNA (Figure 11A) or AR-FL mRNA (Figure 11B) are presented. Optimization of the RT-SIBA conditions cut down the detection time of AR-V7 mRNA by 2,7 minutes, which accounts for 16,6% improvement, and the AR-FL mRNA by 9,4 minutes, accounting for 34,9% improvement. Whereas the optimization of oligonucleotide and enzyme concentrations had a more intense effect on the AR-V7 assay performance, optimization of RT enzyme concentration and incubation temperature improved the performance of AR-FL assay considerably. In addition, the signal (RFU) levels of amplification curves were increased at the optimized conditions for both assays. All the negative control reactions remained negative during the 60-minute SIBA run, and thus their amplification curves are not presented.

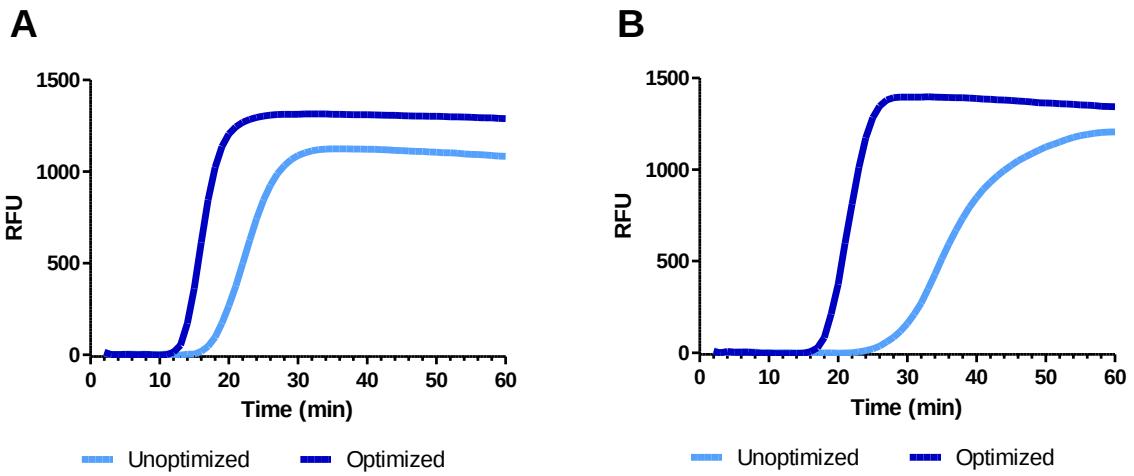

Figure 11A. RT-SIBA amplification curves for 100 cp AR-V7 mRNA from 22Rv1 cells using optimized (10 mM MgAc, 8 U RT, incubation at 41°C) and unoptimized reaction conditions (10 mM MgAc, 16 U RT, incubation at 43,5°C) for the AR-V7 assay. Difference between the average detection times of optimized and unoptimized conditions was 2,7 minutes. **Figure 11B**: RT-SIBA amplification curves for 100 cp AR-FL mRNA from 22Rv1 cells using optimized (10 mM MgAc, 8 U RT, incubation at 41°C) and unoptimized reaction conditions (10 mM MgAc, 16 U RT, incubation at 43,5°C) for the AR-FL assay. Difference between the average detection times of optimized and unoptimized conditions was 9,4 minutes. RFU, relative fluorescence units.

Final, optimized reaction conditions for both developed assays are described in Table 9. For the AR-V7 assay, the forward primer is used at the final concentration of 300 nM, the reverse primer at 200 nM and the IO at 300 nM, and the forward primer at 400 nM, reverse primer at 300 nM and IO at 300 nM for the AR-FL assay; 0,4 mg/ml final concentration of both UvsX and Gp32 enzymes for the AR-V7 assay, and 0,35 mg/ml enzymes for the AR-FL assay; 16 units of reverse transcriptase enzyme and 10 mM magnesium acetate per reaction for both assays; incubation of RT-SIBA reactions at 43,5 °C.

Table 9. Optimized reaction conditions for AR-V7 and AR-FL RT-SIBA assays.

RT-SIBA assay	AR-V7	AR-FL
Forward primer concentration	300 nM	400 nM
Reverse primer concentration	200 nM	300 nM
IO concentration	300 nM	300 nM
UvsX & Gp32 concentration	0,4 mg/ml	0,35 mg/ml
RT enzyme concentration	16 U	
MgAc concentration	10 mM	
Incubation temperature	43,5 °C	

4.5 Evaluation of the SIBA assay performance

4.5.1 Analytical specificity

When 1 ng of each RNA isolate from prostate cancer positive cell lines was amplified in RT-SIBA, both AR-V7 and AR-FL assays detected the three AR-V7 and full-length AR positive cell lines (22Rv1, VCaP and LNCap), but not the AR-V7 and AR-FL negative cell line DU-145. Moreover, the AR-V7 assay detected the AR-V7 synthetic DNA template but not the full-length AR DNA template, whereas the AR-FL assay detected the AR-FL DNA but not AR-V7 DNA. The results suggest, that both assays were only specific to prostate cancer cells expressing AR-V7 and AR-FL mRNA, and that the AR-V7 assay specifically amplified the target AR-V7 sequence and AR-FL assay consistently the AR-FL target sequence. Average detection times and melt temperatures of each cell line RNA isolate as well as the positive and negative controls for both assays are presented in Table 10.

Table 10. Average detection times and melt temperatures (T_m) of 1 ng RNA isolates from 22Rv1, VCaP, LNCaP and DU-145 cells, positive DNA controls and negative controls in both AR-V7 and AR-FL RT-SIBA assays. N/D, no data (negative reaction); cp, copies.

RT-SIBA assay	AR-V7		AR-FL	
	Detection time (min)	T_m (°C)	Detection time (min)	T_m (°C)
1 ng 22Rv1 RNA	14,5	72,5	22,9	73,5
1 ng VCaP RNA	13,2	72,5	14,2	74
1 ng LNCaP RNA	23,1	72,5	40,2	73,5
1 ng DU-145 RNA	N/D	N/D	N/D	N/D
10^3 cp AR-V7 DNA	13,4	72	N/D	N/D
10^3 cp AR-FL DNA	N/D	N/D	18,6	74
negative control	N/D	N/D	N/D	N/D

The AR-V7 assay detected 1 ng of RNA isolate from each AR-V7 positive cell line within 13–23 minutes. Detection of LNCaP RNA was the slowest, but it also had the lowest level of AR-V7 mRNA per nanogram (see Table 4). The AR-FL RT-SIBA assay seemed to be least sensitive for the detection of AR-FL mRNA extracted from the LNCaP cell line, since RNA isolates from 22Rv1 and VCaP cells amplified within 23 and 14 minutes, respectively, whereas the LNCaP RNA was detected within 40 minutes. According to the previous qPCR quantitation (see Table 4), 1 ng of LNCaP RNA extract ought to contain $3,3 \times 10^3$ copies of full-length AR mRNA, which is a similar level than in the 22Rv1 cell line ($1,7 \times 10^3$ copies AR-FL RNA/ng). However, the detection of AR-FL isolate from

22Rv1 is detected 17 minutes faster than the RNA isolate from LNCaP cells. SIBA is not a fully quantitative method (Hoser et al. 2014) and the RNA amount per test does not directly correlate with the detection time. However, the result indicates that there might be differences in the AR-FL assay detection efficiency for different AR-FL positive PCa cell lines, and that the LNCaP cell line used in this study might have a mutation in the AR gene.

The melt temperatures of AR-V7 amplification products were 72°C and 72,5°C, and AR-FL products had T_m of 73,5°C and 74°C. The results were in line with the previous experiments (Table 7). No melt peaks were observed for DU-145 RNA or negative controls, and for AR-FL DNA control in AR-V7 assay or AR-V7 DNA control in AR-FL assay. The results suggest, that the AR-V7 and AR-FL assays amplified their target mRNA sequences with high specificity, and the assays were able to identify the target mRNA from three AR-V7 and AR-FL positive prostate cancer cell lines. Amplification curves for 1 ng of 22Rv1, VCap. LNCaP and DU-145 RNA isolates as well as the positive and negative controls in both AR-V7 and AR-FL RT-SIBA assays are presented in Figure 12.

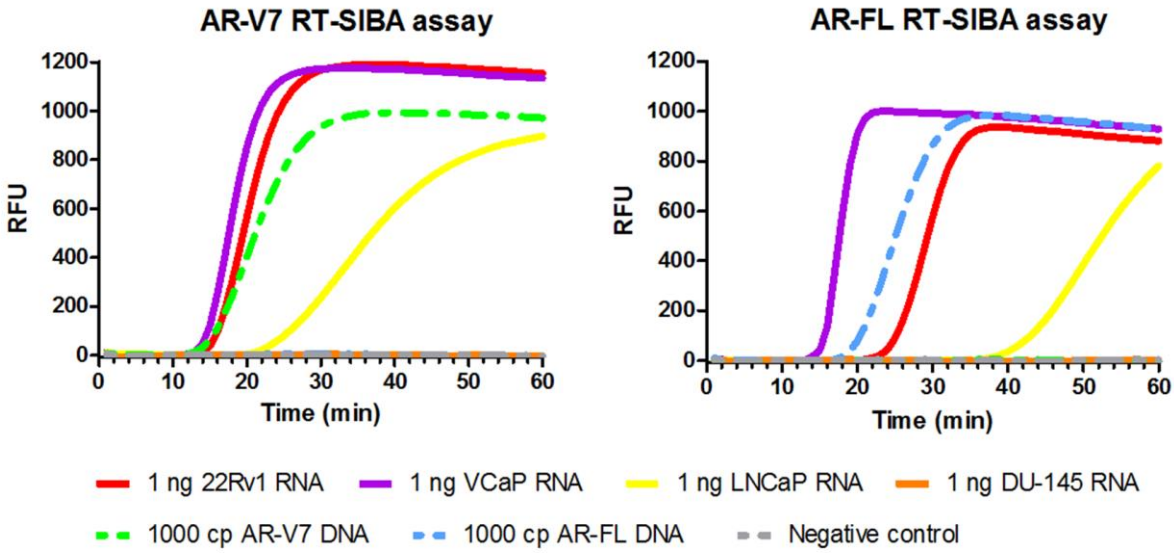

Figure 12. Amplification curves for 1 ng RNA isolates from 22Rv1, VCaP, LNCaP and DU-145 cells, positive AR-V7 and AR-FL DNA controls and negative controls in both AR-V7 and AR-FL RT-SIBA assays. The AR-V7 and AR-FL expressing cell lines; 22Rv1, VCaP and LNCaP, were all detected with both assays. The AR-V7 and AR-FL negative cell line, DU-145, was not detected. The 1000 copies AR-V7 control DNA amplified in the AR-V7 RT-SIBA assay but not in the AR-FL assay, and the 1000 copies AR-FL control DNA only amplified in the AR-FL RT-SIBA assay. Negative controls remained negative. RFU, relative fluorescence units; cp, copies.

4.5.2 Analytical sensitivity

Input data for Probit analysis, *i.e.* the tested AR-V7 and AR-FL mRNA concentrations, the number of replicate reactions and the number of positive reactions for each AR-V7 and AR-FL positive cell line, is presented in Table 11 and Table 12. Output data of the Probit analysis as well as the probability plots are presented in Appendix 6.

Table 11. Input data for Probit analysis to determine the limit of detection of AR-V7 RT-SIBA assay.

AR-V7 mRNA concentration (copies/test)	22Rv1		VCaP		LNCaP	
	No. of replicates	No. of positive	No. of replicates	No. of positive	No. of replicates	No. of positive
1000	10	10	10	10	10	10
500	10	10	10	10	10	10
100	10	10	10	10	10	10
50	10	10	10	10	10	10
10	10	10	10	10	10	10
5	10	9	10	8	10	10
2,5	10	8	10	5	10	8
1	10	3	10	3	10	7

Table 12. Input data for Probit analysis to determine the limit of detection of AR-FL RT-SIBA assay.

AR-FL mRNA concentration (copies/test)	22Rv1		VCaP		LNCaP	
	No. of replicates	No. of positive	No. of replicates	No. of positive	No. of replicates	No. of positive
1000	10	10	10	10	10	10
500	10	10	10	10	10	10
100	10	10	10	10	10	10
50	10	10	10	10	10	10
10	10	8	10	8	10	6
5	10	5	10	5	10	6
2,5	10	3	10	4	10	0
1	10	2	10	2	10	0

The summary of the estimated limits of detection (LoD) is presented in Table 13. The LoD of AR-V7 RT-SIBA assay for AR-V7 mRNA from 22Rv1 cells was determined to be 5,2 copies/test with a 95% confidence interval (CI) of 3,7–14,5 copies/test. Sensitivity of the AR-V7 assay was the weakest for AR-V7 mRNA isolate from VCaP cells, since the

LoD was 7,1 copies/test with 95% CI of 5,0–18,3 copies/test, and the highest for the AR-V7 mRNA from LNCaP cells, since the LoD was 3,8 copies/test. However, the latter value might not be reliable due to the too high rate of positive sample levels; the Probit analysis was unable to provide the 95% CI range for LNCaP AR-V7 mRNA isolate since there were only two levels of positives differing from the total number of replicates tested (10). The experiment should have been repeated with lower concentration levels of AR-V7 mRNA to determine a more reliable LoD for the LNCaP isolate. The average estimated LoD of AR-V7 RT-SIBA assay for the AR-V7 mRNA, calculated from all three PCa cell line isolates, was 5,4 copies/test.

LoDs for AR-FL mRNA isolates from all three PCa cell lines were almost identical: the LoD for 22Rv1 isolate was 14,1 copies/test with 95% CI of 9,8–36,0 copies/test, the LoD for VCaP isolate was 14,5 copies/test with 95% CI of 9,8–43,4 copies/test and the LoD for LNCaP isolate was 14,4 copies/test with 95% CI of 10,8–27,2 copies/test. However, if the zero levels of positives (see the last column of Table 12) were excluded from the Probit analysis, the results showed LoD of 31,6 AR-FL mRNA copies/test instead of 14,4 copies/test. The higher LoD would be in line with the earlier speculation of lower AR-FL RT-SIBA assay sensitivity for the LNCaP mRNA isolate (section 4.5.1), when compared to the two other cell lines. Yet, if the zero levels were to be excluded from the Probit analysis, the rate of positives would again be too high, and no corresponding 95% CI data could be provided for the LNCaP AR-FL mRNA LoD of 31,6 copies/test. The average estimated LoD of AR-FL RT-SIBA assay for AR-FL mRNA was 14,3 copies/test (or alternatively 20,1 copies/test with the higher LNCaP LoD).

Table 13. Estimated limits of detection (LoD) of RT-SIBA assays for AR-V7 and AR-FL mRNA isolates from prostate cancer (PCa) positive cells. At these LoD concentrations, the assays are able to detect 95% of the samples with 95% confidence interval (CI) of described concentration range (CI95%). N/D, no data due to too high positive rate. *If zero levels of positive replicates (see Table 12) were excluded from the Probit analysis, the LoD for AR-FL mRNA from LNCaP was determined to be 31,6 copies/test, with no available CI95% data due to too high rate of positives.

RT-SIBA assay	PCa cell line	Target	LoD (copies/test)	CI95% (copies/test)
AR-V7 assay	22Rv1	AR-V7 mRNA	5,2	3,7–14,5
	VCaP		7,1	5,0–18,3
	LNCaP		3,8	N/D
AR-FL assay	22Rv1	AR-FL mRNA	14,1	9,8–36,0
	VCaP		14,5	9,8–43,4
	LNCaP		14,4*	10,8–27,2

4.5.3 Assay tolerance of sample matrix

The preliminary determination of possible inhibitive levels of human plasma and whole blood showed, that amplification efficiencies of AR-V7 and AR-FL mRNA isolated from the 22Rv1, VCaP and LNCaP cells in the developed AR-V7 and AR-FL RT-SIBA assays were considerably weakened in the presence of >2,5% plasma and blood per test. The amplification was completely inhibited in the presence of >10% plasma and >7,5% blood.

Next, 100 copies of AR-V7 mRNA from LNCaP cells were amplified in the presence of 0–5% human plasma or whole blood per test in the AR-V7 RT-SIBA assay, and 100 copies of AR-FL mRNA in the AR-FL assay. The average detection times for the AR-V7 mRNA are presented in Figure 13. The results suggest that the AR-V7 RT-SIBA assay could tolerate up to 2% of both human plasma and human whole blood per 20 µl reaction volume without remarkable inhibition (under 20% decrease) of AR-V7 mRNA amplification efficacy. When 2% of plasma was present in the RT-SIBA reaction, the detection time of the AR-V7 mRNA slowed down by 4 minutes, accounting for an 18,8% decrease in the amplification efficacy, when measured in minutes. When 2% of the blood was present in the reaction, the amplification was 3,5 minutes slower, accounting for a 16,9% decrease in the amplification efficacy. Blood and plasma concentrations above 2,5% per test caused over 20% decrease in the amplification efficacy and were thus considered as excessively inhibitive levels for the AR-V7 RT-SIBA assay. In addition, blood concentrations above 1% decreased the signal levels of the amplification curves by half (from ~700 RFU to ~300 RFU). No amplification was detected in the negative control reactions. Amplification curves of 100 AR-V7 mRNA copies amplified in the AR-V7 RT-SIBA assay in the presence of 0%, 1% and 2% of human plasma and whole blood are presented in Figure 14.

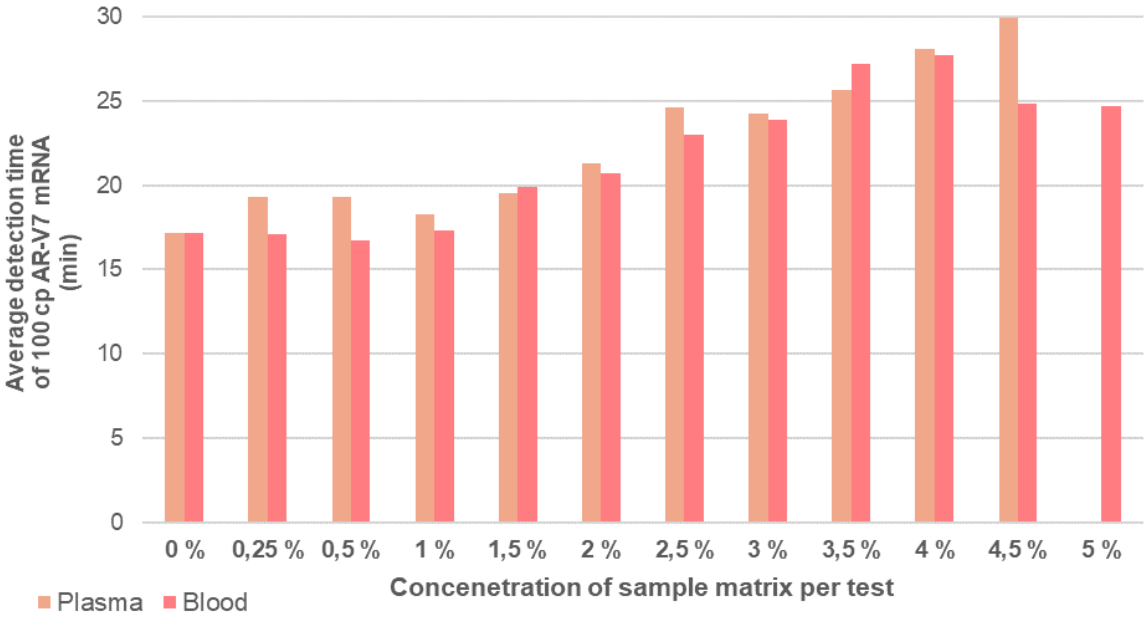

Figure 13. Average detection times of 100 copies of AR-V7 mRNA from LNCaP cells amplified in AR-V7 RT-SIBA assay in the presence of 0%–5% human plasma and whole blood per test. Tolerated level of both plasma and blood was determined to be 2% per test. 5% of plasma per test inhibited the amplification of AR-V7 mRNA completely. Cp, copies.

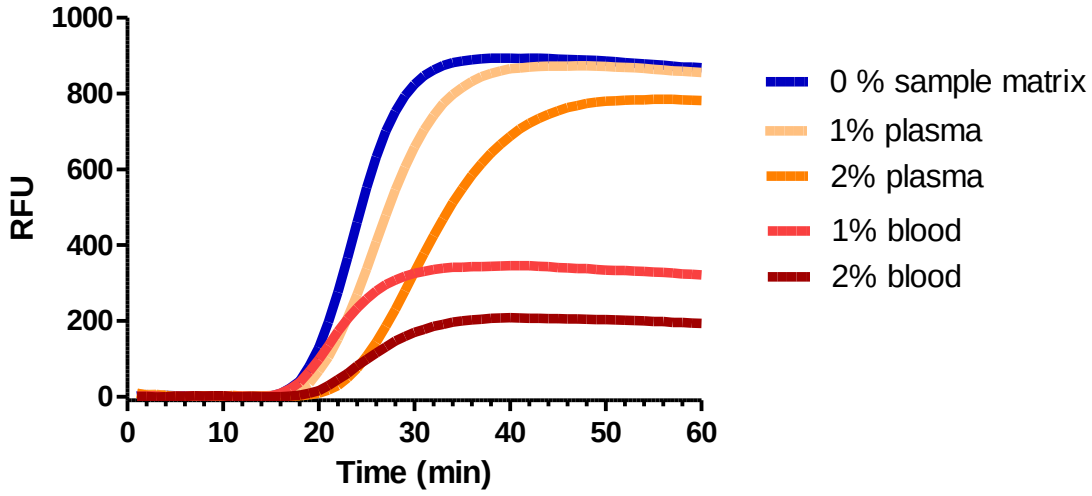

Figure 14. Amplification curves of 100 copies of AR-V7 mRNA from LNCaP cells amplified in the AR-V7 RT-SIBA assay in the presence of 0%, 1% and 2% of human plasma and whole blood per test. Inhibitive effects of blood as sample matrix can be seen as reduced signal levels of the amplification curves (lower RFU values). The AR-V7 RT-SIBA assay was able to tolerate the presence of 2% plasma and 2% whole blood without considerable inhibition in the amplification efficacy. RFU; relative fluorescence units.

The average detection times for 100 AR-FL mRNA copies are presented in Figure 15. When only comparing the detection times, the results suggest that the AR-FL RT-SIBA assay could tolerate up to 1,5% of human plasma and even 4,5% of human whole blood per 20 µl reaction volume without remarkable inhibition of AR-FL mRNA amplification efficacy. When 1,5% of plasma was present in the RT-SIBA reaction, the detection time of the AR-FL mRNA slowed down by 4,4 minutes, accounting for a 14,3% decrease in the amplification efficacy. Plasma concentrations above 2% per test caused over 20% decrease in the amplification efficacy and were thus considered as excessively inhibitive levels for the AR-FL RT-SIBA assay. Negative controls containing the plasma, but no AR-FL, did not show any amplification, suggesting that the assay remained specific in the presence of plasma.

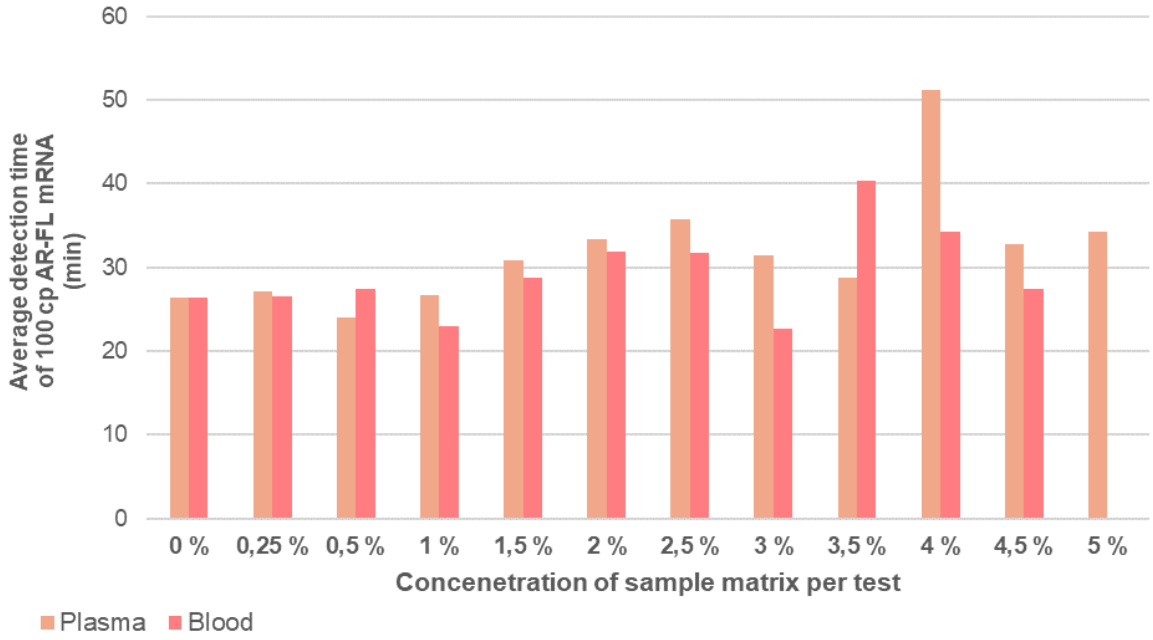

Figure 15. Average detection times of 100 copies of AR-FL mRNA from LNCaP cells amplified in AR-FL RT-SIBA assay in the presence of 0%–5% human plasma and whole blood per test. Tolerated level of plasma was determined to be 1,5% per test. Tolerated level of blood could not be reliably determined due to likely positive AR-FL status of the blood used as sample matrix, but 3,5% blood per test considerably decreased the amplification efficacy and 5% of blood per test inhibited the amplification of AR-FL mRNA completely. Cp, copies.

When 1% and 3% of blood was present in the reaction, the amplification of AR-FL mRNA template was actually faster than in the reactions containing 0% blood. Reactions containing 0,25%–4% blood but no added AR-FL mRNA template showed amplification signals, and the amplicons had the exact same melt temperatures as did the AR-FL

mRNA amplicons: 74°C. The amplification in the no-template reaction containing 1% of blood was detected within the shortest reaction time: 18,7 minutes. The negative control containing 0% blood and no template did not show any amplification. This indicates, that the blood was positive for AR-FL and there was more AR-FL mRNA present in the reactions containing the blood than in reactions without the sample matrix. The melt temperature analysis supported the specificity of the assay for AR-FL mRNA. The results suggest that the AR-FL RT-SIBA assay was able to detect the androgen receptor mRNA from the diluted whole blood within less than 20 minutes. The AR-FL is expressed in several human tissues, including hematopoietic cells of whole blood, and in higher levels in male tissues when compared to female tissues due to hormonal regulation (Sader et al. 2005). Thus, it is possible that the AR-FL RT-SIBA assay possibly detected the AR-FL mRNA from the blood cells present in the whole blood sample used as sample matrix. Unfortunately, no additional information of the blood sample used, including the sex of the donor, was available.

Due to the possible presence of AR-FL mRNA in the whole blood used as sample matrix, the inhibitive levels of blood could not reliably be determined for the AR-FL RT-SIBA assay. However, blood concentrations above 1,5% considerably decreased the signal levels of AR-FL mRNA amplification curves when compared to 0% blood concentration (from ~700 RFU to ~300 RFU). The presence of 5% whole blood completely inhibited the amplification of AR-FL mRNA. Amplification curves of 100 AR-FL mRNA copies amplified in the AR-V7 RT-SIBA assay in the presence of 0%, 1% and 1,5% of human plasma and whole blood are presented in Figure 16.

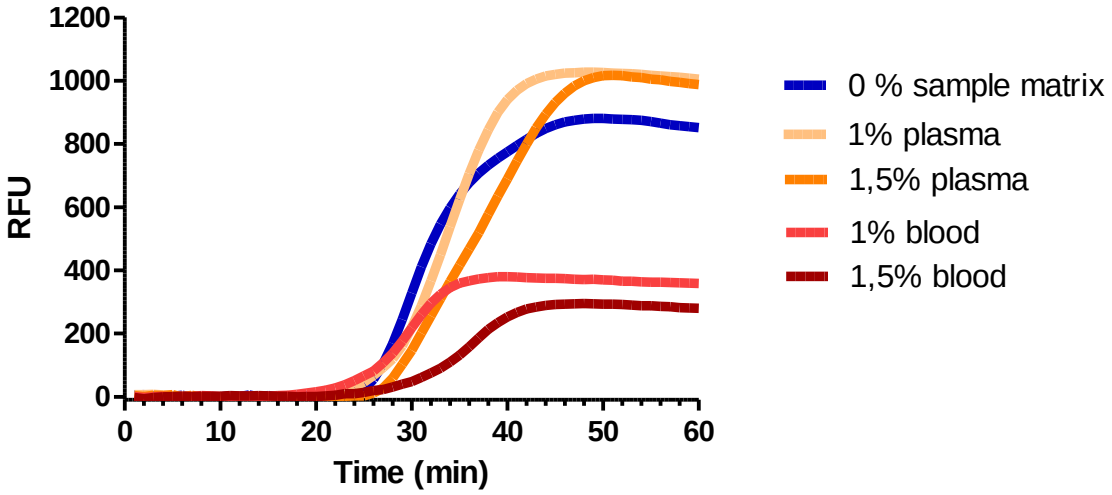

Figure 16. Amplification curves of 100 copies of AR-FL mRNA from LNCaP cells amplified in the AR-FL RT-SIBA assay in the presence of 0%, 1% and 1,5% of human plasma and whole blood per test. Inhibitive effects of blood as sample matrix can be seen as reduced signal levels of the amplification curves (lower RFU values). The AR-FL RT-SIBA assay was able to tolerate the presence of 1,5% plasma and 1,5% whole blood without considerable inhibition in the amplification efficacy. RFU; relative fluorescence units.

When the inhibitive effects of human plasma and whole blood on the AR-V7 and AR-FL RT-SIBA assay performances were considered, the final tolerated level of both plasma and blood was decided to be 1% for both assays, due to the decreased amplification curve signal levels caused by blood concentrations above 1% in both assays. The tolerance of plasma as sample matrix was higher than the tolerance of blood for both assays, but the same 1% level was decided to be used for both matrixes in the future experiments. The differences between the inhibitory effects can be explained by the composition and physiological characteristics of the sample matrixes: plasma is nearly 90% water and rest of the volume is composed of proteins, ions, metabolites and other solutes, whereas blood contains erythrocytes, leucocytes and platelets in addition to the 40–50% liquid blood plasma part and anticoagulants (Kern 2002). Hence, the composition of blood is more complex, and it is also thicker and darker in color. These characteristics of blood as sample matrix were a probable cause for its higher inhibitory level and decreased amplification efficiency of AR-V7 and AR-FL mRNA in the developed RT-SIBA assays. Furthermore, several blood components, including heme, leucocyte DNA and added anticoagulants, have previously been shown as major PCR-inhibitory substances (Al-Soud and Rådström 2001).

4.6 Testing of clinical samples

Average detection times in AR-V7 and AR-FL RT-SIBA assays as well as the C_q values in the in-house RT-qPCR assay for the tested four clinical PCa positive plasma samples are presented in Table 14. As in previous PCR experiments, the AR-V7 primers produced late non-specific amplification in the RT-qPCR. FAM threshold was set to 10 RFU and reactions having C_q values above 32 were considered as AR-V7 negative in PCR. The positive control, 10^3 copies of synthetic AR-V7 mRNA, was detected on average within 15,4 minutes by the AR-V7 RT-SIBA assay having T_m of 72,5 °C, and 10^3 copies of the AR-FL DNA control was detected within 18,8 minutes by the AR-FL RT-SIBA assay having T_m of 74,5°C. In the RT-qPCR, the AR-V7 control DNA had an average C_q value of 30,5, and the AR-FL control DNA C_q of 30,3. The negative controls did not amplify during either RT-SIBA or RT-qPCR runs.

The results suggest that all four samples were negative for AR-V7, since no AR-V7 mRNA was detected by the AR-V7 RT-SIBA assay nor by the RT-qPCR. Two out of four PCa plasma samples were positive for full-length AR in the AR-FL RT-SIBA assay: sample 1b (DLS17-049910-K2 extracted with miRNeasy kit), detected within 20,7 minutes, and sample 2b (DLS17-049930-K2 extracted with miRNeasy kit), detected within 55 minutes. Only one out of two replicates of these samples were amplified in the AR-FL assay, but the amplicons had similar melt temperatures than the AR-FL control DNA (74,5 °C), suggesting that the amplicons were correct sized and specific amplification products of the AR-FL oligonucleotides. The difference in the detection times suggests that the sample 1b probably had considerably higher level of AR-FL mRNA than the sample 2b.

In RT-qPCR, sample 2a (DLS17-049930-K2 extracted with exoRNeasy) was weakly positive for full-length AR, but only one out of two duplicates amplified very late having C_q value of 35,8. The same sample, extracted using different kit (miRNeasy), was also weakly positive for full-length AR in the AR-FL RT-SIBA assay. This suggests, that the results of SIBA and PCR runs are in line, and that the sample DLS17-049930-K2 is most likely positive for AR-FL. However, the sample that was detected within 20,7 minutes by AR-FL RT-SIBA, did not amplify at all in the RT-qPCR. Thus, the developed AR-FL RT-SIBA assay could possibly be more sensitive for the detection of AR-FL mRNA in clinical specimens, than the published RT-qPCR assay used in this study.

Table 14. Average detection times of the plasma samples in AR-V7 and AR-FL RT-SIBA assays, and average Cq values of the samples in the RT-qPCR. Letters after the sample numbers represent the RNA extraction method: (a), exosomal RNA isolated with exoRNeasy plasma kit (Qiagen); (b), cell-free total RNA isolated with miRNeasy plasma kit (Qiagen); (c) 1% of plasma sample per reaction without RNA extraction. N/D, no data (negative reaction); AR-V7^{-}, negative for androgen receptor splice variant 7; AR-FL^{-}, negative for full-length androgen receptor; AR-FL^{+}, positive for full-length androgen receptor; C_q, quantification cycle.

No.	Sample ID	Average detection time in RT-SIBA (min)		SIBA result	Average C_q in RT-qPCR	RT-qPCR result
		AR-V7 assay	AR-FL assay			
1a	DLS17-049910-K2	N/D	N/D	AR-V7^{-} AR-FL^{-}	N/D	AR-V7^{-} AR-FL^{-}
1b	DLS17-049910-K2	N/D	20,7	AR-V7^{-} AR-FL^{+}	N/D	AR-V7^{-} AR-FL^{-}
1c	DLS17-049910-K2	N/D	N/D	AR-V7^{-} AR-FL^{-}	N/D	AR-V7^{-} AR-FL^{-}
2a	DLS17-049930-K2	N/D	N/D	AR-V7^{-} AR-FL^{-}	35,8	AR-V7^{-} AR-FL^{+}
2b	DLS17-049930-K2	N/D	54,4	AR-V7^{-} AR-FL^{+}	N/D	AR-V7^{-} AR-FL^{-}
2c	DLS17-049930-K2	N/D	N/D	AR-V7^{-} AR-FL^{-}	N/D	AR-V7^{-} AR-FL^{-}
3a	DLS17- 050017-K2	N/D	N/D	AR-V7^{-} AR-FL^{-}	N/D	AR-V7^{-} AR-FL^{-}
3b	DLS17- 050017-K2	N/D	N/D	AR-V7^{-} AR-FL^{-}	N/D	AR-V7^{-} AR-FL^{-}
3c	DLS17- 050017-K2	N/D	N/D	AR-V7^{-} AR-FL^{-}	N/D	AR-V7^{-} AR-FL^{-}
4a	DLS17- 050029-K2	N/D	N/D	AR-V7^{-} AR-FL^{-}	N/D	AR-V7^{-} AR-FL^{-}
4b	DLS17- 050029-K2	N/D	N/D	AR-V7^{-} AR-FL^{-}	N/D	AR-V7^{-} AR-FL^{-}
4c	DLS17- 050029-K2	N/D	N/D	AR-V7^{-} AR-FL^{-}	N/D	AR-V7^{-} AR-FL^{-}

5 Discussion

5.1 Applicability of SIBA technology for cancer biomarker detection

This study describes the development of a novel isothermal nucleic acid amplification method for the detection of androgen receptor splice variant 7 (AR-V7) and full-length androgen receptor (AR-FL) mRNA. The developed Reverse Transcription Strand Invasion Based Amplification (RT-SIBA) assays were able to detect low copies of AR-V7 and AR-FL mRNA in the presence of 1% human plasma and whole blood per test. The AR-FL assay also detected the presence of AR-FL in diluted whole blood within 20 minutes, without any RNA isolation or sample treatment performed prior to the RT-SIBA test. The assays only specifically amplified their target mRNA and did not produce unintended amplicons.

Previous studies have demonstrated, that the AR-V7 mRNA can be detected from circulating tumor cells (CTCs) in patients with advanced castrate-resistant metastatic prostate cancer (mCRPC), and that the increased AR-V7 expression is specific for the tumor cells (Antonarakis et al. 2014). Since the CTCs are actively present in the whole blood, no additional CTC isolation from blood is necessarily needed, if the test for the detection of AR-V7 is sufficiently sensitive. Study by Takeuchi et al. (2016) suggests, that in addition to CTCs, AR-V7 mRNA is also expressed in the hematopoietic cells of whole blood. In addition, a recent study on mCRPC cancer markers by Danila et al. (2016) proposes that the direct detection of circulating tumor mRNA in whole blood by ddPCR analysis has similar detection rate of the markers than a CTC isolation-based assay. Thus, whole blood could potentially be used as a liquid biopsy for the identification of ARSI resistance and for the selection of more effective alternative therapies in mCRPC patients.

Recent studies have applied quantitative real-time PCR for the detection of AR-V7 mRNA in clinical specimens (Antonarakis et al. 2014; Onstenk et al. 2015; Scher et al. 2016). Usually, AR-V7 mRNA needs to be isolated from circulating tumor cells in plasma or from other clinical specimens using time-consuming protocols in order to reach results with high sensitivity. In addition, natural components, such as heme and leucocyte DNA, as well as additional anticoagulants such as EDTA present in whole blood samples cause major inhibition of PCR-based technologies (Al-Soud and Rådström 2001). These

characteristics represent the limitations associated with the current PCR-based biomarker detection technologies.

This study demonstrated that the developed RT-SIBA assays detected low copies of AR-V7 and AR-FL mRNA within 20 minutes in the presence of whole blood and plasma. The tolerance of these sample matrixes can enable the use of liquid biopsies for biomarker detection without a need for sample processing prior to the molecular testing. Consequently, the time to result can be considerably faster in contrast to the current PCR-based detection methods. Moreover, the volume of blood samples needed for the RT-SIBA testing is considerably smaller in contrast to the current PCR-based methods, since diluted blood can be added into the RT-SIBA reaction as such. The use of liquid biopsies in combination with novel, easy-to-use molecular diagnostic methods such as RT-SIBA, enables more efficient identification and screening of molecular cancer biomarkers, as here demonstrated with the AR-V7 and AR-FL mRNA.

Moreover, now that the applicability of SIBA for the detection of cancer biomarkers has been demonstrated by using AR-V7 mRNA as a target molecule, additional molecular targets related to alterations in cancer genome could be targeted. The SIBA technology could potentially be applied for the detection of known point mutations in cancer genome, such as mutations in *KRAS* or epidermal growth factor receptor (*EGFR*) gene (Malapelle et al. 2012), since the sensitivity of the method can be extended to a single nucleotide change (Hoser et al. 2014). This could help in the characterization of the cancer on individualized molecular level. RT-SIBA could also be applied for the detection of other common alterations, such as the *TMPRSS2:ERG* (Laxman et al. 2006) or the *BCR-ABL* fusion genes (Melo 1996) resulted from chromosomal translocations, by targeting the sequences of the RNA transcripts, thereby assisting in the cancer diagnosis, prognosis or treatment-planning.

5.2 Limitations of the study

The RT-qPCR conditions used in this study were originally optimized for droplet digital PCR (ddPCR) instead of real-time quantitative PCR (Ma et al. 2016). Hence, the quantities of mRNA isolates from prostate cancer positive cell lines possibly slightly varied, since the RT-qPCR assay was used for the mRNA quantification. The late non-specific amplification or primer dimers produced by the AR-V7 PCR primers likely

affected the reliability of AR-V7 mRNA copy numbers in the quantified cell line isolates. However, since the AR-V7 and AR-FL mRNA ratios were mostly in line with the corresponding ratios in the ddPCR publication by Ma et al. (2016), the quantification results can be considered as relatively reliable.

Use of plasma and blood in LoD determination would have provided more information on the assay performances. Lower levels of AR-V7 and AR-FL mRNA copy numbers could have been used to decrease the high rate of positives. Now, concentrations until 10 copies of AR-V7 mRNA per test, and 50 copies of AR-FL mRNA per test all showed 10/10 positive replicate reactions, and mRNA concentrations below these only provided lower levels of positives.

The most considerable limitation of this study was the lack of truly positive and negative AR-V7 clinical specimens, such as whole blood or plasma samples collected from patients with metastatic castrate-resistant prostate cancer. The clinical plasma samples tested in this study were selected based on their high Gleason scores. However, the Gleason scoring is intended for the grading of localized prostate tumors (Mottet et al. 2017), and it has weaker prognostic value in patients with advanced mCRPC (Fizazi et al. 2016). In addition, the PSA values of the samples were quite low (median 15 ng/ml, see Appendix 1), when compared to common baseline PSA levels measured from mCRPC patients positive for AR-V7; median values ranging between 99,6–239,9 ng/ml (Antonarakis et al. 2014; Del Re et al. 2017; Seitz et al. 2017; Steinestel et al. 2015).

Since increased expression levels of AR-V7 mRNA are common in more advanced metastatic prostate cancer (Antonarakis et al. 2014; Del Re et al. 2017; Seitz et al. 2017; Steinestel et al. 2015), it is highly unlikely that AR-V7 was expressed in any of the plasma samples used in this study, due to the unlikely castrate-resistant stage of the disease. The use of clinical samples with known AR-V7 statuses would have provided more realistic information on the RT-SIBA assay performances. This would also have better indicated the clinical specificity of the assays, and a bigger number of clinical prostate cancer samples are needed to confirm the target-specific detection of both AR-V7 and AR-FL mRNA by the two developed RT-SIBA assays. Unfortunately, additional prostate cancer specimens could not be obtained during this study.

The positivity of the blood sample for AR-FL could not be confirmed due to the lack of an extraction kit intended for RNA purification from whole blood. The RNA from the blood

sample could have been tested with the RT-qPCR assay to ensure the presence of AR-FL mRNA in the blood used as a liquid sample matrix in this study. The known AR-FL status of the sample material, as well as other clinical specimens, would also provide more reliable information on the performances of the developed RT-SIBA assays.

5.3 Further experiments

Further experiments related to this study could include the further optimization of the developed RT-SIBA assays. The results suggested that especially the performance of the AR-FL assay could still be optimized, since now the RT-SIBA conditions were settled to be more optimal for the AR-V7 RT-SIBA assay. The preliminary optimization experiments indicated, that increased magnesium acetate concentration improved the amplification efficacy of AR-FL mRNA by the AR-FL RT-SIBA assay. In addition, the use of probes could enable potential multiplexing of the assays: both AR-V7 and AR-FL mRNA could be amplified in one reaction, and an additional internal control could be used.

For clinical validation of the developed RT-SIBA assays, more clinical mCRPC specimens positive for AR and AR-V7 should be tested. Determination of clinical specificity and sensitivity using a bigger number of clinical samples would describe the diagnostic performance of the developed assays and address the future aspects of the utility of RT-SIBA technology in the field of cancer biomarker diagnostics.

6 Conclusions

The aim of this study was to evaluate the potential applicability of a novel molecular method, Reverse Transcription Strand Invasion Based Amplification (RT-SIBA), for the detection of cancer biomarkers and to develop a RT-SIBA assay targeting androgen receptor splice variant 7 (AR-V7) mRNA. The results of this study demonstrate that the RT-SIBA technology can be applied for the detection of molecular cancer biomarkers, such as AR-V7 mRNA. The AR-V7 has been proposed as a treatment-response biomarker for resistance to androgen receptor signaling inhibitor (ARSI) therapies in patients with advanced metastatic castrate-resistant prostate cancer (mCRPC), and the identification of positive AR-V7 status can guide the selection of efficient treatment for improved outcome. Alternative, enhanced therapies can be developed and applied for the patients identified as resistant to the current ARSI-therapies.

The RT-SIBA technology can possibly be utilized for the rapid detection of AR-V7 mRNA directly from non-invasive liquid biopsies, thus saving time spent on sample processing and mRNA isolation. The technology can act as a fast, sensitive and target-specific alternative for the current RT-qPCR technology and can potentially be performed with low-cost instruments as well as small sample volumes. After carrying out further studies with truly AR-V7 positive clinical specimens from mCRPC patients, the technology could potentially be validated for diagnostic use in the field of oncology.

The use of advanced and easy-to-use molecular methods for the identification of cancer biomarkers provides considerable advantages over the traditional cancer imaging methods. The use of liquid biopsies, such as blood samples, is safer as no surgery is needed for the collection of the biopsy. Rapid sampling and testing of biomarkers with short time-to-result methods can provide valuable tools for cancer screening and diagnosis at the early stages of disease development as well as for monitoring treatment response and therapy planning. The rapid molecular biomarker identification may have a crucial role in the selection of the most efficient therapies. At their best, the novel molecular methods, such as the RT-SIBA, can lead to improved management of the disease and increase the life expectancy of patients with cancer.

7 Acknowledgements

First of all, I would like to express my deepest gratitude to my supervisor Dr. Kevin Eboigbodin for guidance and support, and for always innovating new applications for the SIBA technology. Thank you for being a good and professional, but also understanding and flexible, instructor and co-worker for me. Your ideas are inspiring.

I would like to thank Orion Diagnostica Oy for giving me the opportunity to conduct this study using the laboratory facilities, equipment, reagents and the SIBA-technology provided by the company. I also wish to thank all my co-workers for assistance and advice.

I am grateful to Dr. Anu Moilanen and Leena Kahala from Orion Pharma, and to Prof. Tapio Visakorpi, Prof. Teuvo Tammela, Hanna Selin and Annika Kohvakka from the University of Tampere, for providing me the prostate cancer cell lines and technical support. I would also like to extend my thanks to Dr. Mika Mustonen and Dr. Tarja Ikonen from Orion Pharma for the professional insights on the utility of AR-V7 in prostate cancer diagnostics and treatment.

Finally, I wish to thank my family, friends and loved ones for support, encouragement and trust in me throughout the whole project.

References

Al-Soud W. and Rådström P. (2001). Purification and Characterization of PCR-Inhibitory Components in Blood Cells. *Journal of Clinical Microbiology*, 39 (2): 485–493.

Antonarakis E. S, Lu C, Luber B, et al. (2015). Androgen receptor splice variant 7 and efficacy of taxane chemotherapy in patients with metastatic castration-resistant prostate cancer. *JAMA Oncol*. 1 (5): 582–591.

Antonarakis E. S, Lu C, Luber B. et al. (2017). Clinical Significance of Androgen Receptor Splice Variant-7 mRNA Detection in Circulating Tumor Cells of Men With Metastatic Castration-Resistant Prostate Cancer Treated With First- and Second-Line Abiraterone and Enzalutamide. *J Clin Oncol*, 35 (19): 2149–2156.

Antonarakis E. S, Lu C, Wang H. et al. (2014). AR-V7 and resistance to enzalutamide and abiraterone in prostate cancer. *N Engl J Med*; 371:1028–1038.

Bernard P. S. and Wittwer C. T. (2002). Real-Time PCR Technology for Cancer Diagnostics. *Clinical Chemistry*, 48: 1178–1185.

Bostwick D. G, Burke H. B, Djakiew D, Euling S. et al. (2004). Human prostate cancer risk factors. *Cancer*, 101: 2371–2490.

Bratt O, Damber J. E, Manuelsson M. and Grönberg H. (2002). Hereditary Prostate Cancer: Clinical Characteristics and Survival. *The Journal of Urology*, 167: 2423–2426.

Bray F, Ferlay J, Soerjomataram I, Siegel R, Torre L. and Jemal A. (2018). Global cancer statistics 2018: GLOBOCAN estimates of incidence and mortality worldwide for 36 cancers in 185 countries. *CA: A Cancer Journal for Clinicians 2018*; 0: 1–31.

Burd, Eileen M. (2010). Validation of Laboratory-Developed Molecular Assays for Infectious Diseases. *Clinical Microbiology Reviews*, 23 (3): 550–576.

Bustin S. A, Benes V, Garson J. A. et al. (2009). The MIQE guidelines: Minimum information for publication of quantitative real-time PCR experiments. *Clin Chem*, 55, 611–622.

Bustin S. A. (2000). Absolute quantification of mRNA using real-time reverse transcription polymerase chain reaction assays. *J Mol Endocrinol*, 25 (2):169–93.

Chin L. and J. W. Gray. (2008). Translating insights from the cancer genome into clinical practice. *Nature*, 452 (7187): 553–563.

Crowley E, Di Nicolantonia F, Loupakis F. and Bardelli A. (2013). Liquid biopsy: monitoring cancer-geneticsin the blood. *Nature Reviews Clinical Oncology*, 10 (8): 472–484.

Danila D. C, Samoila A, Patel C. et al. (2016). Clinical Validity of Detecting Circulating Tumor Cells by AdnaTest Assay Compared With Direct Detection of Tumor mRNA in Stabilized Whole Blood, as a Biomarker Predicting Overall Survival for Metastatic Castration-Resistant Prostate Cancer Patients. *The Cancer Journal*, 22 (5): 315–320.

Dehm S. M, Schmidt L. J, Heemers H. V, Vessella R. L and Tindall D. J. (2008). Splicing of a novel androgen receptor exon generates a constitutively active androgen receptor that mediates prostate cancer therapy resistance. *Cancer Res,* 68 (13): 5469–5477.

Del Re M, Biasco E, Crucitta S. et al. (2017). The detection of androgen receptor splice variant 7 in plasma-derived exosomal RNA strongly predicts resistance to hormonal therapy in metastatic prostate cancer patients. *European Urology*, 71: 680–687.

Demir C. and Yener B. (2005). Automated cancer diagnosis based on histopathological images: a systematic survey. Dept. Comput. Sci., Rensselaer Polytechnic Inst., Troy, NY, USA, Tech. Rep. TR-05-09.

Druker, B. J, Talpaz M, Resta D. J, Peng B and Buchdunger E. (2001). Efficacy and safety of a specific inhibitor of the BCR–ABL tyrosine kinase in chronic myeloid leukemia. *New England Journal of Medicine*, 344: 1031–1037.

Eboigbodin K, Filén S, Ojalehto T. et al. (2016). Reverse transcription strand invasion based amplification (RT-SIBA): a method for rapid detection of influenza A and B. *Appl Microbiol Biotechnol,*100: 5559–5567.

Eboigbodin K. E, Moilanen K, Elf S. and Hoser M. (2017). Rapid and sensitive real-time assay for the detection of respiratory syncytial virus using RT-SIBA®. *BMC Infect Dis*,17 (1): 134.

Eboigbodin K. E. and Hoser M. J. (2016). Multiplex Strand Invasion Based Amplification (mSIBA) assay for detection of Chlamydia trachomatis and Neisseria gonorrhoeae. *Scientific Reports*, 3 (6): 2048.

Elf S, Olli J, Hirvonen S, Auvinen P and Eboigbodin K. E. (2018). Molecular Detection of Streptococcus pyogenes by Strand Invasion Based Amplification Assay. *Mol Diagn Ther*, 22 (5): 595–602.

Fizazi K, Flaig T. W, Stöckle M. et al. (2016). Does Gleason score at initial diagnosis predict efficacy of abiraterone acetate therapy in patients with metastatic castrationresistant prostate cancer? An analysis of abiraterone acetate phase III trials. *Ann Oncol*, 27: 699–705.

Fleshner K, Carlsson S. and Roobol M. (2017). The effect of the USPSTF PSA screening recommendation on prostate cancer incidence patterns in the USA. *Nat Rev Urol,* 14 (1): 26–37.

Formosa T. and Alberts B. M. (1986). Purification and characterization of the T4 bacteriophage uvsX protein. *J Biol Chem,* 261(13): 6107–6118.

Gallagher, S.R. (2017). Quantitation of DNA and RNA with absorption and fluorescence spectroscopy. *Current Protocols in Immunology*,116: A.3L.1-A.3L.14.

Guo Z, Yang X, Sun F, Jiang R. et al. (2009). A novel androgen receptor splice variant is up-regulated during prostate cancer progression and promotes androgen depletion resistant growth. *Cancer Res*, 69: 2305–2313.

Haile S. and Sadar M. D. (2011). Androgen receptor and its splice variants in prostate cancer. Cell. Mol. Life Sci., (2011) 68:3971–3981.

Hanahan, D. and Weinberg, R.A. (2000). The hallmarks of cancer. Cell, 100: 57–70.

Hankey B. F, Feuer E.J, Clegg L. X, Hayes R. B. et al. (1999). Cancer surveillance series: interpreting trends in prostate cancer — part I: evidence of the effects of screening in recent prostate cancer incidence, mortality, and survival rates. *J Natl Cancer Inst*, 91: 1017–1024.

Hörnberg E, Ylitalo E. B, Crnalic S. et al. (2011). Expression of androgen receptor splice variants in prostate cancer bone metastases is associated with castration resistance and short survival. *PLoS One*, 6 (4): e19059.

Hoser M. J, Mansukoski H.K, Morrical S. W. and Eboigbodin K.E. (2014). Strand invasion based amplification (SIBA®): a novel isothermal DNA amplification technology demonstrating high specificity and sensitivity for a single molecule of target analyte. *PLoS one*, 9(11): e112656.

Hoser M. J. (2011). Isothermal nucleic acid amplification. Patent Application Publication. US20110123991A1.

Hu R, Dunn T.A, Wei S, Isharwal S. et al. (2009). Ligand-independent androgen receptor variants derived from splicing of cryptic exons signify hormonerefractory prostate cancer. Cancer Res, 69: 16–22.

Jaishree V. and Gupta P. D. (2012). Nanotechnology: A Revolution in Cancer Diagnosis. *Ind J Clin Biochem*, 27 (3): 214–220.

Kainulainen V, Elf S, Susi P, Mäki M. et al. (2018). Detection of human rhinoviruses by reverse transcription strand invasion based amplification method (RT-SIBA). *Journal of Virological Methods,* Accepted in October 2018, in press.

Kern W. F. (2002). PDQ Hematology. People's Medical Publishing House (PMPH), US.

King M, Marks J, Mandell J. B, The New York Breast Cancer Study Group. (2003). Breast and Ovarian Cancer Risks Due to Inherited Mutations in BRCA1 and BRCA2. *Science*, 302 (5645): 643–646.

Kirby M, Hirst C. and Crawford E. D. (2011). Characterising the castration-resistant prostatecancer population: a systematic review. *Int J Clin Pract*, 65 (11): 1180–1192.

Krawetz, Stephen A. and David D. Womble, David D. (2003). Introduction to Bioinformatics: A Theoretical and Practical Approach. Springer Science & Business Media.

Kumar S, Kumar A. and Venkatesan G. (2018). Isothermal Nucleic Acid Amplification System: An Update on Methods and Applications. *J Genet Genom*, 2 (1): 1000112.

Kvåle R, Auvinen A, Adami H.O. et al. (2007). Interpreting trends in prostate cancer incidence and mortality in the five Nordic countries. *J Natl Cancer Inst*, 99: 1881–1887.

Laxman B, Tomlins S, Mehra R. et al. (2006). Noninvasive Detection of TMPRSS2:ERG Fusion Transcripts in the Urine of Men with Prostate Cancer. *Neoplasia*, 8(10): 885–888.

Liang S, Xu Z, Xu X. et al. (2012). Quantitative Proteomics for Cancer Biomarker Discovery. *Combinatorial Chemistry & High Throughput Screening*, 15 (3): 221–231.

Lu C. and Luo J. (2013). Decoding the androgen receptor splice variants. *Transl Androl Urol*, 2 (3): 178–186.

Luo, J. (2016). Development of AR-V7 as a putative treatment selection marker for metastatic castration-resistant prostate cancer. *Asian Journal of Andrology*, 18, 580–585.

Ma, Y, Luk, A, Young, F. P, Lynch, D. et al. (2016). Droplet digital PCR based androgen receptor variant 7 (AR-V7) detection from prostate cancer patient blood biopsies. *Int. J. Mol. Sci*, 17: 1264.

Makkonen H, Kauhanen M, Jääskeläinen T, Palvimo J. J. (2010). Androgen receptor amplification is reflected in the transcriptional responses of Vertebral-Cancer of the Prostate cells. *Molecular and Cellular Endocrinology*, 331: 57–65.

Malapelle U, de Rosa N, Rocco D. et al. (2012). EGFR and KRAS mutations detection on lung cancer liquid-based cytology: a pilot study. *J Clin Pathol*, 65(1):87–91.

Maruvada P, Wang W, Wagner P. D. and Srivastava S. (2005). Biomarkers in molecular medicine: cancer detection and diagnosis. *BioTechniques*, 38: S9–15.

Melo J. V. (1996). The diversity of BCR-ABL Fusion Proteins and Their Realtionship to Leukemia Phenotype. *Blood*, 88 (7): 2375–2384.

Mottet N, Bellmunt J, Bolla M, Briers E. et al. (2017). EAU-ESTRO-SIOG Guidelines on Prostate Cancer. Part 1: Screening, Diagnosis, and Local Treatment with Curative Intent. *European Urology*, 71: 618–629.

Moyer V. (2012). Screening for prostate cancer: U.S. Preventive Services Task Force recommendation statement. *Ann Intern Med*, 157: 120–134.

Nakazawa M, Antonarakis E. S. and Luo J. (2014). Androgen receptor splice variants in the era of enzalutamide and abiraterone. *Horm Cancer*, 5: 265–73.

NCI (National Cancer Institute): Dictionary of Cancer Terms: Prostate cancer. (2018). Available online. Accessed August 2018 >https://www.cancer.gov/publications/dictionaries/cancer-terms/def/prostate-cancer<

NCI (National Cancer Institute): SEER Stat Fact Sheets: Prostate. (2018). Bethesda, MD: National Cancer Institute. Available online. Accessed August 2018. >https://seer.cancer.gov/statfacts/html/prost.html<

Onstenk W, Sieuwerts A. M, Kraan J. et al. (2015). Efficacy of cabazitaxel in castration-resistant prostate cancer is independent of the presence of AR-V7 in circulating tumor cells. *Eur Urol*, 68 (6): 939–945.

Paez, J. G, Jänne P. A, Lee J. C, Tracy S. et al. (2004). EGFR mutations in lung cancer: correlation with clinical response to gefitinib therapy. *Science*, 304: 1497–1500.

Pegram M. and Slamon D. (2000). Biological rationale for HER2/neu (c-erbB2) as a target for monoclonal antibody therapy. *Semin. Oncol*, 27: 13–19.

Postel M, Roosen A, Laurent-Puig P, Taly V. and Wang-Renault S-F. (2018). Droplet-based digital PCR and next generation sequencing for monitoring circulating tumor DNA: a cancer diagnostic perspective. *Expert Review of Molecular Diagnostics*, 18 (1): 7–17.

Ririe K. M, Rasmussen R. P. and Wittwer C. T. (1997). Product Differentiation by Analysis of DNA Melting Curves during the Polymerase Chain Reaction. *Analytical Biochemistry*, 245, 154–160.

Sader, M. A, McGrath K. C. Y, Hill M. et al. (2005). Androgen receptor gene expression in leucocytes is hormonally regulated: implications for gender differences in disease pathogenesis. *Clinical Endocrinology*, 62: 56–63.

Sawyers C. L. The cancer biomarker problem. (2008). *Nature*, 452 (7187): 548–552.

Scher H. I, Lu D, Schreiber N. A. et al. (2016). Association of AR-V7 on Circulating Tumor Cells as a Treatment-Specific Biomarker with Outcomes and Survival in Castration-Resistant Prostate Cancer. *JAMA Oncol*, 2 (11): 1441–1449.

Schiffman J. D, Fisher P. G. and Gibbs P. (2015). Early Detection of Cancer: Past, Present, and Future. *Am Soc Clin Oncol Educ Book*, 57–65.

Seitz A. K, Thoene S, Bietenbeck A. et al. (2017). AR-V7 in Peripheral Whole Blood of Patients with Castration-resistant Prostate Cancer: Association with Treatment-specific Outcome Under Abiraterone and Enzalutamide. *European Urology*, 72: 828–834.

Shen M. M. and Abate-Shen C. (2010). Molecular genetics of prostate cancer: new prospects for old challenges. *Genes & Development*, 24 (18): 1967–2000.

Siegel R, Naishadham D, Miller K, Jemal A. Cancer statistics. (2018). *CA Cancer J Clin*, 68: 7–30.

Stamey, T.A, Yang N, Hay A.R, McNeal, F.S. Freiha F. S, and E. Redwine. (1987). Prostate-specific antigen as a serum marker for adenocarcinoma of the prostate. *New England Journal of Medicine,* 317: 909–916.

Steinestel J, Luedeke M, Arndt A. et al. (2015). Detecting predictive androgen receptor modifications in circulating prostate cancer cells. *Oncotarget; Advance Publications 2015*.

Stump M. D, Cherry J. L. and Weiss R. B. (1999). The use of modified primers to eliminate cycle sequencing artifacts. *Nucleic Acids Research*, 27 (23): 4642–4648.

Takeutchi T, Okuno Y, Hattori-Kato M, Zaitsu M, Mikami K. (2016). Detection of AR-V7 mRNA in whole blood may not predict the effectiveness of novel endocrine drugs for castration-resistant prostate cancer. *Research and Reports in Urology*, 8: 21–25.

Tan J-L, Sathianathen N, Geurts N. et al. (2017). Androgen receptor targeted therapies in metastatic castration-resistant prostate cancer - The urologists' perspective. *Urological Science*, 28: 190–196.

Taylor S, Wakem M, Dijkman G, Alsarraj M and Nguyen M. (2010). A practical approach to RT-qPCR – Publishing data that conform to the MIQE guidelines. *Methods*, 50 (4): S1–S5.

Wadowsky K.M and Koochekpour S. (2017). Androgen receptor splice variants and prostate cancer: From bench to bedside. Oncotarget, Vol. 8, (No. 11): 18550–18576.

Zhu Y, Sharp A, Anderson C. M. et al. (2017). Novel Junction-specific and Quantifiable In Situ Detection of AR-V7 and its Clinical Correlates in Metastatic Castration-resistant Prostate Cancer. *European Urology*, 73: 727–735.

Appendix 1.

Information about the Prostate carcinoma positive plasma samples obtained from Magellan Research Sample Biobank (Discovery Life Sciences Inc, CA)

Product ID	DLS17-049910-K2	DLS17-049930-K2	DLS17-050017-K2	DLS17-050029-K2
Origin	Russia	Russia	Russia	Russia
Matrix	K2 EDTA Plasma	K2 EDTA Plasma	K2 EDTA Plasma	K2 EDTA Plasma
Age	68	64	68	69
Gender	M	M	M	M
Ethnicity	White	White	White	White
Sample Date	02-Feb-18	22-Jan-18	06-Feb-18	12-Feb-18
Test 1	Staging	Staging	Staging	Staging
Test Data 1	II; T2cNxM0G2	IV; T3bN1M0G3	III; T3aNXM0G3	II; T2bNXM0G3
Gleason score	Gleason 6	Gleason 9	Gleason 8-9	Gleason 7-8
PSA value	12.3 ng/mL	18.3 ng/mL	15.2 ng/mL	14.0 ng/mL
Treatment Status	Pre-Treatment	Pre-Treatment	Pre-Treatment	Pre-Treatment
Clinical Diagnosis	Prostate Carcinoma	Prostate Carcinoma	Prostate Cystadenocarcinoma	Prostate Carcinoma
Smoking History	Former; 10-20 cigs/day for 20-25 years	Current; 10-15 cigs/day for 40 years	Former; 10-20 cigs/day for 35 years	Former; 12-15 cigs/day for 20 years
Initial Primary Tumor Diagnosis	MRI, Ultrasound, Clinically	CT, Ultrasound, Clinically	CT, Ultrasound, Clinically	MRI, Ultrasound, Clinically
Diagnosis date	17-Jan-2018	26-Dec-2017	12-Jan-2018	18-Jan-2018
Site of Primary Tumor	Prostate gland	Prostate gland	Prostate gland	Prostate gland
Current Medications	None	None	None	Ranitidine; Perindopril; Nifedipine
Any Previous Form of Cancer	No	No	No	No

Appendix 2.

Sequences of the synthetic DNA control templates commercially synthetized by Invitrogen, Thermo Fisher Scientific Inc. (USA)

AR-V7 GeneArt Strings™ DNA Fragment (980 bp):

CATTATCAGGTCTATCAACTCTTGTATTTGTTCTCCCAGGGAAACAGAAGTACCTGTGCGCCAGCAGAAA
TGATTGCACTATTGATAAATTCCGAAGGAAAAATTGTCCATCTTGTCGTCTTCGGAAATGTTATGAAGCA
GGGATGACTCTGGGAGAAAAATTCCGGGTTGGCAATTGCAAGCATCTCAAAATGACCAGACCCTGAAGAA
AGGCTGACTTGCCTCATTCAAAATGAGGGCTCTAGAGGGCTCTAGTGGATAGTCTGGAGAAACCTGGCGT
CTGAGGCTTAGGAGCTTAGGTTTTTGCTCCTCAACACAGACTTTGACGTTGGGGTTGGGGGCTACTCTCT
TGATTGCTGACTCCCTCCAGCGGGACCAATAGTGTTTTCCTACCTCACAGGGATGTTGTGAGGACGGGCT
GTAGAAGTAATAGTGGTTACCATTCATGTAGTTGTGAGTATCATGATTATTGTTTCCTGTAATGTGGCTT
GGCATTGGCAAAGTGCTTTTTGATTGTTCTTGATCACATATGATGGGGGCCAGGCACTGACTCAGGCGGA
TGCAGTGAAGCTCTGGCTCAGTCGCTTGCTTTTCGTGGTGTGCTGCCAGGAAGAAACTTTGCTGATGGGA
CTCAAGGTGTCACCTTGGACAAGAAGCAACTGTGTCTGTCTGAGGTTCCTGTGGCCATCTTTATTTGTGT
ATTAGGCAATTCGTATTTCCCCCTTAGGTTCTAGCCTTCTGGATCCCAGCCAGTGACCTAGATCTTAGCC
TCAGGCCCTGTCACTGAGCTGAAGGTAGTAGCTGATCCACAGAAGTTCAGTAAACAAGGACCAGATTTCT
GCTTCTCCAGGAGAAGAAGCCAGCCAACCCCTCTCTTCAAACACACTGAGAGACTACAGTCCGACTTTCC
CTCTTACATCTAGCCTTACTGTAGCCACACTCCTTGATTGCTCTCTCACATCACATGCTTCTCTTCATCA

AR-FL GeneArt Strings™ DNA Fragment (980 bp):

CTTCAAAAGAGCCGCTGAAGGGAAACAGAAGTACCTGTGCGCCAGCAGAAATGATTGCACTATTGATAAA
TTCCGAAGGAAAAATTGTCCATCTTGTCGTCTTCGGAAATGTTATGAAGCAGGGATGACTCTGGGAGCCC
GGAAGCTGAAGAAACTTGGTAATCTGAAACTACAGGAGGAAGGAGAGGCTTCCAGCACCACCAGCCCCAC
TGAGGAGACAACCCAGAAGCTGACAGTGTCACACATTGAAGGCTATGAATGTCAGCCCATCTTTCTGAAT
GTCCTGGAAGCCATTGAGCCAGGTGTAGTGTGTGCTGGACACGACAACAACCAGCCCGACTCCTTTGCAG
CCTTGCTCTCTAGCCTCAATGAACTGGGAGAGAGACAGCTTGTACACGTGGTCAAGTGGGCCAAGGCCTT
GCCTGGCTTCCGCAACTTACACGTGGACGACCAGATGGCTGTCATTCAGTACTCCTGGATGGGGCTCATG
GTGTTTGCCATGGGCTGGCGATCCTTCACCAATGTCAACTCCAGGATGCTCTACTTCGCCCCTGATCTGG
TTTTCAATGAGTACCGCATGCACAAGTCCCGGATGTACAGCCAGTGTGTCCGAATGAGGCACCTCTCTCA
AGAGTTTGGATGGCTCCAAATCACCCCCCAGGAATTCCTGTGCATGAAAGCACTGCTACTCTTCAGCATT
ATTCCAGTGGATGGGCTGAAAAATCAAAAATTCTTTGATGAACTTCGAATGAACTACATCAAGGAACTCG
ATCGTATCATTGCATGCAAAAGAAAAAATCCCACATCCTGCTCAAGACGCTTCTACCAGCTCACCAAGCT
CCTGGACTCCGTGCAGCCTATTGCGAGAGAGCTGCATCAGTTCACTTTTGACCTGCTAATCAAGTCACAC
ATGGTGAGCGTGGACTTTCCGGAAATGATGGCAGAGATCATCTCTGTGCAAGTGCCCAAGATCCTTTCTG

Appendix 3.

Primers and probes for RT-qPCR detection of AR-FL and AR-V7 mRNA after publication by Ma et al. (2016):

Target mRNA	Forward primer (5'-3')	Reverse primer (5'→3')	Probe (5'→3')
AR-FL	GGAATTCCTGTGCATGAAAGC	CGATCGAGTTCCTTGATGTAGTTC	[HEX]CTTCAGCATTATTCCAGTG[BHQ1]
AR-V7	CGGAAATGTTATGAAGCAGGGATGA	CTGGTCATTTTGAGATGCTTGCAAT	[6FAM]CGGAATTTTTCTCCCAGA[BHQ1]

RT-qPCR protocol used for the detection of AR-FL and AR-V7 mRNA after publication by Ma et al. (2016):

Reverse transcription	50 °C	10 min	
Initial denaturation	95 °C	10 min	
Denaturation	95 °C	30 s	× 40 cycles
Annealing	55 °C	60 s	

Appendix 4.

Target mRNA sequences for AR-V7 and AR-FL RT-SIBA assays.

The E3/C3 junction nucleotides on the AR-V7 mRNA sequences are marked with red. The target exons (E3/CE3) of the AR-V7 assays are located in the AR-V7 transcript, and the target exon sequences (E4/E5, E4, E7/E8) of the AR-FL assays are located in the full-length AR transcript.

RT-SIBA assay	Target sequence (5'→3')	Sequence length	Target exons
AR-V7 assay 1	CTTGTCGTCTTCGGAAATGTTATGAAGCAGGGATGACTCTGGGA**GA**AAAATTCCGGGTTGGCAATTGCAA	70 bp	E3/CE3
AR-V7 assay 2	TCTTCGGAAATGTTATGAAGCAGGGATGACTCTGGGA**GA**AAAATTCCGGGTTGGCAATTGCAAGCATCTC	70 bp	E3/CE3
AR-V7 assay 3	TGTTATGAAGCAGGGATGACTCTGGGA**GA**AAAATTCCGGGTTGGCAATTGCAAGCATCTCAAAATGACCA	70 bp	E3/CE3
AR-V7 assay 4	ATGCTTGCAATTGCCAACCCGGAATTTTT**CT**CCCAGAGTCATCCCTGCTTCATAACATTTCCGAAGACGACAAGA	75 bp	E3/CE3
AR-V7 assay 5	GCAATTGCCAACCCGGAATTTTT**CT**CCCAGAGTCATCCCTGCTTCATAACATTTCCGAAGACGACAAGAT	70 bp	E3/CE3
AR-FL assay 1	TCAATGAGTACCGCATGCACAAGTCCCGGATGTACAGCCAGTGTGTCCGAATGAGGCACCTCTCTCAAGA	70 bp	E4/E5
AR-FL assay 2	TGAGGAGACAACCCAGAAGCTGACAGTGTCACACATTGAAGGCTATGAATGTCAGCCCATCTTTCTGAAT	70 bp	E4
AR-FL assay 3	TCCGTGCAGCCTATTGCGAGAGAGCTGCATCAGTTCACTTTTGACCTGCTAATCAAGTCACACATGGTGA	70 bp	E7/E8

Appendix 5.

Selected oligonucleotides for the alternative AR-V7 and AR-FL RT-SIBA assays.

RT-SIBA assay	Forward primer (5' - 3')	Reverse primer (5'→3')	IO (5'→3')	Amplicon size
AR-V7 assay 1	CTTGTCGTCTTCGGAAATGTT	GCAATTGCCAACCCGG	CCCCCCCCCC AATGTTATGAAGCAGGGATGACTCTGGGmAmGmAmAmAmAmUmUmCmC	68 bp
AR-V7 assay 2	TCTTCGGAAATGTTATG	AGATGCTTGCAATTGCCAA	CCCCCCCCCC CCAACCCGGAATTTTTCTCCCAGAGTCA mUmCmCmCmUmGmCmUmUmC	69 bp
AR-V7 assay 3	TTATGAAGCAGGGATG	TGGTCATTTTGAGATGCTT	CCCCCCCCCC CTTGCAATTGCCAACCCGGAATTTTTCT mCmCmCmAmGmAmGmUmCmA	68 bp
AR-V7 assay 4	TGCTTGCAATTGCCAAC	TCGTCTTCGGAAATGT	CCCCCCCCCCCC ACCCGGAATTTTTCTCCCAGAGTCATCC mCmUmGmCmUmUmCmAmUmAmAmCmAmU	69 bp
AR-V7 assay 5	CAATTGCCAACCCGGAA	TTGTCGTCTTCGGAAAT	CCCCCCCCCCCC AATTTTTCTCCCAGAGTCATCCCTGCTT mCmAmUmAmAmCmAmUmUmUmC	66 bp
AR-FL assay 1	CAATGAGTACCGCATG	TCTTGAGAGAGGTGCCTCAT	CCCCCCCCCC TGCACAAGTCCCGGATGTACAGCCAGmUmGmUmGmUmCmCmGmAmAmUmGmA	69 bp
AR-FL assay 2	AGGAGACAACCCAGAA	AGAAAGATGGGCTGAC	CCCCCCCCCC AAGCTGACAGTGTCACACATTGAAGGmCmUmAmUmGmAmAmUmGmUmCmA	64 bp
AR-FL assay 3	GTGCAGCCTATTGCG	CATGTGTGACTTGATTA	CCCCCCCCCC CGAGAGAGCTGCATCAGTTCACTTTTGmAmCmCmUmGmCmUmAmAmUmC	63 bp

Appendix 6A.

Output data of Probit analysis for the determination of LoD for AR-V7 mRNA from 22Rv1 cells.

Probit Analysis: No.of positive; No. of replicate versus Copies/reaction

Distribution: Normal

Response Information

Variable	Value	Count
No.of positive	Event	70
	Non-event	10
No. of replicates	Total	80

Estimation Method: Maximum Likelihood

Regression Table

Variable	Coef	Standard Error	Z	P
Constant	-0,743284	0,496719	-1,5	0,135
Copies/reaction	0,461272	0,179466	2,57	0,01
Natural Response	0			

Log-Likelihood = -15,147

Goodness-of-Fit Tests

Method	Chi-Square	DF	P
Pearson	1,52006	6	0,958
Deviance	1,56618	6	0,955

Tolerance Distribution

Parameter Estimates

Parameter	Estimate	Standard Error	95,0% Normal CI Lower	95,0% Normal CI Upper
Mean	1,61138	0,636737	0,363395	2,85936
StDev	2,16792	0,843463	1,01127	4,64747

Table of Percentiles

Percent	Percentile	Standard Error	95,0% Fiducial CI Lower	95,0% Fiducial CI Upper
1	-3,43195	2,32074	-22,1455	-0,790211
2	-2,84098	2,09856	-19,6722	-0,439283
3	-2,46603	1,95852	-18,105	-0,214692
4	-2,18396	1,85377	-16,9272	-0,044487

5	-1,95453	1,769	-15,9702	0,094912
6	-1,75924	1,69722	-15,1564	0,214345
7	-1,58801	1,63459	-14,4435	0,319741
8	-1,4347	1,5788	-13,8058	0,414717
9	-1,29527	1,5283	-13,2264	0,50165
10	-1,16692	1,48206	-12,6936	0,582194
20	-0,213187	1,14815	-8,75674	1,2031
30	0,474521	0,925121	-5,96216	1,69499
40	1,06214	0,757749	-3,64161	2,1826
50	1,61138	0,636737	-1,6033	2,76902
60	2,16061	0,572722	0,13988	3,65056
70	2,74823	0,588472	1,4332	5,1654
80	3,43594	0,707435	2,3227	7,56237
90	4,38967	0,975314	3,12873	11,3141
91	4,51802	1,01633	3,22209	11,8341
92	4,65745	1,06175	3,32123	12,4013
93	4,81077	1,11261	3,42788	13,0273
94	4,982	1,17039	3,54453	13,7289
95	5,17728	1,23738	3,67492	14,5318
96	5,40672	1,31732	3,82514	15,478
97	5,68878	1,41713	4,00626	16,6448
98	6,06373	1,55189	4,24233	18,2006
99	6,6547	1,76787	4,60646	20,6607

Probability Plot for No. of positive

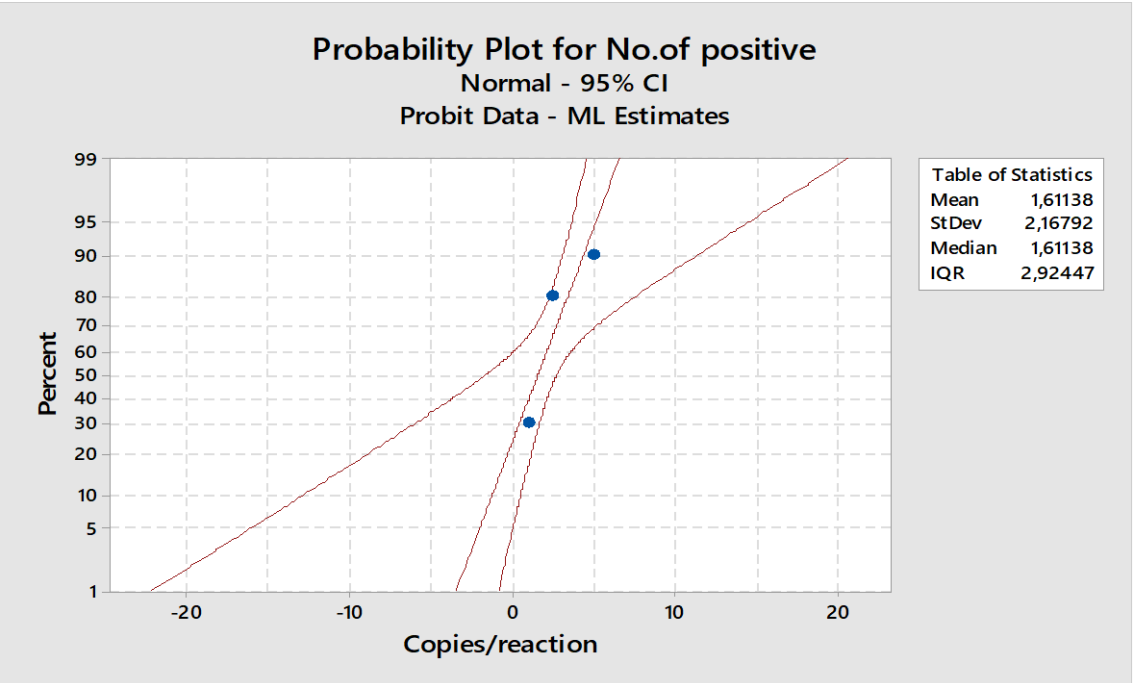

Appendix 6B.

Output data of Probit analysis for the determination of LoD for AR-FL mRNA from 22Rv1 cells.

Probit Analysis: No.of positive; No. of replicate versus Copies/reaction

Distribution: Normal

Response Information

Variable	Value	Count
No.of positive	Event	58
	Non-event	22
No. of replicates	Total	80

Estimation Method: Maximum Likelihood

Regression Table

Variable	Coef	Standard Error	Z	P
Constant	-0,988607	0,366613	-2,7	0,007
Copies/reaction	0,18631	0,0656941	2,84	0,005
Natural Response	0			

Log-Likelihood = -23,065

Goodness-of-Fit Tests

Method	Chi-Square	DF	P
Pearson	0,0336086	6	1
Deviance	0,0336243	6	1

Tolerance Distribution

Parameter Estimates

Parameter	Estimate	Standard Error	95,0% Normal CI Lower	95,0% Normal CI Upper
Mean	5,30624	1,17778	2,99784	7,61464
StDev	5,36739	1,89257	2,68921	10,7128

Table of Percentiles

Percent	Percentile	Standard Error	95,0% Fiducial CI Lower	95,0% Fiducial CI Upper
1	-7,18018	4,28735	-33,7014	-2,0835
2	-5,71703	3,79272	-29,0079	-1,17532
3	-4,78872	3,4821	-26,0366	-0,592402

4	-4,09038	3,25059	-23,8061	-0,149308
5	-3,52233	3,06397	-21,9954	0,214755
6	-3,03884	2,90656	-20,4573	0,527747
7	-2,61491	2,76982	-19,1115	0,804984
8	-2,23533	2,64855	-17,9091	1,05582
9	-1,89012	2,53936	-16,818	1,28642
10	-1,57235	2,4399	-15,816	1,50108
20	0,788929	1,74915	-8,48864	3,21398
30	2,49158	1,35401	-3,49828	4,74233
40	3,94643	1,16479	0,202651	6,61139
50	5,30624	1,17778	2,73961	9,28057
60	6,66605	1,37017	4,41832	12,808
70	8,1209	1,70615	5,72837	17,0679
80	9,82355	2,18838	7,0035	22,3115
90	12,1848	2,93029	8,59264	29,7627
91	12,5026	3,03373	8,79838	30,7735
92	12,8478	3,14677	9,02044	31,8732
93	13,2274	3,27178	9,26304	33,0838
94	13,6513	3,4122	9,5323	34,4376
95	14,1348	3,57323	9,83747	35,9835
96	14,7029	3,7635	10,1938	37,802
97	15,4012	3,99874	10,629	40,0404
98	16,3295	4,31336	11,2035	43,02
99	17,7927	4,81268	12,102	47,7233

Probability Plot for No. of positive

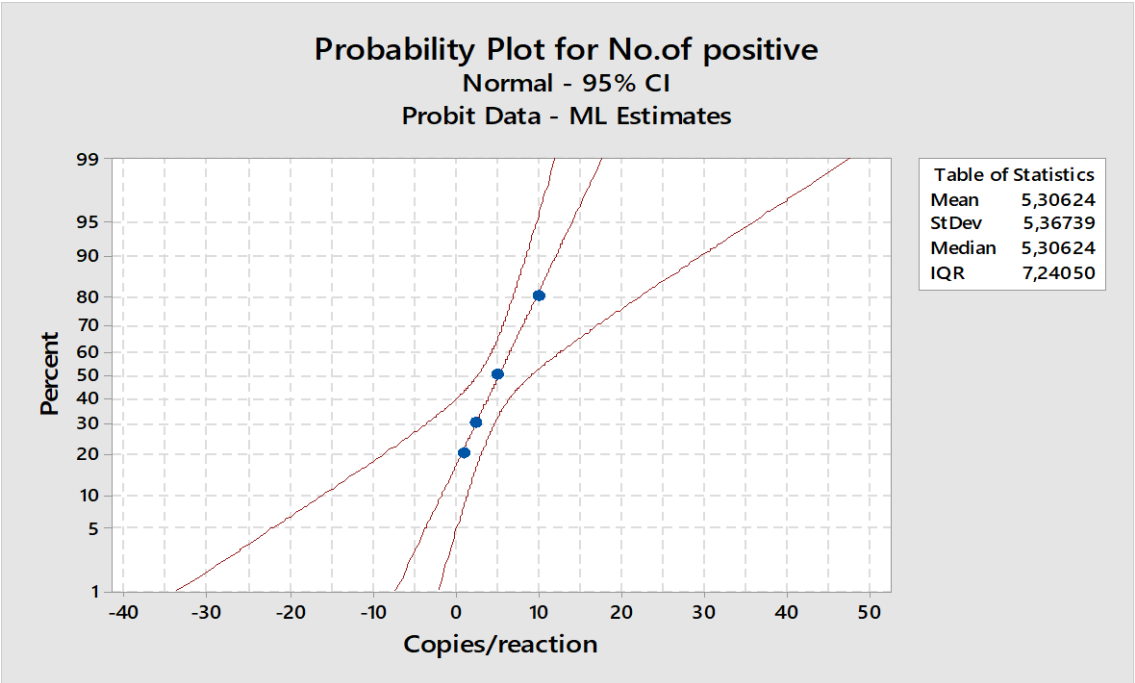

Appendix 6C.

Output data of Probit analysis for the determination of LoD for AR-V7 mRNA from VCaP cells.

Probit Analysis: No.of positive; No. of replicate versus Copies/reaction

Distribution: Normal

Response Information

Variable	Value	Count
No.of positive	Event	66
	Non-event	14
No. of replicates	Total	80

Estimation Method: Maximum Likelihood

Regression Table

Variable	Coef	Standard Error	Z
Constant	-0,903762	0,444229	-2,03
Copies/reaction	0,359512	0,132108	2,72
Natural Response	0		

Log-Likelihood = -18,088

Goodness-of-Fit Tests

Method	Chi-Square	DF	P
Pearson	0,0516344	6	1
Deviance	0,0869484	6	1

Tolerance Distribution

Parameter Estimates

Parameter	Estimate	Standard Error	95,0% Normal CI Lower
Mean	2,51386	0,680778	1,17956
StDev	2,78155	1,02212	1,35363

Table of Percentiles

Percent	Percentile	Standard Error	95,0% Fiducial CI Lower	
1	-3,95699	2,58033	-21,5865	-0,942569
2	-3,19874	2,31243	-18,8981	-0,480111
3	-2,71766	2,14387	-17,1953	-0,183726
4	-2,35576	2,018	-15,9163	0,0411989

5	-2,06138	1,91632	-14,8775	0,225676
6	-1,81082	1,83037	-13,9945	0,383964
7	-1,59113	1,75551	-13,2215	0,523867
8	-1,39442	1,68895	-12,5303	0,650146
9	-1,21552	1,62883	-11,9027	0,765936
10	-1,05084	1,57389	-11,3258	0,873414
20	0,172848	1,18282	-7,07987	1,71253
30	1,05521	0,934145	-4,10547	2,40485
40	1,80916	0,767719	-1,71253	3,14498
50	2,51386	0,680778	0,228411	4,13244
60	3,21856	0,686759	1,65817	5,63109
70	3,9725	0,793025	2,65111	7,77122
80	4,85487	1,00393	3,46134	10,6277
90	6,07856	1,37167	4,35954	14,8146
91	6,24323	1,42475	4,47133	15,3871
92	6,42213	1,48306	4,59124	16,0106
93	6,61884	1,54786	4,72151	16,6978
94	6,83854	1,62099	4,86528	17,467
95	7,0891	1,70522	5,02737	18,3461
96	7,38348	1,80517	5,21562	19,3812
97	7,74538	1,92925	5,44439	20,6563
98	8,22646	2,09589	5,74485	22,355
99	8,98471	2,36153	6,21204	25,0388

Probability Plot for No. of positive

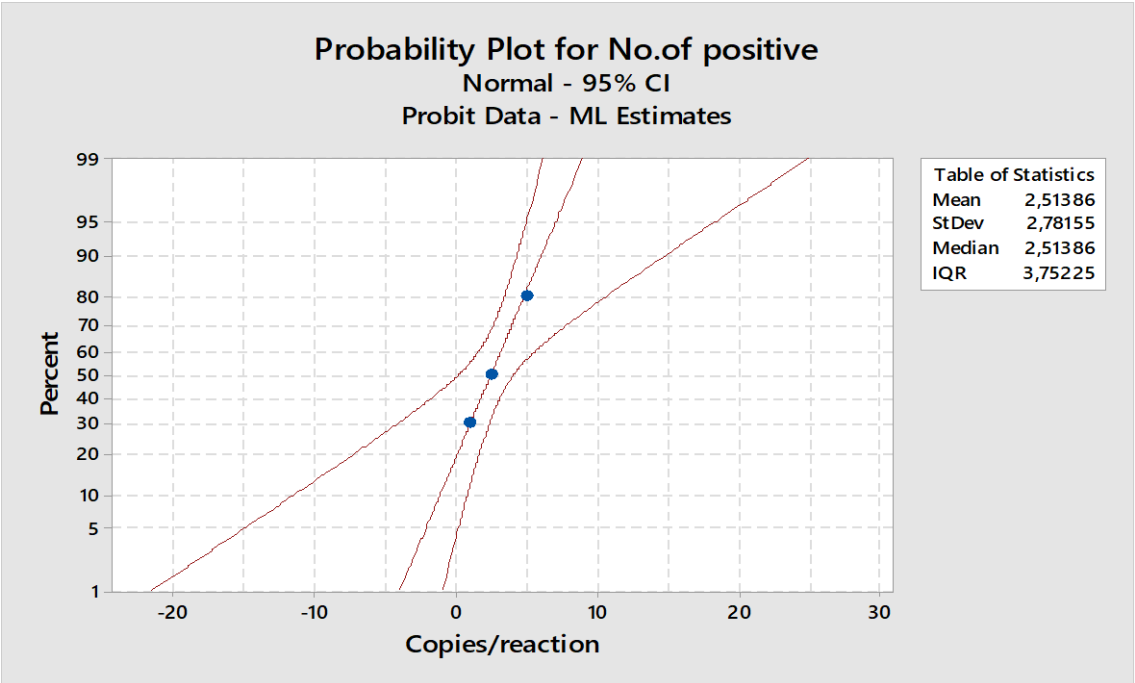

Appendix 6D.

Output data of Probit analysis for the determination of LoD for AR-FL mRNA from VCaP cells.

Probit Analysis: No.of positive; No. of replicate versus Copies/reaction

Distribution: Normal

Response Information

Variable	Value	Count
No.of positive	Event	59
	Non-event	21
No. of replicates	Total	80

Estimation Method: Maximum Likelihood

Regression Table

Variable	Coef	Standard Error	Z	P
Constant	-0,85134	0,359104	-2,37	0,018
Copies/reaction	0,172247	0,0650543	2,65	0,008
Natural Response	0			

Log-Likelihood = -23,825

Goodness-of-Fit Tests

Method	Chi-Square	DF	P
Pearson	0,30883	6	0,999
Deviance	0,310251	6	0,999

Tolerance Distribution

Parameter Estimates

Parameter	Estimate	Standard Error	95,0% Normal CI Lower	Upper
Mean	4,94254	1,23645	2,51914	7,36594
StDev	5,80561	2,19266	2,76928	12,1711

Table of Percentiles

Percent	Percentile	Standard Error	95,0% Fiducial CI Lower	Upper
1	-8,56332	5,07203	-45,9989	-2,7236
2	-6,98071	4,49428	-39,9466	-1,77395
3	-5,9766	4,13066	-36,1127	-1,16529

4	-5,22125	3,8591	-33,2329	-0,703241
5	-4,60683	3,63976	-30,8936	-0,324094
6	-4,08386	3,45438	-28,9054	0,0014441
7	-3,62532	3,293	-27,1646	0,289409
8	-3,21475	3,14956	-25,6083	0,549592
9	-2,84135	3,02011	-24,1951	0,788445
10	-2,49764	2,9019	-22,8965	1,01046
20	0,056422	2,0676	-13,3518	2,76582
30	1,89808	1,56209	-6,73731	4,29936
40	3,47171	1,28021	-1,66094	6,18523
50	4,94254	1,23645	1,86615	9,16557
60	6,41338	1,42684	3,98918	13,55
70	7,98701	1,80602	5,47597	19,0254
80	9,82866	2,36507	6,85201	25,7975
90	12,3827	3,22937	8,53486	35,4146
91	12,7264	3,34987	8,75175	36,7184
92	13,0998	3,48153	8,98571	38,1364
93	13,5104	3,62712	9,24118	39,6975
94	13,9689	3,7906	9,52459	41,4428
95	14,4919	3,97805	9,84568	43,4355
96	15,1063	4,19947	10,2204	45,7791
97	15,8617	4,47314	10,678	48,6635
98	16,8658	4,83903	11,2819	52,502
99	18,4484	5,41943	12,2261	58,5598

Probability Plot for No. of positive

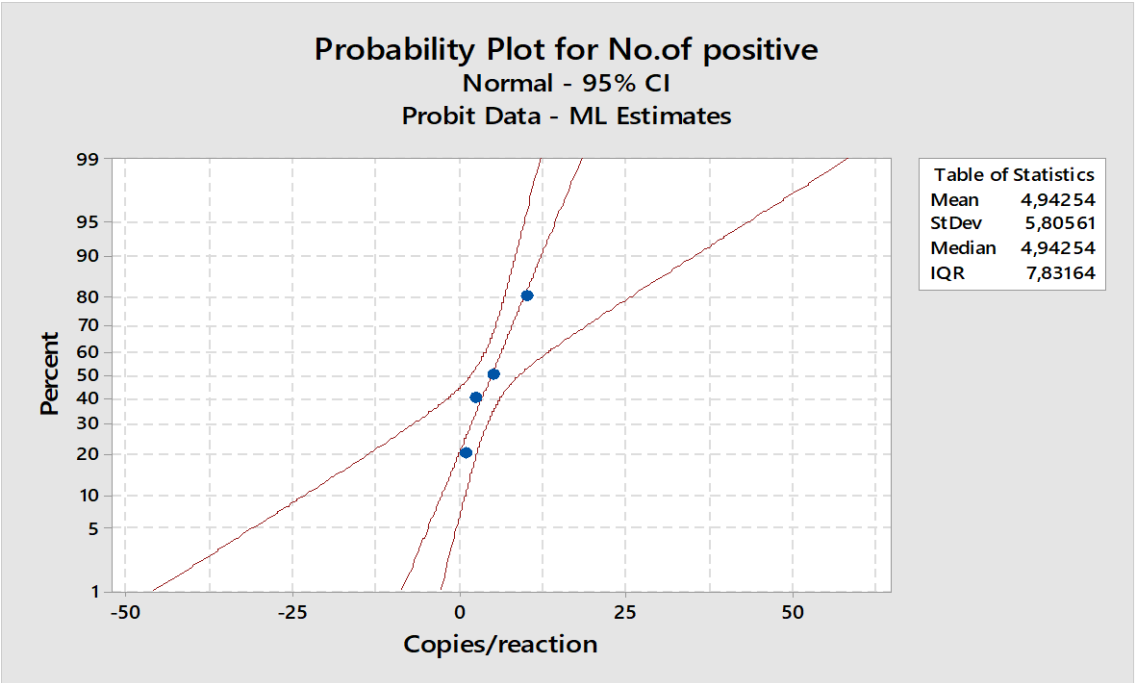

Appendix 6E.

Output data of Probit analysis for the determination of LoD for AR-V7 mRNA from LNCaP cells.

Probit Analysis: No.of positive; No. of replicate versus Copies/reaction

Distribution: Normal

Response Information

Variable	Value	Count
No.of positive	Event	75
	Non-event	5
No. of replicates	Total	80

Estimation Method: Maximum Likelihood

Regression Table

Variable	Coef	Standard Error	Z	P
Constant	-0,025217	0,577943	-0,04	0,965
Copies/reaction	0,436955	0,26006	1,68	0,093
Natural Response	0			

Log-Likelihood = -11,425

Goodness-of-Fit Tests

Method	Chi-Square	DF	P
Pearson	0,494423	6	0,998
Deviance	0,625506	6	0,996

Tolerance Distribution

Parameter Estimates

		Standard	95,0% Normal CI	
Parameter	Estimate	Error	Lower	Upper
Mean	0,0577102	1,29338	-2,47727	2,59269
StDev	2,28857	1,36207	0,712785	7,34798

Table of Percentiles

		Standard	95,00 % Fiducial CI	
Percent	Percentile	Error	Lower	Upper
1	-5,26629	4,32092	*	*
2	-4,64243	3,95474	*	*
3	-4,24661	3,72293	*	*
4	-3,94885	3,54888	*	*

5	-3,70665	3,40754	*	*
6	-3,50049	3,28743	*	*
7	-3,31973	3,18229	*	*
8	-3,15789	3,08828	*	*
9	-3,0107	3,00292	*	*
10	-2,8752	2,92445	*	*
20	-1,8684	2,34604	*	*
30	-1,14241	1,93682	*	*
40	-0,522091	1,59674	*	*
50	0,0577102	1,29338	*	*
60	0,637512	1,01699	*	*
70	1,25784	0,784064	*	*
80	1,98382	0,685576	*	*
90	2,99063	0,94194	*	*
91	3,12612	0,999111	*	*
92	3,27331	1,06467	*	*
93	3,43516	1,14018	*	*
94	3,61591	1,22795	*	*
95	3,82207	1,33162	*	*
96	4,06427	1,45719	*	*
97	4,36203	1,61582	*	*
98	4,75785	1,83197	*	*
99	5,38171	2,18084	*	*

Probability Plot for No. of positive

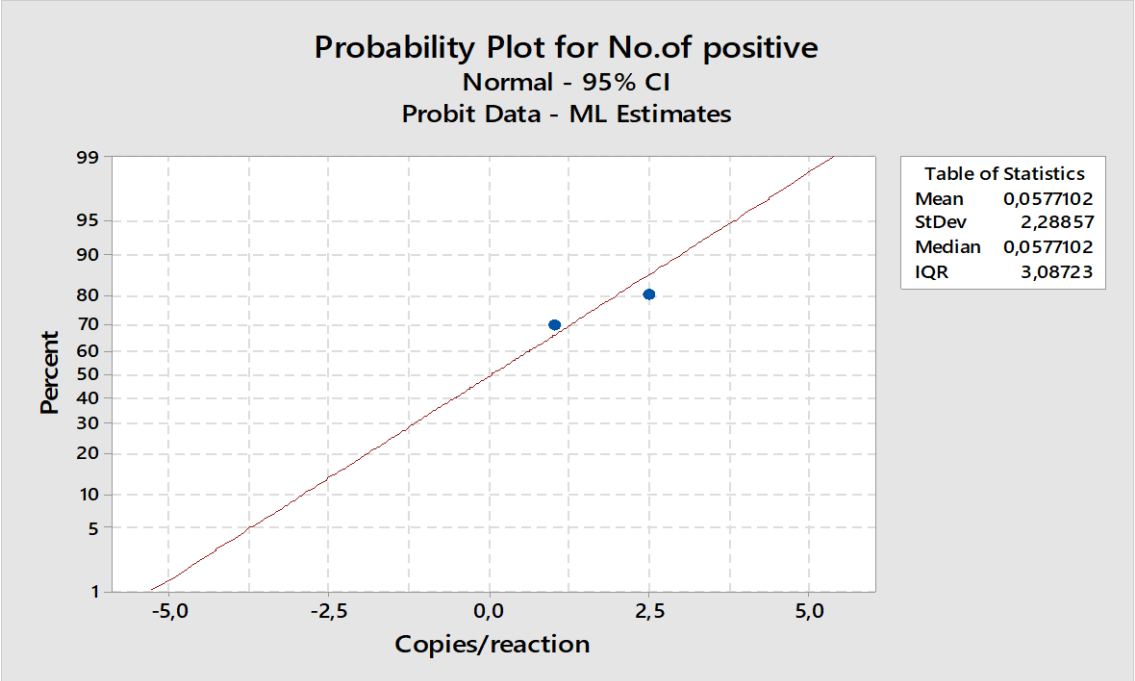

Appendix 6F.

Output data of Probit analysis for the determination of LoD for AR-FL mRNA from LNCaP cells.

Probit Analysis: No.of positive; No. of replicate versus Copies/reaction

Distribution: Normal

Response Information

Variable	Value	Count
No.of positive	Event	52
	Non-event	28
No. of replicates	Total	80

Estimation Method: Maximum Likelihood

Regression Table

Variable	Coef	Standard Error	Z	P
Constant	-1,8077	0,481272	-3,76	0
Copies/reaction	0,240326	0,0724668	3,32	0,001
Natural Response	0			

Log-Likelihood = -17,977

Goodness-of-Fit Tests

Method	Chi-Square	DF	P
Pearson	8,10051	6	0,231
Deviance	9,03332	6	0,172

Tolerance Distribution

Parameter Estimates

Parameter	Estimate	Standard Error	95,0% Normal CI Lower	Upper
Mean	7,52187	1,12601	5,31492	9,72881
StDev	4,16101	1,25469	2,30426	7,51391

Table of Percentiles

Percent	Percentile	Standard Error	95,0% Fiducial CI Lower	Upper
1	-2,15809	2,58777	-14,0023	1,17961
2	-1,0238	2,27576	-11,2906	1,95417
3	-0,304136	2,0827	-9,58073	2,45622
4	0,237243	1,9408	-8,30187	2,84129

5	0,677613	1,828	-7,26756	3,16047
6	1,05244	1,73423	-6,39236	3,43729
7	1,38108	1,65399	-5,62963	3,68467
8	1,67535	1,58395	-4,95105	3,91051
9	1,94297	1,52196	-4,33806	4,12006
10	2,18932	1,4665	-3,77781	4,31696
20	4,01987	1,1246	0,19401	5,97137
30	5,33983	1,00202	2,66583	7,55646
40	6,46769	1,01603	4,34716	9,34161
50	7,52187	1,12601	5,57074	11,3581
60	8,57605	1,30598	6,57104	13,5978
70	9,7039	1,54842	7,50236	16,133
80	11,0239	1,87116	8,49501	19,1972
90	12,8544	2,35716	9,7834	23,5351
91	13,1008	2,42472	9,95205	24,1236
92	13,3684	2,49855	10,1343	24,7638
93	13,6626	2,5802	10,3338	25,4688
94	13,9913	2,67193	10,5553	26,2573
95	14,3661	2,77716	10,8068	27,158
96	14,8065	2,90155	11,1006	28,2176
97	15,3479	3,05543	11,4598	29,5224
98	16,0675	3,2614	11,9343	31,2597
99	17,2018	3,58868	12,6768	34,0035

Probability Plot for No. of positive